

University of Nottingham
UK | CHINA | MALAYSIA

Department of Mechanical, Materials and Manufacturing Engineering

Faculty of Engineering

Design and Modelling of a Reconfigurable Parallel Kinematic Machine with Customisable Leg Layout for Enhanced Performance

By:

Josue Israel Camacho Arreguin

Thesis submitted to the University of Nottingham for the degree of Doctor of Philosophy

September 2021

Abstract

Parallel Kinematic Machines (PKMs) are well know for their high rigidity and precision, as several struts work collaboratively to achieve the desired activations, minimising accumulative errors and providing stiff configurations. As such PKMs have seen successful applications as machine tools, rapid positioners and high precision pointers for antennas and lasers. However, their wide application has been severely limited due to small workspaces (compared to the machine size), singularities in the workspace and complexity of implementation. For these reasons PKMs have been limited to operate in well prepared environments, such as those of workshops and laboratories. Nevertheless, currently robotic systems require to be highly adaptive to different task and scenarios. Adaptive PKMs or also known as reconfigurable PKMs represent a possibility to overcome the limitations of PKMs, as their modifiable architectures can be utilised to optimise their workspace, avoid singularities and in general enable systems capable to adapt to different environments. Furthermore, given the redundancy of actuators PKMs can be utilised as walking machine tools. Nevertheless, providing walking capabilities to a robotic system represents a complicated task . For this reason, most walking robots are based on fixed configurations that are selected according to desired environments and walking conditions, and their performance may be hindered if the ideal requirements are modified. For instance, mammal-inspired walking robots can transport heavy loads at high walking speeds thanks to their vertically-configured legs. Conversely, insect-inspired robots (e.g. hexapods) can traverse complicated terrains, as they can maintain three or more limbs in contact with the ground at any time, with higher stability coefficients than bipeds and quadrupeds. Thus, the number, distribution, and configuration of the legs play a crucial role in the performance of walking robots

(e.g. speed, stability coefficients, actuation torque, etc.). Therefore, designing a Reconfigurable Parallel Kinematic Machine could bridge the current gap for PKMs , enabling its wider use as walking machine tools. Furthermore, enabling the reconfigurable capabilities PKMs could be exploited to walk on different terrains and optimise their performance during machining operations.

In the research of this PhD thesis, the concept and design and test of a walking Reconfigurable Parallel Kinematic Manipulator (RPKM) is proposed. By presenting a reconfigurable kinematic architecture, the system is enabled to operate in many different configurations Furthermore, this thesis presents the kinematic and gait analysis for machining and walking operations. Special attention is presented to singularity avoidance, where an efficient methodology is presented to analyse the workspace and create singular-free paths.

A novel methodology is presented to perform the safe walking of the proposed RPKM over different terrain conditions (e.g. flat and inclined terrain at different slopes). Furthermore, several configurations are implemented to show the advantages of a reconfigurable system with minimal walking errors.

Publications

The research in this thesis has contributed in part or full for the following publications:

[1] J. Camacho, M. Wang, X. Dong, and D. Axinte, "A Novel Class of RPKM Concepts and Fourier-base Singularity Analysis " Mechanism and Machine Theory, vol. 153, 2020.

[2] J. Camacho, M. Wang, Matteo Russo, X. Dong, and D. Axinte, " Novel reconfigurable walking machine tool enables symmetric and non-symmetric walking configurations " IEEE/ASME Transactions on Mechatronics. Pending.

[3] N. Ma , Xin Dong, David Palmer, Josue Camacho Arreguin, Zhirong Liao, Mingfeng Wang, Dragos Axinte.., "Parametric vibration analysis and validation for a novel portable hexapod machine tool attached to surfaces with unequal stiffness," Journal of Manufacturing Processes, vol. 47, pp. 192-201, 2019.

[4] X. D. Ma Nan , Josue Camacho Arreguin., "A Novel Shape Memory Alloy (SMA) Wire-Based Clutch Design and Performance Test," In Annual Conference Towards Autonomous Robotic Systems, no. Springer,Cham, pp. 369-376, 2020.

Acknowledgements

I would like to thank all who have contributed to the development of this thesis. Without your support, I could not have completed this journey. Special thanks are due to the following:

My wife Martha, for all her love, support and encouragement to pursue our goals together.

To my family for all their love and support throughout my life. Thank you for giving me the strength, the support, the encouragement and the examples to chase my dreams. Especially I want to thank my parents Rodolfo and Imelda for their understanding and support.

To my principal supervisor, Prof. Dragos Axinte, for all his support, guidance and constant encouragement to become a better researcher.

My co-supervisors Xin Dong and Mingfeng Wang for all their help and efforts in technical discussions, designs and experimental tests.

To my colleagues in the University of Nottingham for their company and encouragement.

To the Consejo Nacional de Ciencia y Tecnología (CONACyT) for its Financial Support through my PhD studies.

Table of Contents

Abstract II
Publications IV
Acknowledgements V
Table of Contents VI
List of Figures IX
List of Tables XIII
Nomenclature XIV
Chapter 1 ..... Introduction 1
1.1 Background 1
1.2 Problem Definition 2
1.3 Objectives 4
1.4 Structure of the Thesis 6
1.5 Highlights and Contributions 8
Chapter 2 ..... Literature Review 10
2.1 Introduction 10
2.2 In-Situ Repair and Maintenance 13
2.3 Review of Parallel Kinematic Machines 14
2.3.1 PKM Joints 17
2.3.2 Singularities of PKMs 21
2.4 Review of Walking Robots 24
2.4.1 Early Implementations 25
2.4.2 Mature Solutions 31
2.4.3 The Current Trend in Walking Machines 32
2.5 Review of Walking Machine Tools 33
2.5.1 Stability Analysis 36
2.5.2 Foot Ground Contact 38
2.6 Conclusions 39
2.7 Challenges 41
Chapter 3 ..... Concepts of Reconfigurable Parallel Kinematic Manipulators 43
3.1 Disadvantages and challenges of the existing Parallel Kinematic Machines 43
3.1.1. Limited workspace 44

3.2 Singularities on the workspace 45
3.3 Redundancy 47
3.4 Conceptual designs for Reconfigurable Parallel Kinematic Manipulator 48
3.4.1. Concept 1 49
3.4.2. Concept 2 50
3.4.3. Concept 3 51
3.4.4. Concept 4 52
3.5 Concept Summary 54
3.6 Reconfiguration concept selection 55
3.7 Proposed overall RPKM Requirements 58
3.8 Conclusions 59
Chapter 4 ..... Kinematic Analysis 61
4.1 Inverse Kinematic Analysis of the class of RPKMs 61
4.2 Reachable Workspace Analysis 64
4.2.1. Key component constrains 65
4.2.2. Collision constraints 66
4.2.3. Workspace 69
4.3 Singularity Analysis and Optimisation 77
4.3.1. Singularity analysis 77
4.3.2. Singularity Optimisation of the RPKM 85
4.3.3. Validation of singularity analysis and optimisation 88
4.4 Conclusions 92
Chapter 5 ..... Design 94
5.1 Conceptual design 94
5.2 Design overview 97
5.3 Platform Design 98
5.4 Smart Actuation System 99
5.4.1. SMA-clutch mechanism 102
5.4.2. SMA wire characterisation 104
5.4.3. Knot Referencing Mechanism 114
5.5 Limbs 115
5.6 Conclusions 121
Chapter 6 ..... Gait Analysis 122

6.1 Kinematics and stability analysis 122
6.1.1. Singularity Analysis 123
6.1.2. Coordinate systems 123
6.1.3. Kinematic Analysis 124
6.1.4. Comparing the different walking configurations 133
6.2 Force Analysis 136
6.3 Walking Performance Analysis 142
6.3.1. Levelled Ground 142
6.3.2. Inclined ground 147
6.4 Results 151
6.4.1. Gait selection for the different configurations 152
6.4.2. Flat ground 154
6.4.3. Inclined ground at 4 degrees 160
6.4.4. Inclined ground at 10 degrees 162
6.5 Discussion of Results 164
6.6 Conclusions 166
Chapter 7 ..... Conclusions and further research 167
7.1 Discussion on challenges in PKMs vs project objectives 167
7.1.1. To Study suitable architectures to allow a reconfigurable parallel kinematic machine 170
7.1.2. To propose the kinematic models that describe the safe actuation of an RPKM 170
7.1.3. To optimise the architecture of an RPKM to enhance its workspace 171
7.1.4. To propose a novel design of an RPKM 172
7.1.5. To develop the kinematics for enabling the RPKM to walk in different terrain conditions 172
7.2 Overall Achievement 174
7.3 Further Research 174
7.3.1. Feet 174
7.3.2. Walking 174
7.3.3. Machining 175
7.3.4. Power Consumption 175
7.4 Conclusion 176
References 177

List of Figures

Figure 2-1. Ultra Motion GS- platform; Zoom of the spherical and universal joints on the Ultramotion GS platform [34]. 19
Figure 2-2. a) Invex V100 [IndexV100], b)Sprint Z3 [37]. 20
Figure 2-3. Delta robot DR [42]; b) X Delta 3+1 [43]. 21
Figure 2-4. The actuation mechanism of NINJA I. 29
Figure 2-5. LAURON III 31
Figure 2-6. LEMUR [80]I. 32
Figure 2-7. a) Hexagonal configuration; b) Insect configuration 38
Figure 3-1. Illustration of Concept 1, configuring a revolute joint between the limbs and the moving platform. 49
Figure 3-2. Illustration of concept 2, configuring a prismatic joint on the moving platform and each limb 51
Figure 3-3. Illustration of Concept 3, configuring a revolute and a prismatic joint between the limbs and the moving platform. 52
Figure. 3-4. Illustration of Concept 4, configuring a universal and a prismatic joint between the limbs and the moving platform. 53
Figure 3-5. Illustration of three configurations for Concept 1: a)Hexagonal for walking on uneven ground; b) Rectangular for walking on constrained spaces; c) Asymmetrical for inclined terrain. 58
Figure 4-1. Kinematic model of the family of the proposed RPKMs. 62
Figure. 4-2. Component constrains of: a) P-joint ($|\text{Lacti}| \in [\text{Lmin}, \text{Lmax}]$*) and b) S-joint (*$\phi i \in [0, \theta Sl]$*)).* 66
Figure. 4-3 Illustrations for collision analysis: a) scenarios of possible impacts between elements of the RPKM; b) Zoom of the scenario for one limb and the spindle of an RPKM. 67
Figure. 4-4 Illustration of the limit search for the workspace. a) The search is performed dividing the space into planes; the centroid of each plane is the starting point for the search in the next plane. b) Illustration of the polar search on each plane. 70
Figure 4-5. Flow diagram to evaluate the reachable workspace. 71
Figure. 4-6. A case study on the workspace analysis of the proposed RPKM under a highly asymmetrical configuration where feet are placed at uneven heights and slides orientation are unsymmetrically distributed and tilted with respect to the moving platform in: (a) a 3D view, (b) xy plane, (c) xz plane and (d) a 3D view with detailed workspace. 72
Figure 4-7. Illustration of RPKM based on Concept 2. a) The RPKM on uneven surfaces with a symmetrical configuration; b) Top view of the platform. c) Zoom to one of the slides showing the orientation and position of the slide. 74
Figure 4-8. Workspace volume dependant of slide position and orientation of slide. 75
Figure 4-9. Results of maximum workspace volume considering slide orientation and joint position on slide. 76

Figure. 4-10. Illustration of TCP approaching an element of the workspace with a direction angle α and tilt angle β. 78
Figure. 4-11. A case study on singularity analysis for an element of the workspace. a) variation of the Jacobian determinant; b) configuration of the RPKM in both isometric and top views. 79
Figure 4-12. Signal composed by five sinusoid waves. 80
Figure 4-13. Sctrum analysis of amplitude coefficients. 82
Figure 4-14. Spectrum analysis of phase coefficients. 82
Figure. 4-15. a) Spectrum analysis results of Jacobian profile for an element of WS: (a) Jacobian determinant surface; b) Jacobian profile at tilt angle of 0.25π; c) amplitude vs frequency; d) phase vs frequency. 84
Figure 4-17. Flowchart for the DFA of the Jacobian for a given TCP position. 84
Figure. 4-18. Comparison between the original Jacobian profile and reconstructed one by DFA. 85
Figure 4-19. Flowchart for the configuration optimisation to avoid unstable configurations. 86
Figure. 4-20. Results after optimisation using GA for: a) Jacobian surface for an WS element; b) Jacobian profile at tilt angle of 0.25π; c) frequency vs Jacobian. 87
Figure. 4-21. A case study for a proposed path considering a circular trajectory with an inclination of 0.25 π 87
Figure. 4-22. Element of planned path against the determinant value of the Jacobian. a) Non optimised configuration Jacobian values; b) non optimised joints layout; c) optimised configuration Jacobian values; d) optimised joints layout. 88
Figure. 4-23. An FEA model used to evaluate the stiffness of the proposed RPKM. 90
Figure. 4-24. Stiffness of the RPKM when conducting a circular path in Fig. 14a: a) Jacobian stiffness model vs FEA-based model; b) percentage of error between both models. 91
Figure. 4-25. Stiffness of the RPKM when conducting a circular path after an optimisation; a) Jacobian stiffness model vs FEA-based model; b) percentage of error between both models. 91
Figure 5-1. Illustration of the proposed RPKWM design. 95
Figure 5-2 Reconfigurable Parallel Kinematic Manipulator. The illustration presents the capability of the RPKM to place its limbs on complicated to operate environments for in-situ repair. 97
Figure 5-3. Illustration of the platform design, the design considered: a) the integration of the electronics on the platform to increase autonomy. b) Integration of the SAS clutch system on the platform for improved performance. 99
Figure 5-4. Illustration of the proposed RPKM design over a scenario with uneven surfaces: a driving pulley/motor (orange) actuates a wire-rope band to reposition six upper S-joints. 101
Figure 5-5. Illustration of the SMA-clutch with its main components. 103
Figure 5-6. Illustration of the SMA-clutch with its working modes; a) SMA inactive, the shift pads are engaged, the position is locked; b) SMA active, the sift pads grasp the wire-rope band, displacement follows the wire-rope band actuation. 104

Figure 5-7 Illustration of the test rig for the characterisation of the SMA wire with the main components. 105
Figure 5-8. Illustration of the mechanical and electrical connections for the test rig. 106
Figure 5-9. Relation between force time and current provided. 108
Figure 5-10. Characterisation of SMA wire. a) force vs current; b) Cooling time vs current; c) Heating time vs current; d) Efficiency vs current. 109
Figure 5-11. Illustration of the clutch mechanism highlighting the SMA wire and the springs for the pretension of the SMA wire. 111
Figure 5-12. Testing of the cutch mechanism to validate the grasping force exerted on the wire rope. 113
Figure 5-13. Illustration of knot referencing system. 115
Figure 5-14. Illustration of the limbs. a) Actuation package of the S-joints; b) main reference frames for the actuation of the S-joint. 117
Figure 5-15 Illustration of the design and components of the 3-DoF limbs. 118
Figure 5-16. Required variation of length toto operate the S-Joint within the operational limits. a) Plot of the centre of the lower end of the S-joint. Required delta length for: b) Tendon 1; c) Tendon 2; d) Tendon 3 119
Figure 5-17. Illustration of the test set-up for the actuation validation. 120
Figure 5-18. Trajectories recorded from the motion tracking system. 120
Figure 6-1. Schematic of the RPKM on an inclined surface considering the pitch, yaw and roll angles for the kinematic model in the gait analysis. 124
Figure 6-2. a) Illustration representing the repositioning of a limb without contacting the ground; b) limbs interacting with the ground to produce the displacement of the platform. 127
Figure 6-3. Illustration of the methodology for interaction between the feet and the ground in the gait analysis. 129
Figure 6-4. Schematic of selected gaits. a) Tripod gait: Limbs 1, 3 and 5 being swung between Pi_1 to Pi_2, limbs 2, 5 and 6 supporting the RPKM. b) Table of the tripod gait. Metachronal gait: a) Limb 1, swung between Pi_1 to Pi_2, limbs 2 to 6 supporting the RPKM. b) Table of the metachronal gait. 131
Figure 6-5. Illustration of the stability criteria considered for the walking analysis. 132
Figure 6-6. Illustration of the RPKM with insect configuration Insect. 133
Figure 6-7. Illustration of the RPKM with Insect configuration. 134
Figure 6-8. Illustration of the RPKM with G-S configuration 135
Figure 6-9. Illustration of the RPKM with Asy-Hex configuration. 136
Figure 6-10. Illustration of the FEA, the end result is the reaction forces on the feet and the moments exerted on the upper joints. 138
Figure 6-11. Representation of the moments actuating on the limbs 139
Figure 6-12. Determinant of matrix T. 141
Figure 6-13. Maximum step length comparison a) Maximum step length vs height, showing limitations to extend steps size) insect configuration; c) Sym-Hex configuration. 144
Figure 6-14. Force analysis for the tendons. Sym-Hex configurations: a) Tripod gait max force; b) Wave gait max force; c) Difference between gaits. Insect

configuration: d) Tripod gait max force; e) Wave gait max force; f) Difference between gaits. 146
Figure 6-15. RPKM over an inclined surface. a) Illustration of the RPKM, the platform is considered parallel to the inclined surface; b) Stability margins between 0 and 10 º of inclination for the inclined surface. 148
Figure 6-16. Illustration of the RPKM showing the effect of the attitude angles of the platform with respect to the ground. 149
Figure 6-17. Case study for the optimal attitude of the RPKM. Variation of the stability coefficients considering different platform inclinations and ground inclinations. a) Gough-Stewart configuration stability coefficients; b) Sym-Hex configuration stability coefficients. 149
Figure 6-18. Illustration of the RPKM operating at a high inclined surface. The frontal limbs work at the top of the workspace, while the rear limbs operate at the bottom of the workspace, limiting the displacement of the RPKM. 151
Figure 6-19. Motion tracking implementation. a) Image of the locations where the markers have been located; b) Illustration of the recorded motion, the markers are traced at each state of the terrain traverse. 153
Figure 6-20. Snapshots of the recorded motion. A) G-S configuration during the first 5 steps of the walking; b) Snapshots of the gait between full steps. 154
Figure 6-21. a) Illustration of the: a) Insect configuration; b) Sym-Hex configuration. c) First five steps of the Insect configuration; d) First five steps of the Sym-Hex l configuration. 155
Figure 6-22. Recorded motion of the moving platform for the: a) Sym-Hex configuration; b) Insect configuration 156
Figure 6-23. a) Illustration of the: a) Sym-Hex configuration; b) G-S configuration. c) First five steps of the Sym-Hex configuration; d) First five steps of the G-Sl configuration. 158
Figure 6-24. Comparison between the Sym-Hex and Insect configurations. a) Displacements of the Sym-Hex and Insect configuration against the ideal displacement. b) Displacement error. c) Direction error. 159
Figure 6-23. a) Illustration of the: a) Sym-Hex configuration; b) G-S configuration. c) First five steps of the Sym-Hex configuration; d) First five steps of the G-S configuration. 161
Figure 6-25. Comparison between the Sym-Hex and G-S configurations. a) Displacements of the Sym-Hex and G-S configuration against the ideal displacement. b) Displacement error. c) Direction error. 162
Figure 6-26. Comparison Asy-Hex configuration. a) Displacements of the Asy-Hex configuration against the ideal displacement. b) Displacement error. c) Direction error. 163

List of Tables

Table 3-1. Mechanical characteristics of the family of reconfigurable PKMs proposed. 55
Table 3-2. Concept summary 56
Table 4-1 Main harmonics of the selected Jacobian profile in Figure 15. 83
Table 5-1. Pondering table for the working conditions of the SMA wire. 110
Table 5-2. Coordinates and unit vectors for SMA wire. 112
Table 5-3. Error calculated from tracking motion system and estimated trajectories from kinematics. 120
Table 4. Table of comparison between Insect and Sym-Hex configuration for maximum step size over flat terrain. 143
Table 6-5. Performance Comparison of the Insect, Sym-Hex, G-S and Asy-hex configurations. 165

Nomenclature

Variable	Description
A_i	Matrix describing the positions of the *ith* foot of the RPKM
${}^{O}A_{Ang_i}$	Rotation angles describing the orientation of the *ith* foot of the RPKM
V_j	Location of virtual base vertices
${}^{O_v}R_O$	Rotation matrix from the global reference frame to the machine coordinate system
B_i	Vector describing the positions of the *ith* joint of the RPKM
$\boldsymbol{L_{act_i}}$	Vector of the *ith* limb of the RPKM
$\boldsymbol{K_i}$	Vector defined normal to surface of the *ith* foot
ϕ_i	Angle formed between the limbs and the *ith* joint.
$\boldsymbol{D}$	Vector between two elements under collision analysis
$\boldsymbol{L}$	Vector describing the geometrical characteristics of element 1 for collision analysis
$\boldsymbol{S}$	Vector describing the geometrical characteristics of element 2 for collision analysis
a	Coefficient linked to element L for collision analysis
b	Coefficient linked to element S for collision analysis
$S(\theta)$	Represents a periodic signal
a_n	Amplitude coefficient of the nth component of a signal (cosine component)
b_n	Amplitude coefficient of the nth component of a signal (sine component)

c_n	Amplitude coefficient of the nth component of a signal as the sum of phased sine waves
ω_n	Frequency at which a wave n operates
φ_n	Phase angle of a given signal
K	Stiffness matrix of a PKM
J	Jacobian matrix
K_l	Stiffness matrix for the limbs of a PKM
ΔX	Deformation matrix of a PKM
θ_1	Direction angle for the actuation of a limb
θ_2	Amplitude angle for the actuation of a limb
T_i	Position of the tendon guides
${}^{Os}R_{Ol}$	Rotation matrix from the limb reference frame to the S-joint reference frame
n	Vector defined as the reference where the rotation of the leg is declared to occur
T_{length_i}	Nominal length of the *ith* tendon
$\boldsymbol{P_v}$	Neutral vector to evaluate intersection with the surface to be traversed.
$\boldsymbol{N_v}$	Vector normal to the surface of the moving platform in the RPKM
t_v	Coefficient for Nv to intersect the surfaced traversed
P_i	Vector defining the position of each foot against the neutral position
A	Coefficient defining the aperture of each foot
$\boldsymbol{N_{slide}}$	Projected vector of the *ith* slide on the traversed surface
P_{i_1}	Forward limit position of the *ith* foot
P_{i_2}	Afterward limit position of the *ith* foot

F_i	Force exerted by *ith* tendon.
$\boldsymbol{r_i}$	Vector from the centre of the spherical joint to the lower tendon guide.
$\boldsymbol{D_i}$	Direction vector for the *ith* tendon (as a unit vector).
$\boldsymbol{W_l}$	Mass of the limbo f the RPKM.
$\boldsymbol{r_w}$	Radius of action of the limb's mass.
$\boldsymbol{g}$	Acceleration produced by the gravity.
$\boldsymbol{r_f}$	Radius of action of the reaction force of the foot.
$\boldsymbol{R_f}$	Reaction force on the foot.
T_{Wlimb}	Torque exerted by the weight of the limb and
T_{Feet}	Torque exerted by the reactions on the feet.
$T_{i\%}$	Percentage of difference between maximum tensile forces between insect and wave gaits.
T_{Ti}	Maximum tensile force on the *ith* tendon with the tripod gait
T_{Wi}	Maximum tensile force on the *ith* tendon with the wave gait

Chapter 1 **Introduction**

1.1 **Background**

Since 2010 the demand and request of robotic systems have seen a steady increment [1]. This response relies on the current needs of the manufacturing industry, where more processes are being automated to increase production rates and quality requirements. The applications where robotic systems are being applied go from pick and place to more complicated operations such as polishing, drilling, milling, welding, etc. However, most of these robots rely on serial architectures, which under high loads are prone to larger deformations and accuracy errors [2]. To compensate these drawbacks, specialised systems relying on Computer Numerical Control (CNC) have been designed with particular attention to improving accuracy and rigidity. The approach by conventional CNC machine tools relies on the creation of robust and bulky machines, which result in stiff but heavy equipment requiring dedicated facilities and workshops [3, 4]. Another trend in the search to increase accuracy during machining operations is based on parallel architectures. Parallel Kinematic Machines (PKMs) have been known for their good performance under high payload and high dynamic capabilities since their first successful applications by Gough and Stewart [5]. However, one of the main drawbacks of parallel architectures is its small workspace/machine size ratio. Moreover, conventional PKMs are constrained to operate between a fixed platform (that works as a base) and a moving platform (that connects the end-effector) by several actuators working together [6]. However, these conventional PKMs are still limited to work on particular tasks, as the architectures limit their applications to well-dedicated spaces (i.e. workshops and laboratories). Furthermore, as mentioned in[7]that the future of

robotics will highly rely on versatility, as adaptive robotic systems could conform to different scenarios and tasks allowing to overcome the high cost associated with specialised systems for a single task/condition. One of these scenarios is the in-situ repair and maintenance, which demands highly adaptive machines. As a successful application, FreeHex, is a compact portable machine tool capable of performing 5-axis operations (i.e. milling and threading) at high precision [8]. This machine based its design on a conventional Gough-Stewart machine with one significant difference; the fixed base was removed, allowing its actuators to position directly over the site of intervention (i.e. free form surfaces). This machine overcame several challenges such as the calibration against the features to machine, proving significant advantages against conventional PKMs and the common trend on CNC machines. However, the FreeHex posed limited adaptability and required human intervention to place it in the intervention site. Nevertheless, this project developed an innovative non-conventional PKMs and opened new possibilities for adaptive PKMs. This possibilities are focused on increasing the adaptability of PKMs to overcome its current limitations, such as reduced workspaces, singularities and further providing capabilities as walking machine tools.

1.2 **Problem Definition**

The main goal of this thesis is to design and build a novel Reconfigurable Parallel Kinematic Manipulator (RPKM) capable of modifying its performance for machining and walking operations. Nevertheless, to operate as a walking machine (in contrast to conventional machines), two primary requirements are desired from the proposed RPKM:

(1) It must not only perform as a machine for inspection and repairs, but also be able to displace autonomously (walk) to the place of intervention.

(2) It must be capable to readapt its configuration to optimise between the walking and the machining operations, as the required optimal configurations between walking and machining are different. .

Although, several PKMs have been reported with successful applications (e.g. machining centres, flight simulators, precision manipulators, etc.), those are still constrained between two platforms, a fixed one that works as the base for the system and a moving platform where the end-effector/tools are attached to perform the required operations. These conventional systems are limited to particular applications, as some of the main limiting conditions as follows:

1. **The reduced workspace/machine ratio**. Although the parallel architecture is well known for its advantages for stiffness and precision, its workspace is reduced compared to serial architectures. As a result, these machines have been constrained to applications where high stiffness and precision in a small workspace are the primary targets.
2. **The inability to adapt to free form surfaces.** In conventional PKMs a fixed platform provides a robust base for the system. However, it becomes one of the main drawbacks as it forms a flat plane where the limbs are attached, preventing PKMs of adapting to free forms (i.e. irregular heights or curved surfaces on the place of intervention). Furthermore, the fixed platform forms a barrier between the machine and the intervention surfaces, preventing the use of the struts as limbs (that can directly attach and displace the complete system).

3. **The fixed configuration and workspace.** Conventional PKMs pose fixed locations of their joints for consistent workspace conditions and require complex kinematic and control algorithms for the safe operation. These safe operations often involve the workspace analysis to operate in safe regions (to avoid collisions or singularities). However, these analyses are often resource consuming and are evaluated only on the design stages (as conventional PKMs maintain the same workspace during their operational life).

Even though removing the lower fixed base has already been implemented, allowing non-conventional PKMs to adapt to different surfaces, its performance is constrained by the surface and the configuration on the moving platform. Other approaches could increase the adaptability of RPKM more precisely in terms of their performance (i.e. workspace volume, singularity avoidance, stiffness). For instance, the repositioning of the upper joints would mean a further advantage to prevent unstable configurations that limit the workspace (i.e. singularities and possible collisions, joint limits, etc.).

Therefore, a parallel kinematic manipulator capable of modifying its performance for autonomous walking and in-situ operations is proposed. The theoretical challenges in the academic and industrial context will be addressed to increase the practicality of the PKMs and provide a more in-depth understanding.

1.3 **Objectives**

The main aim of this thesis is to develop a reconfigurable parallel kinematic manipulator, capable of performing autonomous walking and in-situ repairs. For this, the proposed RPKM must consider several conditions, such as singularity avoidance

and metamorphic capabilities, which can improve its performance when acting like a machine (i.e. improved stiffness and workspace). Nevertheless, as a non-conventional and walking machine-tool, the proposed RPKM must adapt to different scenarios (i.e. flat and inclined terrains, obstacles and stairs) during its autonomous walking. The specific objectives to achieve in this thesis are listed as follows:

- Propose a novel RPKM that is capable of performing both autonomous walking and in-situ repairs. PKMs are well known for their high performance in terms of precision and high load capacity as several actuators work collaboratively to position an end-effector. However, the redundancy of actuators could be exploited not only for positioning an end-effector but further allowing walking capabilities, where the actuators could alternate between supporting and translating phases. This also represents a system that can modify its kinematic chain between optimal machining and walking configurations.
- Develop the kinematic models that describe the metamorphic characteristics of the proposed novel RPKM. Several PKMs have been developed, but often these designs consider a single configuration for the operational life of the proposed PKM. However, in an RPKM, the workspace, collision avoidance and desired actuation must be evaluated before any operation. This requires an efficient methodology to obtain the kinematic characteristics of an RPKM.
- Develop the optimal algorithm to obtain an best possible configuration of the RPKM for machining operations and the avoidance of singularities. As one drawback of PKMs is the presence of singularities in the workspace that can lead to loss of control and damage to the PKMs, this thesis aims to overcome

this issue by taking advantage of the reconfiguration capabilities of the design to be proposed.

- Propose the novel gait analysis of the RPKM to achieve optimised walking by considering different conditions such as the terrains and obstacles. Most walking robots are based on fixed configurations that are selected according to desired environments and walking conditions. However, their performance may be hindered if the ideal conditions are modified. An RPKM with a methodology to obtain the ideal configuration would enable RPKMs in several industrial applications. Furthermore, the configurations of the RPKM could be modified to enhance the speed of translations, load capabilities and stability margins.

1.4 Structure of the Thesis

Chapter 2 presents a review of the existing PKMs covering different architectures and corresponding applications. Special attention is paid to reconfigurable designs and the actuation utilised. Furthermore, several walking robots are also reviewed, with a particular focus on the evolution of the systems and their applications. Finally, the research gaps and challenges for a novel RPKM are identified.

Chapter 3 introduces the challenges and disadvantages existing in the current PKMs designs, especially the main limitations to industrial applications. With respect to these disadvantages, a family of novel RPKMs is presented to increase the flexibility and adaptability of PKMs. These 4 concepts are presented, increasing the flexibility of the kinematic chains by actuating the upper and lower joints.

Chapter 4 presents the inverse kinematics of the family of RPKM concept designs presented in chapter 3. Furthermore Chapter 4 serves as a foundation to select the most suitable configuration of the concepts presented in chapter 3 and as a means to finalise the design presented in Chapter 3. The challenges introduced in chapter 3 are solved by a practical analysis under consideration of the collision avoidance and the geometrical characteristics of the proposed RPKMs. Moreover, an efficient workspace calculation method and a singularity avoidance evaluation algorithm are performed for the optimisation of the workspace, which is later utilised to effectuate the design of the moving platform. Once the platform geometry is selected, a novel methodology for singularity detection is introduced based on furrier analysis. Furthermore, this novel methodology is combined with genetic algorithms to propose optimised configurations to avoid singularities in the tasks to be performed.

Chapter 5 presents the mechanical design, where a novel clutch mechanism is presented, based on Shape Memory Alloys. This novel system allows the actuation and reconfiguration of the upper joints with significant advantages to the conventional mechanism, such as weight reduction and adaptive capabilities.

Chapter 6 presents the models used to perform the walking of the RPKM considering different environments and conditions (i.e. approach angles to the terrain and inclination of the ground). This chapter presents the optimal configurations for different conditions, ensuring stable and safe traverse.

Then the chapter presents the experiment results related to the walking capabilities of the proposed RPKM. Furthermore, the walking tests with

various gaits on flat, inclined and a mixture of slopes are presented, with comparison to the theoretical results showing the advantages of a metamorphic RPKM.

Chapter 7 concludes and discusses the outputs of this research work, with special attention to the contributions presented in this thesis and the future academic and industrial work that could be developed in the field.

1.5 Highlights and Contributions

This thesis details the work and contribution of the research developed under the RAIN project; the main highlights of this project are:

1. A family of novel RPKMs were proposed. The concepts differ from existing PKMs, as the upper joints are repositionable on the moving platform by several mechanical systems (i.e. slides, universal joints) and the lower joints are free from a fixed based. The family of RPKMs looks to increase the adaptability of PKMs to enhance its possible applications in a variety of environments. Furthermore, a kinematic model was developed to describe the kinematic adaptability and workspace of the concepts introduced.
2. The concept, design and demonstration of a novel RPKM as a walking machine tool is presented. Theoretical and experimental analyses have shown that the proposed RPKM can displace itself to the place of intervention, reconfigure from optimal walking configurations to later operate as a machine tool.
3. A novel SMA-based actuation mechanism for the repositioning of the upper joints is presented and demonstrated. This novel design has shown its novelty and advantage in terms of actuating several joints separately or simultaneously

with a single motor, which significantly reduces the weight of the system (compared with conventional actuation structures).

4. A novel Fourier-based method is proposed to analyse the Jacobian of the RPKM. This method is proved to reduce the burden on the identification of unstable configurations, especially as the workspace changes on each configuration of the RPKM. More importantly, this method is combined with genetic algorithms to present an enhanced stiffness configuration free of singularities in the task to develop, achieving an efficient methodology to use the workspace and ensuring a stable operation of the RPKM.
5. The optimal configurations for the walking of RPKM are presented and evaluated. Specifically, these configurations are obtained not only by considering the interaction between the RPKM and the ground (i.e. inclination and friction), but also by evaluating the stable and optimal actuation of the limb.

Chapter 2 **Literature Review**

2.1 Introduction

Robotic systems are known to reduce production times and increase the quality of products and services (i.e. repair, maintenance, inspection). As a result, robotic systems have seen an increased demand for the manufacturing of electronics, automobiles, aerospace components, food processing and energy generation. These applications are from as simple as those of pick-and-place, to more complicated ones such as painting, welding, and product testing. However, robotic systems are still facing restrictions for other activities (e.g. machining tools), especially when high specifications are required (e.g. high material-removing rates, manufacturing/repair of large components). These restrictions are often related to serial architectures, which are the most common ones in robotic systems. As a result, when high payloads and high precision are required in machining operations, the current trend is to create large and bulky systems. However, these systems look to increase the stiffness and prevent undesired deformations but often are limited to operate in dedicated facilities, as their large size and high weight restrict the portability. These characteristics have led to the disassembling and transportation of large components requiring repair with high-quality controls to dedicated workshops, which significantly increases maintenance and repair costs. Nevertheless, new methods and systems capable of achieving high precision and practical transport are required to reduce downtimes and costs of repairing complex mechanical systems.

One industrial sector requiring high precision and transportability is the in-situ repair and maintenance of large components. The basic idea of in-situ repair is to bring the repairing machine to the equipment requiring the intervention. This strategy aims to

reduce the cost involved in the disassembly and transportation processes of large mechanical components. However, in-situ operations require machines with a high level of adaptability to operate in environments that have not considered the ideal manufacturing conditions. Nevertheless, in-situ repair equipment must be light-weighted as these systems must be transported, deployed, and mounted over the place of intervention to perform high-quality services. As a result, the current trend in portable machine tools is to create systems with moderate precision and accuracy, limiting their operation for non-critical repair tasks.

PKMs are one of the promising technologies to overcome these issues, present high stiffness and excellent dynamic characteristics, leading to increased accuracies. However, disadvantages such as small workspace volumes, complicated control algorithms and singular conditions are still limiting the applications. To overcome these drawbacks, first, researchers have been focused on improving the workspace by optimising the layouts of the actuators to reduce singularities and increase the workspace volume. However, these efforts are focused on achieving a single configuration for a specific task, and thus restricting the adaptability to different conditions. Then, other studies have been relied on the creations of hybrid PKMs (creating a combination of serial and parallel architectures) to exploit the characteristics of PKMs over larger volumes. However, most of these systems are still focused on the intervention of dedicated workshops and laboratories, limiting the applications for the in-situ repair sector. Moreover, another research trend has been established to explore the reconfigurable PKMs for enhanced performance and adaptability. This approach may benefit several sectors (e.g. aeroengines, nuclear plants, etc.), as a single robotic system could adapt to different environments and operations, allowing to reduce the cost involved in designing and manufacturing

specialised robotic systems. Nevertheless, the exposure of human labour could be reduced in environments that represent a threat to human health (e.g. nuclear environments). Furthermore, if robotic systems are intended to replace human intervention in hazardous environments, these must include self-propelling capabilities (i.e. walking).

The development of walking robots has extensively relied on nature-inspired mechanisms (e.g. mammals, insects, reptiles) in search of more efficient, higher load capabilities and increased gait adaptability [9]. For instance, mammal inspired walking robots (vertically configured legs) have been considered to transport heavy loads at optimal walking speeds [10], while insect-inspired ones (e.g. hexapods) have been used to traverse over-complicated terrains given the number of limbs in contact with the ground and their higher stability. In this regard, the number, distribution, and configuration of legs play very important roles in the performance of walking robots (e.g. speed, stability margin, actuation torque, etc.). Currently, on one hand, most walking robots are based on fixed configurations, which normally represent a trade-off between the environment and walking performance, and their performance can be hindered when the conditions change from the ideal ones. However, on the other hand, adaptive walking robots, thanks to their reconfigurable capabilities, represent a clear advantage against their conventional counterparts when the terrain or applications constantly vary [11]. Even though some researchers have focused on developing metamorphic walking robots, few researchers have focused on creating adaptive walking machine tools. These issues arise as the requirements for efficient walking differ from those required for machining. This literature survey aims to identify the research gaps for developing a Reconfigurable Parallel Kinematic

Machine capable of optimising its performance with respect to locomotion and manufacturing/repair operations.

2.2 In-Situ Repair and Maintenance

Maintenance involves the necessary activities to keep a system in optimal conditions to achieve its ideal performance through its operational life cycle, playing a crucial role in high-value products such as aero-engines, nuclear plants, defence and medical equipment [12]. Poor maintenance practises are often linked to prolonged downtimes, reduced productivity and lower profits [13]. However, maintenance often represents an expensive necessity as it can represent up to 40 per cent of the total cost of production of goods [14]. In this regard, the industry is paying more attention to technologies that reduce maintenance costs. More importantly, [15] concludes that the future profitability of maintenance is based on new information, technology and methods.

Some maintenance approaches are focused on transporting the maintenance tools to the intervention site, in contrast to conventional methodologies. One of these strategies aims to increase the portability of the machine tools necessary to perform repairs [16], as the downtimes and costs related to disassembly and transport of components could be reduced [17], especially for large components. Furthermore, large components with complex shapes represent a complicated problem for the machine tool industry. The current trend is to create machines that suit the size of the part to be manufactured, requiring immense machine tools [18]. Nevertheless, specialised tools have reported successful results in the repair and inspection of large components in the energy sector [19], shipbuilding [20] and aerospace industries [21].

One example of this approach is found in [22] with the development of a 6-DoF serial and track-mounted portable machine (called SCOMPI) for the repair of hydraulic turbines, with successful applications for welding and grinding operations. Although the authors report on the limitations related to high human dependency and vibrations issues associated with low stiffness of the system. In this regard, [23] reports on the low stiffness and deviations generated by the use of serial architectures in the machining of large components. However, other architectures, such as PKMs, have attracted the attention of researchers, thanks to their low weight and high performance in terms of rigidity and precision. More importantly, thanks to their low weight and high precision PKMs represent a possibility to overcome the current limitations of portable machines.

2.3 Review of Parallel Kinematic Machines

As defined by Merlet [6], a PKM is a moving platform/an end-effector connected to a fixed base by at least two independent kinematic chains (in a closed-loop chain). Even though PKMs had attracted the attention of mathematicians since 1645 when Christopher Wren proposed closed-loop structures [24], the first successful applications were reported related to Gough in [25] and Stewart in [5], under the name Gough-Stewart platform. Although these machines proved to be efficient in their applications as a 6-DoF testbed for tires and a platform for a flight simulator, the complex control algorithms and limited computational resources of the 1960s constrained a broader series of applications. It was until the mature development, distribution and availability of computational resources when PKMs became more popular and commercially available [26], more precisely in the forms of Delta robots. The first successful application of Delta robots considered the rapid

positioning of components in the manufacturing sector, opening the interest of PKMs for more industrial applications. As a result, in 1994, two companies presented two prototypes of the Gough-Stewart platform as milling machines [27], although inefficient controllers and design flaws limited the success of these prototypes[6].

Nevertheless, the reappearance of the Gough-Stewart platform opened several challenges and research topics that inspired the studies for a more profound knowledge of parallel mechanisms. Since then, PKMs have been studied extensively, from the kinematic models and the singularities existing in the workspace to control these mechanisms. Nevertheless, several challenges of the PKMs continue to inspire researchers to optimise and expand the applications of these mechanisms, representing an important topic for academic and industrial interest.

Parallel mechanisms have been classified into two major groups: complete mobility PKMs and reduced mobility PKMs. The first group possess mobility in 6-DoF while the reduced mobility possesses five or fewer DoFs. However, mechanisms capable of achieving 5-DoF (3 translations and two rotations) are capable of complying with most industrial applications, as usually the third rotation is provided by the spinning of the tools added to the PKMs (i.e. drillers, miller, spindles). In this context, it is worth mentioning the most widely applied and studied PKMs: the Delta and the Gough-Stewart platform. These two configurations have achieved their success thanks to their high rigidity, good dynamic performance and high accuracy. More importantly, PKMs do not accumulate errors as serial manipulators do in their links (as the errors add up serially). However, the main disadvantage of PKMs are small workspaces (compared with serial manipulators), complex kinematics and singularities existing in their workspace. As a result, applications requiring high

rigidity and precision in a small workspace are the ideal scenarios for PKMs, limiting a wider popularisation. These applications are often as milling machines, manipulators in assembly lines, positioning of antennas and telescopes and even as medical devices.

Furthermore, researchers have proposed reconfigurable mechanisms capable of modifying its performance (e.g. mobility, stiffness, workspace volume, load capacity, dexterity) to different tasks and conditions. The basic idea behind these concepts relies on the capabilities of the mechanisms to modify its kinematic chains or components. Further, in an era of rapid developments, a robotic system capable of adapting and increasing its flexibility is highly valued and could increase its use in several industrial applications [28]. For example, Pallpacelli et al. [28] presented a mechanism for a lockable spherical joint (S-joint). This joint could modify its kinematic characteristics between an S- and a U-joint joint for a 3-CPU (cylindrical-prismatic-universal) PKM with adaptive mobility, whose working modes can transform between pure translation and pure rotation. Other researchers focused on developing reconfigurable PKMs with interchangeable elements to adapt to specific requirements between different tasks to create a map between elements of the PKM and application s[29]. However, these approaches still represent a small workspace for the PKMs proposed. High efforts have been invested in increasing the workspace and have successfully proven other concepts as autonomous repositioning PKMs [30], [31]. Similarly, Reid [32] proposed a system where a PKM was mounded on an automated guided vehicle to displace the mechanism and to achieve high precision for drilling and fastening operations (reporting precisions of 0.3 mm). Nevertheless, these systems rely on a series of wheeled vehicles or slides for

repositioning and then preventing their service in unprepared environments for its operation (i.e. uneven surfaces and complex industrial sites).

Other researchers have proposed PKMs to operate in complicated environments for manufacturing and repair, introducing a novel class of PKMs [8] [33] to perform in-situ operations of industrial installations. The FreeHex, whose fixed base was removed and replaced by six re-locatable feet, allowed to position each strut independently, permitting the system to adapt to complex surfaces. Furthermore, [8] proved high versatility against conventional PKMs and opened the interest in the research of highly adaptive PKMs. These aspects comprehend the capability to modify the locations of the upper joints to avoid unstable configurations during machining operations and during the traverse of different ground conditions (e.g. low friction between the feet and ground, inclined surfaces). Even with the modifications proposed by previous works, to the authors' best knowledge, there exists an opportunity to develop an intelligent Reconfigurable Parallel Kinematic Manipulator (RPKM) capable of adapting its configuration to different tasks in unconditioned environments for manufacturing and repair with particular attention to optimising workspace and stability of PKMs (avoiding singular configurations). However, special attention must be placed on the selection of the components conforming to an RPKM.

2.3.1 PKM Joints

The main objective of the joints is to provide a mean to transfer loads of the PKM and allow the required DoF for the mechanism, playing a crucial role in the task to develop. Furthermore, joints control the DoF of the PKMs, preventing undesired

displacements. Therefore, it is essential to notice that different applications require a combination of joints to achieve the desired kinematic constraints.

For instance, six struts with a Spherical-Prismatic-Universal (SPU) joint configuration form the Gough-Stewart platform. These joints were selected for the Gough-Stewart platform as the lengths of the limbs control the position and orientation of the platform. More precisely, by extending and contracting each strut, the platform is brought to the desired positions; this represents that the P-joint is active while the U and S- joints are passive. Furthermore, PKMs consist of iterated components and their selection becomes critical, as these element dictate crucial characteristic of the static and dynamic behaviour of the PKMs. For these reasons, a summary of the joints used in PKM is presented.

The advantages of using spherical joints is their capability to allow the relative rotation between the platforms and the limbs, as 3-DoF are permitted (all being rotations). However, to prevent the twist of the struts, spherical joints are usually paired with universal joints (Figure 2-1). A universal joint is considered as a pair of revolute joints with each axis intersecting orthogonally. Therefore, universal joints possess 2-DoFs (rotational). Universal and spherical joints are, in the majority of designs considered as passive joints.



Figure 2-1. Ultra Motion GS- platform; Zoom of the spherical and universal joints on the Ultramotion GS platform [34].

Prismatic joints are probably the most extensively used joints in PKM, as most PKM control their orientation and position by changing the length of the struts. Prismatic joints restrict the axis of two mechanical components to become parallel and concentric, permitting the displacement along the coincident axis. Rotary motors often drive these prismatic joints, but transmissions are often needed to convert the rotary movement of the motor to linear displacement. These displacements can be indirectly measured with encoders on the rotary motors, or directly measure the positions and relative displacement on the prismatic joint.

Another approach to the use of prismatic joints is the use of linear stages. The use of linear stages has been reported in several PKMs designs. More importantly, the use of linear stages and other heavy components on fixed and rigid support bases assists the reduction of mass on the moving platform, increasing its performance on high dynamic applications [35] and contributing to expanding the workspace of PKMs. Furthermore, linear stages can support the PKM and constrain undesired movements,

as the heavy masses are utilised to diminish vibration and undesired displacements. However, this is limited to maintain the linear stages on the fixed base of the PKMs. Some successful applications are reported for several PKMs as the V100 [36], the Sprint Z3 and A3 [37], [38], as shown in Figure 2-2. Nevertheless, fixed rigid bases restraint portability and limit the use of PKMs in workshops and laboratories.

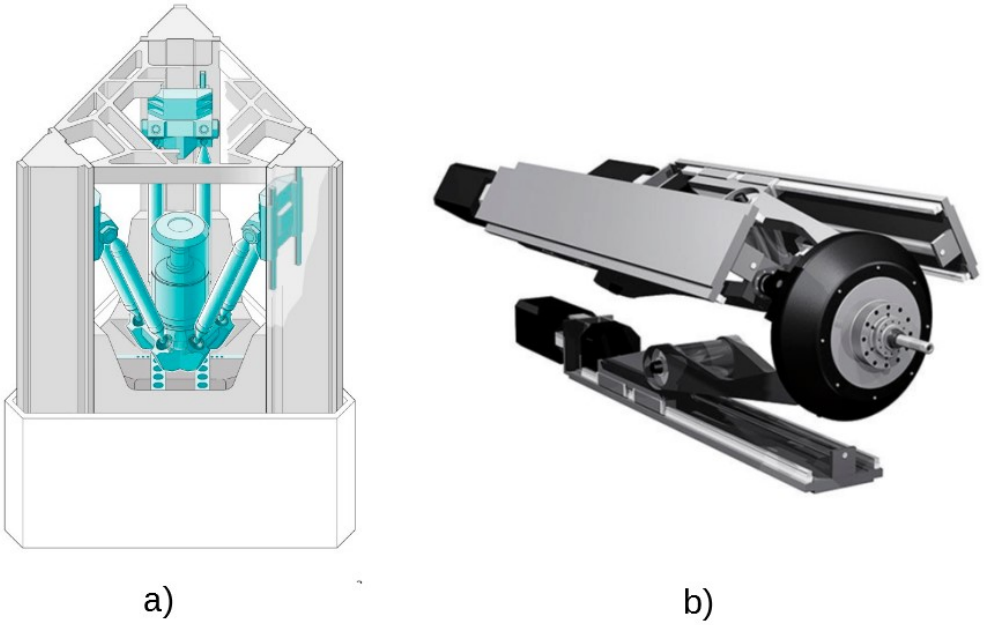


Figure 2-2. a) Invex V100 [IndexV100], b)Sprint Z3 [37].

Revolute joints conform to a single axis permitting the relative rotation of two bodies along a common axis. Similarly to prismatic joints, revolute joints can be passive or active. The active revolute joints are commonly known as rotary actuators. Those are driven mainly by electrical motors in robotic applications (i.e. direct current, stepper motors, alternating current motors, and servos) [39]. Although, rotary actuators are mainly present in Delta PKMs, which are mostly used for pick-and-place applications in electronics, the food industry and others. Delta PKMs have seen their extensive thanks to their low moving masses, permitting them to achieve high speeds and accelerations [40]. The rotary actuators are placed on the static base to reduce the moving masses (as shown in Figure 2-3) of the system and deliver excellent

dynamic performance of the system [41]. This consideration also connects to the reduced torques produced by rotary actuators but very high speeds of operation.

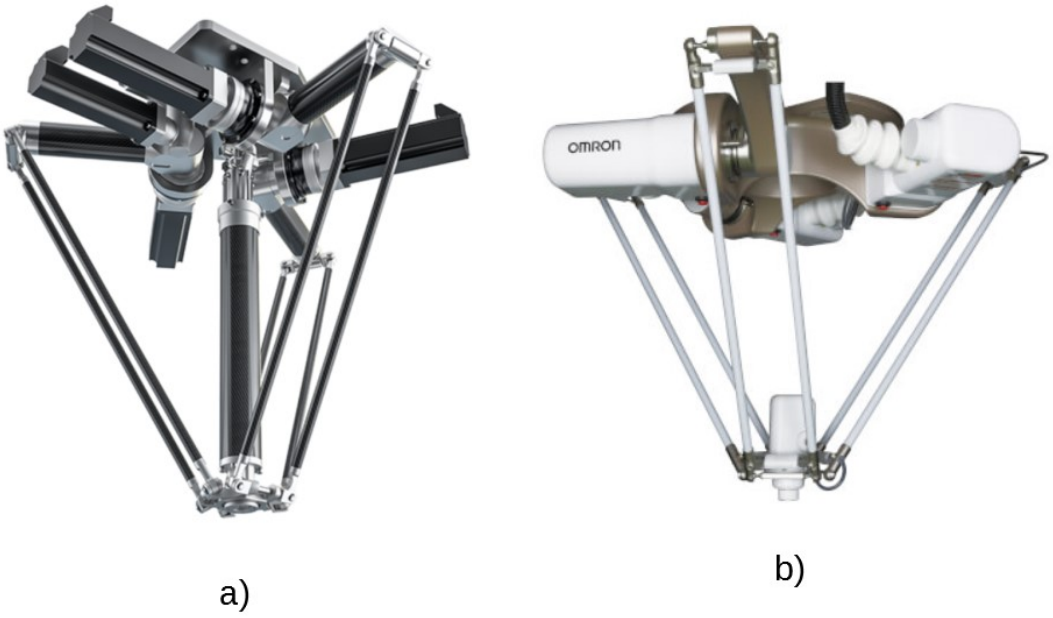


Figure 2-3. Delta robot DR [42]; b) X Delta 3+1 [43].

More importantly, an adequate selection of the joints is targeted to provide a means to constrain undesired displacements and reduce the effects created by rapid movements of PKMs. In this regard, designers have considered the use of heavy components only for fixed components (foundations elements) while maintaining the moving components as light as possible. Furthermore, another aspect controlling undesired displacement is related to the existence of singular configurations in the workspace. These conditions are connected to the constraints provided by the joints and the geometrical poses reached by the PKMs.

2.3.2 Singularities of PKMs

Singularities are poses where a PKM gains or loses one or more DoF; in PKMs these are classified into two groups:

Type I- refers to a pose that the end-effector is incapable of reaching, requiring an infinite actuation of its joints.

Type II- refers to a pose where the end-effector can not resist an external force, leading to a loss of control. Parallel singularities also represent a pose where the total stiffness of the PKM is null, leading to steep increments in the forces exerted on the joints.

Furthermore, singularities represent dangerous conditions that can damage PKMs and, as such, must be avoided. One of the conventional approaches for locating unstable zones relies on the identification of the singularity locus in the task space of a PKM. Then singularity avoidance methodologies can be applied to operate the PKMs safely. Some of these methodologies limit the workspace to zones without singularities affecting the full usable workspace of PKMs. Garcia and Campos [44] proposed to find the safe reachable workspace by utilising standard kinematic analysis combined with the screw theory. This method considered the geometrical limitations and the singular free task space. However, they simplified the safe region to be the geometry of a sphere and neglected other regions of the reachable workspace, meaning that some of the useful space of the PKM is lost. Other researchers have presented methodologies to optimise the identification of singularities using visual approaches, such as the one presented in [45], which proposed a graphical approach to simplify a series of rules based on screw theory for 2 DoF mechanisms. Although this methodology identifies the singularities of a defined configuration, it cannot suggest a configuration free of singularities (avoidance algorithm). One solution for this problem could be the iteration of

random configurations until an optimised reconfiguration for the mechanisms is found. Nevertheless, proposing several configurations without any clear strategy would result in disadvantage, especially for higher DoF mechanisms, as a high number of positions and orientations should be analysed.

Liu et al [46] presented an evolutionary methodology to identify the singular configurations in the workspace of a 6-DoF PKM; based on screw theory, a series of rules (collinearities and Jacobian determinant values) are proposed to identify unstable configurations. Later, an evolutionary strategy was used to search for the singularities in the workspace, based on extreme values of the proposed rules. The method proved to be efficient from the computational point of view. However, as the method only considered the analysis of the conventional PKMs (i.e. Gough-Stewart platform), no strategy to reduce the presence of singularities was proposed, and a random search of configurations would become the nullifier of its advantage. Similarly, [47] proposed a geometric methodology based on screw theory to identify singular configurations. This methodology proposed two rules that could be simplified as the existence of two lines intersecting 4 struts of the PKM under analysis. More importantly these rules were proved against setups known to be singular. However, the foundations of the methodology is left as an open conjecture for all singular conditions and as a topic of future research.

Although several researchers have focused on the singularity analysis for PKMs, the complication for reconfigurable parallel kinematic manipulators is that it requires, to perform the workspace analysis, identify singularities and optimise its final configuration efficiently before any operation, representing an intelligent and highly adaptive machining tool requiring intensive computational resources for its safe operation. Therefore, it is concluded that an efficient approach for singularity and

workspace analysis of RPKM is critical when the system must adapt (i.e. optimise its kinematic morphology) to compensate its performance in non-conventional places of intervention (e.g. power plants, hazardous industrial environments, large aerospace components, etc.).

2.4 Review of Walking Robots

For a long time, humankind has found inspiration in nature to develop solutions that facilitate and improve life. These inspirations go from the creation of tools to more efficient and rapid methods of transport. Often this inspiration has found its roots in animals, more precisely, mammals and insect have served to inspire researchers for their ability to adapt and traverse irregular terrains. More importantly, new designs of mechanisms aim to build intelligent robotic systems to replace human intervention in dangerous and complicated environments.

Walking robots attend to fulfil these aims and as such several multi-legged systems have been proposed. One of the most critical characteristics of walking robots is the redundancy in their legs, which directly relates to stability and displacement speeds. When describing walking robots, two significant classifications can be considered: statically stable robots and dynamically stable robots. Statically stable robots consider low displacement speeds, and as such neglect, the effects of inertial forces when performing its gaits; dynamically stable robots consider rapid displacements and must ponder the effects of inertial forces when conducting its gaits. However, in both cases, the redundancy in the number of limbs used for the gaits is a common approach. Nevertheless, a precise selection of the design and number of limbs must be considered when a new walking robot is proposed.

These efforts can be seen in projects such as BigDog and Cheetah 3 from MIT [48], [49]. These robots base the advantages of their walking in their optimal design but even more in their control algorithms, capable to adapt to complicated terrains and traverse them safely. Nevertheless, these advanced robots only mention some possible task that could be performed by adding additional extremities to be used as positioners, but no formal task is presented. However, these efforts are focused on replicate complicated movements and performances seen in nature, but complicated task involving missions related to industrial robots are still to be developed.

To present to the reader further insight into the development of the walking robots and to identify the possible research gaps in these developments this section presents a compilation of the walking robots that have contributed to creating a more profound knowledge of walking machines.

2.4.1 Early Implementations

In 1966 Bob McGhee and A. Frank [50, 51], presented the first computer-based control implementation of a quadruped robot, known as Phony Pony. Although Phony Pony presented limited mobility, its control strategy proposed two sequential states for the actuation of the limbs in a walking robot: supporting the robot on the ground or swinging in the air. This synthesis later settled the basis for future studies related to control and stability of walking robots. Later in 1969, R. Mosher [52] aware of the limitations of the computing power and the complications involved for the analysis and control of walking robots introduced the design of a quadruped maned vehicle called the "walking truck". This concept took advantage of the judgement, and psychomotor capabilities of a man controlled vehicle (walking truck) to enhance characteristics such as force and load capacity when compared to other concepts. However, relying on an operator to evaluate and perform all the

movements of the walking truck resulted as an exhausting task for the operator. Other approaches, such as the KUMO [53] proposed to reduce the complication of walking robots at the time (number of components required and sequences), and as such, they proposed a simplified design where each of the four legs was actuated by a single motor and a clutch mechanism. This strategy later proved to be inefficient in terms of energy consumption, as the design would dissipate the actuation energy as heat [53]. Simultaneously in 1976, Masha et al. developed a tubular hexapod with 3-DoF limbs capable of sensing and displacing over-complicated terrain (soft soil) [54, 55], settling the ground for more complicated control theories. Further, in 1977, McGhee and Gofrey [56] developed the Ohio State University hexapod, capable of sensing the terrain to be traversed and modify its gait where unsuitable placements were required. The concepts developed by the implementation of this robot generated opened the doors of topics such as compliance with the terrain. However, when the terrain became too complicated, the system would become deadlock; to prevent this situation a preselection of the path to traverse was required. In 1978 the PV-II [53, 57] became the first walking robot capable of climbing stairs thanks to a pair of sensors in the toes, which provided feedback on the contact and attitude of the limbs. Furthermore, its design evolved from the KUMO, focusing on the reduction of the energy necessary to operate its gaits thanks to a gravitational decoupled actuation system.

Later in 1983, Sutherland and Raibert [58, 59] constructed a hexapod to be the first walking robot to integrate a human operator and a computer-based controller interface. This computer-based controller effectuated the safe gaits in terms of static stability criteria, evaluated and performed a better distribution of the load on the

limbs to actuate them within the operational safe ranges to reduce the operational burden of the operator. Nevertheless, the operator would always be in control of the crawling direction and the attitude of the hexapod. Following the development of walking robots by the Tokyo Institute of Technology, the TITAN III [53] presented a novel design. It incorporated the use of composite materials and shape memory alloys as actuators and sensing contact devices. More importantly, not only the integration of these new materials helped to reduce the total weight of the system but also created an intelligent system, combining the use of novel materials, posture sensors and a unique control system for adaptive static walking [53, 60]. Keneth and Waldron [61] followed a similar approach with the Adaptive Suspension Vehicle, which also combined several microprocessors and sensing systems to evaluate and effectuate the low-level control and a human operator to drive the system. These sensing systems supposed a novel approach in its time, and included a scanner of the terrain that combined the control algorithms and vehicle to generate the appropriated gaits.

Other design of walking machines considered the advantage of autonomy to replace human operators in hard to reach zones or hazardous environments. As such, in 1985, the AQUAROBOT prototype performed inspection operations of structures under-water (at 50m depth) and flatness measurements of rock foundations [62]. For these purposes, the AQUAROBOT had a camera mounted in one additional manipulator which combined an ultrasonic measurement system and a transponder system as a navigation device, proving the value of robotic systems with the same accuracy as a human diver.

By 1987 researchers had focused not only on static gaits but started to explore the dynamic gaits. Raibert's quadruped [63] proposed to couple the legs in his design to

propose three dynamically stable gaits, and with this forbidding its application for static stable gaits. Although the actuation of the limbs lacked accuracy, it was able to perform fast enough for dynamic applications. Later, TURTLE I [64] proposed a design to perform straight-line displacements by using two actuators per limb. By the use of a microcomputer, TURTLE I achieved static stable and quasi-dynamic gaits but its limbs design had a small workspace and limited more complicated movements, such as rotations and avoidance of obstacles. Other approaches proposed to reduce the weight of robots while maintaining their autonomous capabilities. Angle and Brooks proposed a robot called Attila [65]; their idea relied on the creation of a robotic system capable of operating autonomously without previous knowledge of the terrain to traverse, as it was intended for planetary exploration. Attila was composed of 24 actuators, 150 sensors, batteries capable of operating the system for 30 minutes and several solar cells to recharge it, with a total weight of 1.6 kg. This design was completely contra posed by Mecant I [66] with a total weight of 1050 kg. The Mecant I was a hydraulic-six-legged walking robot relaying on a combustion engine to provide the required energy to operate autonomously in outdoor, mainly to adapt to operations in forestall locations. Its main characteristic came from the modular design between the integration of software and hardware to produce stable gaits on natural terrain combined with different modes of operation to enhance the machine performance. Certainly, the 90s marked the path to more intelligent robotic systems, and by 1995 Ilg and Berns [67] presented the first walking robot to optimise its gait based on Reinforcement Learning, this robot was called LAURON and served more as a testbed for these control algorithms rather than an improvement to the mechanical components of the walking robots. Similarly, the second generation of LAURON (LAURON II [68]),

presented an optimised structure, which used aluminium and included several more sensors, resulting in a total weight of 20 kg. As with its predecessor the LAURON II served as a testbed for advanced learning techniques.

NINJA I and II [69, 70], on the other hand, focused on improving the mechanical design to create a wall-climbing robot. To achieve these objectives, Hirose et al. proposed a lightweight actuation mechanism (presented in Figure 2-4) with high force capabilities based on a parallel mechanism and combined with feet capable of creating high suction forces (1500 N per leg) for each limb, which also provided the required 3-DoF for climbing walls.

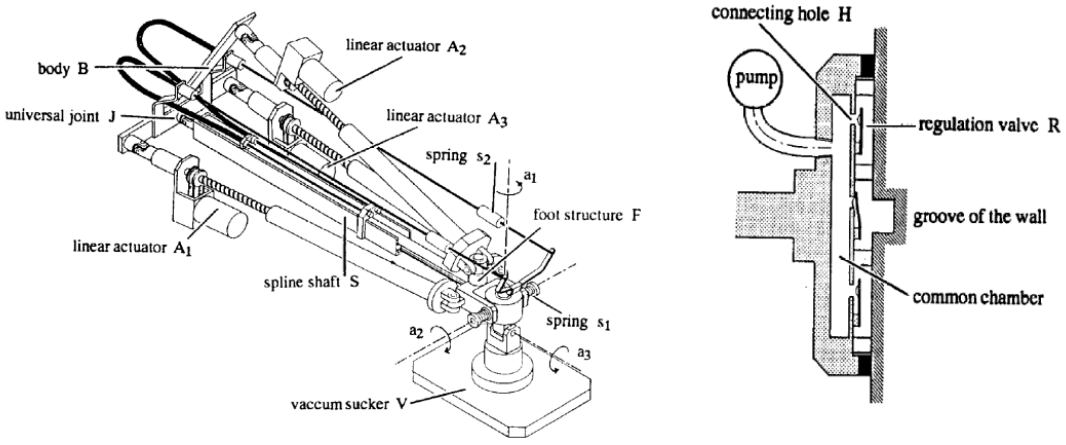


Figure 2-4. The actuation mechanism of NINJA I.

Similarly, the SHERPA (hexapod robotised system for nuclear applications, by its French acronym) [71] was conceived to operate in dangerous zones for human intervention. Its design relied on an axis-symmetrical and six-legged configuration. The use of ball screws on the legs allowed it to increase the operational length of the legs and to operate in nuclear facilities, traversing over stairs and inclined terrains with payloads up to 300 kg. More importantly, the system relied on a series of cameras and a manipulator, which allowed remote inspection of hazardous areas. Following the success of its predecessors, the TITAN VIII [72]presented a new design approach based on an insect configuration, which considered a device capable

of being accessed by several researchers. The main target with these assumptions was to reduce the price and the complexity of the operations. For it, Arikowa and Hirose focused on the design of the limbs for the TITAN VIII, which relied on actuation by wires, eliminating complicated mechanical components, such as ball-screws and linear guides.

By 1997, Nelson et al. [73, 74] presented an innovative design based on the insect "Blaberuss" as this insect is capable of achieving rapid speeds and climbing over different terrains. Their design was based on pneumatically actuated legs to represent the movements similar to those produced by muscles. In 1998 Mena et al. Presented the REST climbing robot [75, 76], which was designed to transport heavy loads (up to 100 kg) on ferromagnetic surfaces. Furthermore, the development of this robot supposed new gaits to perform the climbing of vertical walls, for which the authors proposed a new gait called sawing gait. This gait consisted of a four-phase discontinuous gait which also considered the optimisation on the forces exerted on each limb to improve energy consumption. The development of the LAURON III (Figure 2-5) arrived in 1999 and with it a new perspective from its designers [77, 78]. This time they moved from the reinforced learning techniques and focused on the creation of a testbed for reactive systems in rough terrains, such as those found in mountainous terrains. However, the walking speeds saw an negative impact; the robot made the walking analysis based on a reactive architecture from the inputs encountered by its sensors, and as such required to walk at a slow phase. The authors also reported some issues with the legs of the robot slippering on inclined grounds. However, the system was reported to be used with the integration of different systems for the sensing of its environment and different control strategies, such as a

hierarchical control where different layers of the gait analysis are pondered to produce a stable traverse on rough terrains.

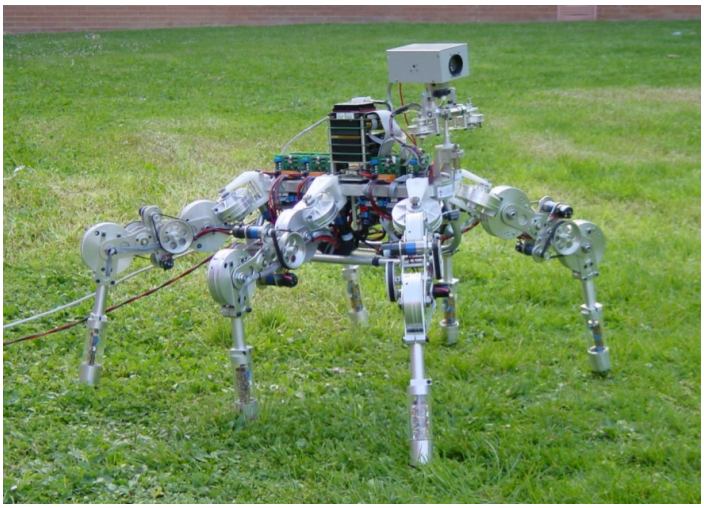


Figure 2-5. LAURON III

2.4.2 Mature Solutions

By the end of the 90s and beginning of 2000, walking robots achieved a good level of maturity, and several applications started to emerge. An example is seen in the ROWER [79], a walking robot developed for welding in the shipbuilding industry, capable of using its legs to lock between the ground and floor of the ships and increase its stiffness. Similarly, the LEMUR I, consider its application for inspection, maintenance and repair of orbital installations [80]. To comply with these requirements, the LEMUR I (shown in Figure 2-6)had an insect configuration with six legs aligned in two rows. Furthermore, its design focused on the simplicity of mechanisms of actuation to reduce its total weight. However simple the design accomplished to be, its design also helped to achieve complicated postures and task, as it was capable of achieving 4-DoF per limb and attach different tools.

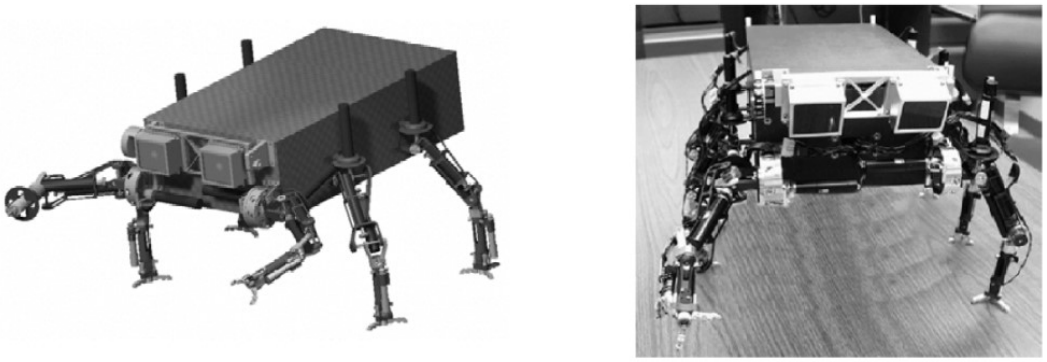


Figure 2-6. LEMUR [80]I.

Similarly to LEMUR I, the TITAN IX proposed a robot to reduce the risk of human intervention in dangerous environments[81], in this case, a landmine detection robot. TITAN IX was capable of displacing over rough terrains and use its legs as manipulators for demining operations of the terrain, and as such considered a system to store and provide a different tool in its main body. Furthermore, it also considered possible damage to the limbs, for which the design considered long legs to prevent damage to the main body.

2.4.3 The Current Trend in Walking Machines

In 2005, BigDog was developed by Boston Dynamics, to be the most advanced hydraulic robot; composed of several systems working together to provide the power, actuation, sensing and communications (i.e. internal combustion engine, hydraulic pressure system and actuators and 50 sensors)[48]. The advantages of BigDog came from its capability to adapt to rough terrain and rapidly react to external perturbations. Later by 2011, Boston Dynamics presented the LittleDog, intended for rapid research of rough terrain legged locomotion [82]. The novelty of this design lays on the capacity to rapidly gain knowledge and improve locomotion

technology, as it provided a common platform for research. Later in 2014 came the Cheetah, a quadruped capable achieve speeds of 6 m/s which based its design in the motion capabilities of a Cheetah with a total weight of 32 kg [83]. More importantly, the knowledge gained during the development of these robots gave origin to towards high-performance systems that mimic applications found in nature inspiring the creation of more advanced robots that can traverse and operate over very complicated terrains and perturbations [49, 84]. These developments have served to inspire researchers to develop more sophisticated walking robots. Furthermore, sectors with interest on walking robots require benefits in operations (e.g. inspection, machining, repair, etc.) apart from the already complicated task of locomotion.

2.5 Review of Walking Machine Tools

In terms of operational capabilities, Parallel Kinematic Machines (PKMs) have attracted the attention of researchers, as PKMs are well known for their performance on accuracy, stiffness and dynamic performance. Furthermore, PKMs naturally consider the redundancy of actuators, and as such, these machines could be exploited as legged robots capable of traversing over several environments and surfaces. Additionally, if the legs layouts can reconfigure, the PKMs could adapt to irregularities of the terrain as other robotic systems do. Further, this capacity to place their legs over complex surfaces provides an advantage to constrain and relocate the feet on unprepared environments for other activities than walking (i.e. repair and inspection tasks).

PKMs have also proved their capability as walking machines, specially in environments with hazardous conditions representing a risk for human intervention (e.g. nuclear industry). Such as in the case of Saltaren et al.[85] that presented the

design of a modified Gough-Stewart platform as a climbing robot for the nuclear industry. The proposed PKM in [85] based its configuration on a kinematic and singularity analysis to ensure its claiming capabilities, although no other task is reported (i.e. inspection, machining, etc.).

Similarly, [86] reported a 6-DoF PKM and walking machine named REMORA for manufacturing applications. REMORA consisted of four limbs, each comprising two actuators, and a specially prepared surface (base with clamping pins). More importantly, [86] presented the kinematic models that allowed the system to exploit its redundancy to alternate between support phases and swinging phases. However, the system required a series of locking pins on the ground, essential to provide stability to the robot, forbidding its use in common industrial sites/environments. More importantly, the need of pins on the ground represents one of the main disadvantages of the system, not only as the environment must be specially designed for REMORA but as it results forbidding to other equipment (i.e. pneumatic wheeled vehicles) and for human intervention, as locating pins could represent a hazard when walking. Later the WalkingHex was proposed [33, 87] to be a PKM capable of walking autonomously and performing machining operations, considering automatic calibration and auto-referencing against critical features in the intervention site. Although the WalkingHex proved to be an autonomous walking PKM and perform precise operations with its end-effector (e.g. milling/drilling/tapping), the authors did not consider the existence of unstable configurations inside the workspace and with this the need to readapt to the intervention task.

Nevertheless, PKMs have not been fully exploited in their potential, mainly by the complicated mechanical design and control compared to other designs (i.e. wheeled vehicles). The kinematics of legged robots are more complicated than those of

conventional PKMs (i.e. Gough-Stewart platform) as the number of mechanical components that must be controlled are significantly increased [88, 89]. More importantly, precise control of the limbs is required to interact effectively with the environment to traverse [90]. Further interactions with the ground, obstacles and the own components of the walking robot must be included in the analysis to prevent collisions and possible damages of the mechanical components. Nevertheless, these problems have inspired studies and projects focused on the gaits of multi-legged robots. However, idealisations have been included to simplify the problems to address. These idealisations go from reduced or no consideration between the frictional forces between feet and the ground, simplified orientations of the main body of the walking robot. Further, it is necessary to properly coordinate the gait configuration and sequences in different conditions (flat and low friction surfaces, inclined terrains, obstacle avoidance) to ensure a safe traverse. To address these complications, researchers have relied on nature-inspired configurations, proposing multi-legged robots with zoomorphic configurations (e.g. mammal, insect, reptiles). For instance, designers have considered mammal inspired walking robots (vertically configured legs) to transport heavy loads at optimal walking speeds [10]. Other designers have used insect inspired walking robots (e.g. hexapods) to traverse over complicated terrains as several limbs are in contact with the ground, and thus presenting higher stability margins. In this regard, the number of legs, distribution, and configuration play an important role in the performance of walking robots (e.g. speed, stability margins, actuation torques, etc.). However, this often represents a trade-off between the environment and the performance of walking robots, and fixed configuration walking robots may be affected in different environments.

Furthermore, a realistic kinematic model must consider the ground interaction, gait stability and power consumption.

Although the most significant walking robots and their contributions have been mentioned so far, to the author's consideration, these developments have based on a progressive and steady foundation of research over the years. Proposing different solutions to address the three main challenges of walking robots: stability, foot ground contact and energy consumption. In this regard, adaptive walking robots, more precisely RPKM represent a clear advantage against conventional walking robots, especially as terrain and applications often change even in the same environment. However, when adaptive configurations are taken into account, the analysis becomes more complicated as several conditions for safe operation must be accounted (i.e. stability analysis, possible impacts between components, location of the centre of mass, conditions of support, etc.).

2.5.1 Stability Analysis

Stability analysis is one of the fundamental principles to understand possible risks to walking robots. Further, it also represents the possibility of not complying with the task to be developed, as the system can become unstable. McGhee et al.[50] presented the first study of static stability criteria by considering the projection of the centre of mass to the support polygon, represented by the limbs in contact with the ground. Then the stability margins were described as the smallest distance to the sides of the support polygon. Min et al. [91] proposed a gait to maximise the stability margins with variations to the feet positioning and the maximum allowable strokes. Later Hirose et al. presented new stability criteria considering the normalised stability values[92], for which they considered the relative positions of the centre of

mass between the initial state and the highest position in the tumbling state. Finally using this criterion to propose the best possible gaits for a quadruped robot. Later Santos and Jimenez [93] considered the advantages of different gaits, mainly discontinuous and wave gaits. They defined the discontinuous as the gaits that alternate between support and placement of the feet and the wave gaits as a continuous process of support and displacement. More importantly, concluding the discontinuous gaits to perform better in terms of stability and energy consumption.

Wang et al. [94] pointed out the advantages of the two most common configurations of gaits for hexapods: the hexagonal (axis-symmetrical) and rectangular or insectoid (two rows of three legs) as shown in Figure 2-7. They concluded the benefits of insect configuration to consume less energy at the expense of decreased stability margins, while the hexagonal provides better performance for changing the walking direction. Concerning the insectoid configurations, its control becomes relatively straightforward as all the limbs are displacing in the same direction, but requires unique turning gaits. .However, Santos et al. [9] evaluated the design and location of the limbs of a hexapod to reduce the forces acting on each limb and concluded a hybrid design, which considers a semi-rectangular configuration with the centre limbs extended out of the corner limbs, although this conclusion needs to be proved on other architectures.

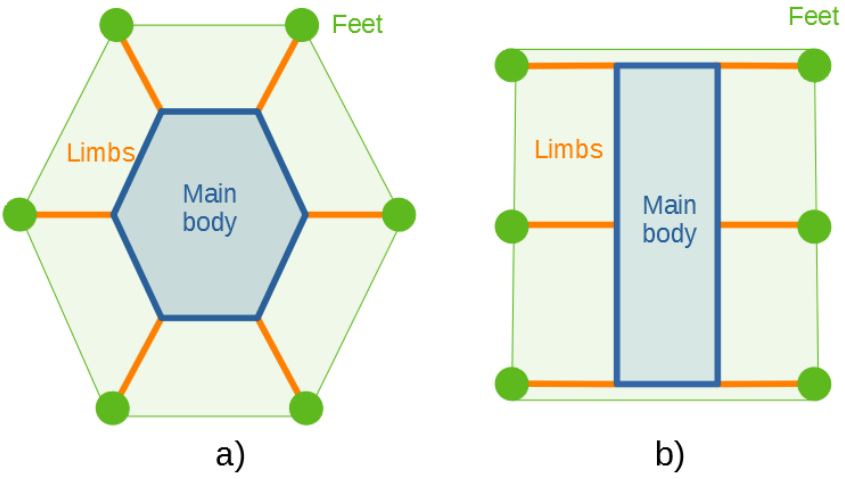


Figure 2-7. a) Hexagonal configuration; b) Insect configuration

2.5.2 Foot Ground Contact

The magnitude of the Contact Force- between the feet of the robot and the ground has a significant impact on the performance of the walking robots. Conditions of low friction can lead to slippage and even induce damage to the system. Therefore, the interaction between frictional forces of the ground is an essential part of the analysis of walking robots. However, most of the recent studies focus on two types of interactions [95]:

i) The contact between the ground and feet is modelled as a fixed contact (no slippage considered).

ii) The contact with the ground considers a normal reaction and two tangential forces (friction). Creating two possible alternatives: static friction conditions or dynamic friction conditions [96].

Furthermore, the interaction of the limbs must consider the required forces and torques on the actuators. Further, a very detailed model should consider interactions

of the limbs, such as impacts with the ground when transitioning between support and placement (swinging legs in the air). However, to prevent such a complicated interaction, the control and design must consider a precise positioning of the system. Requiring previous information of the terrain to be considered in the kinematic model. However, highly detailed friction interactions complicate the walking analysis and prevent a practical application. In contrast, a simplified model providing rapid feedback to gait stability would be advantageous.

2.6 Conclusions

The maintenance and manufacturing industry require agile and flexible tools to perform in-situ operations such as inspection and repair processes (i.e. drilling, milling). There are have been several efforts to comply with these demands. However, the proposed solutions often represent a trade-off between portability and performance. Parallel Kinematic Machines represent an opportunity to bridge the trade-off between performance and portability. However, conventional PKMs suffer from reduced workspaces and present complex behaviour with respect to stiffness and singularities. Furthermore, reconfigurable parallel kinematic machines represent a significant advantage to adapt to complex environments of intervention and even improving the benefits of conventional PKMs. Reconfigurable PKMs are considered to overcome these disadvantages and present the possibility of improved performance against the task to develop. However, novel designs and methodologies are required for their characterisations. As their performance is pose dependant, a metamorphic solutions represents a continuous challenge to trace and improve the performance of a reconfigurable PKM through its operational life.

Several walking machines exist with great capabilities to traverse complicated environments, but these are mainly focused on a good performance for walking. Some of these designs consider the possibility to perform other tasks than walking. However, few evaluated the development of highly specialised operations (i.e. drilling milling). PKM represent a possibility to create a walking machine capable of performing other tasks than traversing environments. More importantly, most of the work developed for walking robots relies on nature-inspired mechanism (mammals and insect configurations) with fixed configurations. Currently, most of walking robots are based on fixed configurations, which normally represent a trade-off between the environment and walking performance, and may be affected in different environments. However, adaptive walking robots, thanks to the reconfigurable capabilities in either the leg mechanism or entire configuration, represent a clear advantage against the conventional walking robots when the terrain or applications vary. However, not much work has been developed to exploit metamorphic configurations, taking advantages in multiple terrain conditions and tasks. Furthermore, sectors with interest on walking robots require added values in operations (e.g. inspection, machining, repair, etc.) apart from the already complicated task of locomotion. In both cases, a Reconfigurable Parallel Kinematic Manipulator capable of optimising on different terrains (e.g. inclined, uneven ground) and tasks (e.g. drilling, milling, etc.) could bridge the present limitations of walking machine tools.

Therefore, to the authors best knowledge there exist an opportunity to develop a Reconfigurable Parallel Kinematic Manipulator capable of optimising its performance according to locomotion and manufacturing/repair operations. However, this means that several challenges must be overcome.

2.7 Challenges

From researching state of the art in the fields of maintenance, PKMs and walking robotic systems, the following objectives have been identified:

1. To propose a reconfigurable PKM capable of modifying its kinematical configuration with respect to machining and walking operations. Furthermore, this design must consider the reconfigurations mechanisms to be light-weighted to comply with good dynamic and static performances.
2. To develop the kinematical models that describe a highly configurable PKM for machining and walking through its operational life cycle. In a reconfigurable system such as the one proposed in this thesis, the evaluation of the reachable workspace, collision avoidance and singularity analysis must be performed prior any operation to ensure the safe operation of the RPKM. Furthermore, these models must have the capability to operate several tool such as milling and drilling tools, and operate those in 6 DoF conditions. This represents a system able to perform highly complex machining operations for repair and maintenance. Similarly, the kinematic models must be able to allow different configurations to operate in a variety of terrains.
3. To develop the optimisation methodologies for proposing improved configurations for machining and walking. Similarly, the proposed methodologies must be able to propose optimised configurations for increasing the capabilities of the system, such as proposing new

configurations free of singularities, increased workspace and increased stiffness. However, the methodologies proposed must be able to provide a clear path to select the optimal gaits for different terrain and load conditions.

Chapter 3 **Concepts of Reconfigurable Parallel Kinematic Manipulators**

Parallel Kinematic Machines have demonstrated their capabilities in different sectors such as milling/drilling machines, flight simulators, radio telescopes and medical devices. Furthermore, these machines have demonstrated their capabilities for applications where critical precision is required. However, its broader application in the industry has been limited due to some disadvantages present in current designs. In this chapter, the disadvantages of the existing PKMs are introduced. Furthermore, several designs of PKMs are introduced to reduce the disadvantages of conventional PKMs.

3.1 **Disadvantages and challenges of the existing Parallel Kinematic Machines**

Conventional Parallel kinematic Machines consist of a moving platform (where the end-effector is usually placed) connected to a fixed platform by several actuators; these actuators provide the positioning of the moving platform and give the stiffness for the moving platform. The actuators are connected to the moving platform and fixed platform by means of spherical and universal joints, and as a result, its elements are allowed to work only under compressive and tensing loads. Nevertheless, the positions of the joints on the moving and fixed platforms are fixed, and thus their workspace is well defined during its operational life. However, this type of design results in a small workspace compared to serial manipulators. Furthermore, the presence of singularities in the workspace further reduces the

functional workspace as the total stiffness of the system becomes null in specific regions, and to prevent it these locations are discarded.

3.1.1. Limited workspace

The orientations and reachable positions for the moving platform are constrained by the geometrical limitations of the actuators and joints (spherical or universal) and possible collisions between the elements of the PKMs. In conventional PKMs the positions of the joints are fixed in the moving and fixed platform, resulting in a small workspace. However, repositioning the location of the joints on the moving platform could enhance the operational workspace reducing possible collisions and improving the response to joint limits and strokes of the actuators. Furthermore, removing the fixed platform would allow the modification of the workspace and further enhance the adaptability of PKMs on unprepared environments for in-situ repair and machining as proved by Allen et al [8]. However, these reconfiguration capabilities present the challenge of the evaluation of the workspace for safe operation. This means that the workspace must be evaluated prior to any task to prevent the operation of PKMs in conditions that may damage the components (exceed operational limits) or lead to an impact between the components of the PKM. The workspace must be evaluated prior to any operation, but it must be done efficiently to reduce analysis times.

In this chapter, several concepts are presented to increase the adaptability and increase the workspace of PKMs, considering the repositioning of the joints on the moving platform and considering the lower joints free of a fixed base.

3.2 **Singularities on the workspace**

As defined by Merlet, a singularity is a condition where the PKM can gain or lose one or more degrees of freedom, resulting in a loss of control of the PKM. This type of instabilities must be traced before any operation and must be avoided to prevent the loss of control and even damage to the PKMs. In terms of theoretical study, the identification of singularities is of critical importance for the functionality of the PKMs as the performance is affected and can lead to damage. Amine et al. [97] mentioned that a singularity is a pose when the PKM losses or gains one DoF. To avoid this instability, it is necessary to obtain the distribution of the singularity locus in the task space of a PKM and then, further explore singularity avoidance[98]. A new method was proposed in [44] to find the safe reachable workspace by utilising standard kinematic analysis and the screw theory. This method considered the geometrical limitations and the singular free task space. However, they simplified the safe region to be the geometry of a sphere and neglected other regions of the reachable workspace, meaning that some of the useful space of the PKM is lost. Other researches have presented methodologies to optimise the identification of singularities such as the one presented in [45], which proposed a graphical approach to simplify a series of rules based on screw theory for 2 DoF mechanisms. However, the methodology is not able to propose an optimised reconfiguration for the mechanisms while being able to analyse for singularities of existing configurations. Nevertheless, proposing several iterations of the configuration would result in disadvantage, especially for higher DoF mechanisms, as a high number of positions and orientations should be analysed. Other authors [46] presented a methodology to extract the singular configurations in the workspace of a 6-UCU PKM. Based on screw theory, a series of rules (collinearities and Jacobian determinant values) have

proposed to identify unstable configurations in [46]. Later, an evolutionary strategy was used to search for the singularities in the workspace, based on extreme values of the proposed rules. The method proved to be efficient from computational point of view, but as it was intended to analyse the conventional PKMs, no strategy to reduce the presence of singularities is proposed, and a random search of configurations would become the nullifier of its advantage. Further, based on the Kennedy theorem a methodology was proposed in [47], where a series of geometrical relations are used to define rules for the identification of singular conditions, this rules are proved against setups known to be singular. However, one of the foundations of the methodology is left as an open conjecture and as a topic of future research. Although several researchers have focused on the singularity analysis for PKMs, the complication for an reconfigurable parallel kinematic manipulators is that it requires, to perform the workspace analysis, identify singularities and optimise efficiently its final configuration prior to operation, representing an intelligent and highly adaptive machining tool. It can be found that an efficient approach for singularity and workspace analysis of RPKM is critical when the system must adapt (i.e. optimise its kinematic morphology) to compensate its performance in non-conventional places of intervention (e.g power plants, hazardous industrial environments, large aerospace components, etc).

However, these approaches result useful for conventional PKMs as their workspace remains unaltered during their operational life cycle. Nevertheless, for reconfigurable PKMs these approaches result time consuming and even unfeasible as several configurations must be analysed prior to operation. This is related as each position of the workspace must be analysed considering different approaching angles (azimuth and elevation).

The complication of singularities not only relies on mechanical systems capable of avoiding these instabilities but efficient methodologies capable of predicting these phenomena and proposing new configurations to achieve the desired task. More importantly, the combination of innovative PKMs combined with efficient algorithms for the identification and prevention of these undesired effects could further increase the application and flexibility into more industrial applications. To overcome these disadvantages the work of this thesis proposes a new methodology based on the Fourier Analysis. This methodology is capable to identify configurations with singularities present and is as capable to propose new configurations free of singularities, enabling the operation of the RPKM to complete the desired task.

3.3 **Redundancy**

Part of the natural design of PKMs includes the redundancy of its actuators, which, as presented by Rushworth et al [99] can be used to provide self-displacement capabilities to these machines. Several authors have worked on multi-legged robots to negotiate on complicated terrains, basing their designs on nature-inspired systems. Some examples of these designs rely on systems such as CHeetha, Bigdog, ANYmal, among others. However, most of these systems have been designed with the only capability to traverse complicated environments but cannot perform precise operations such as machining or milling capabilities. Therefore, PKMs could use their redundancy to replicate the movements present in insect or multilegged animals. However, the capabilities required for negotiating over different terrains and conditions differ from those configurations required for machining operations. For this reason, to the authors best knowledge, a reconfigurable parallel kinematic

manipulator could bridge the gap between an efficient machine tool and an improved performance walking machine tool.

3.4 Conceptual designs for Reconfigurable Parallel Kinematic Manipulator

Since the RKM to be implemented must be capable of performing walking and machining operations, it is essential to consider different reconfigurable mechanisms that allow it to enhance its performance for both types of operation. This means improving their performance concerning workspace volume, singularity avoidance, collision prevention, walking stability, and displacement. To achieve these goals, the proposed family of RPKMs are proposed to consist of a virtual base (free positioning feet), an upper moving platform connected by a series of joint mechanisms to enable the repositioning of six identical Spherical-Prismatic-Spherical (SPS) limbs. It is worth noting that different from the existing ones, in the proposed family of RPKMs, not only the lower joints can be relocated, but also the upper ones can be adjusted on the moving platform, which can significantly improve the adaptability as an RPKM. Furthermore, thanks to the repositioning of the upper joints, the performance can be enhanced as the orientations of the limbs and joints can be improved to increase specific characteristics (e.g. the work volume and singularities) during the operations. This idea is based on the Jacobian of a PKM, more specifically of that of a hexapod, as the Jacobian relates the displacements of the actuators to those experienced by the end-effector. Modifying the positions with respect to the end-effector could significantly modify the characteristics of the proposed RPKMs.

To accomplish an enhanced PKM four concepts of RPKMs are presented with different mechanisms between the upper moving platform and SPS limbs to provide different conditions for the repositioning of the upper joints. The limbs considered

for the concepts proposed rely on the design presented by Rushworth et al. composed of an active-passive spherical joint. This design has been selected for the proposed reconfigurable PKMs by its highly adaptive qualities between the walking and machining operations. Furthermore, this design has now been thoroughly tested, and its novel characteristics have proved to bridge the gap for the implementation of novel mechanisms such as the WalkingHex. This design is presented as an SPS limb in the next chapters.

3.4.1. Concept 1

Concept 1 (Figure 3-1) configures a Revolute joint (R-joint) connecting the SPS limbs to the platform. This configuration allows 1-DoF mobility (rotation, i.e. red arrow) to rotate each upper S-joint by a constant radius around the rotation axis of the R-joint (i.e. red dashed line).

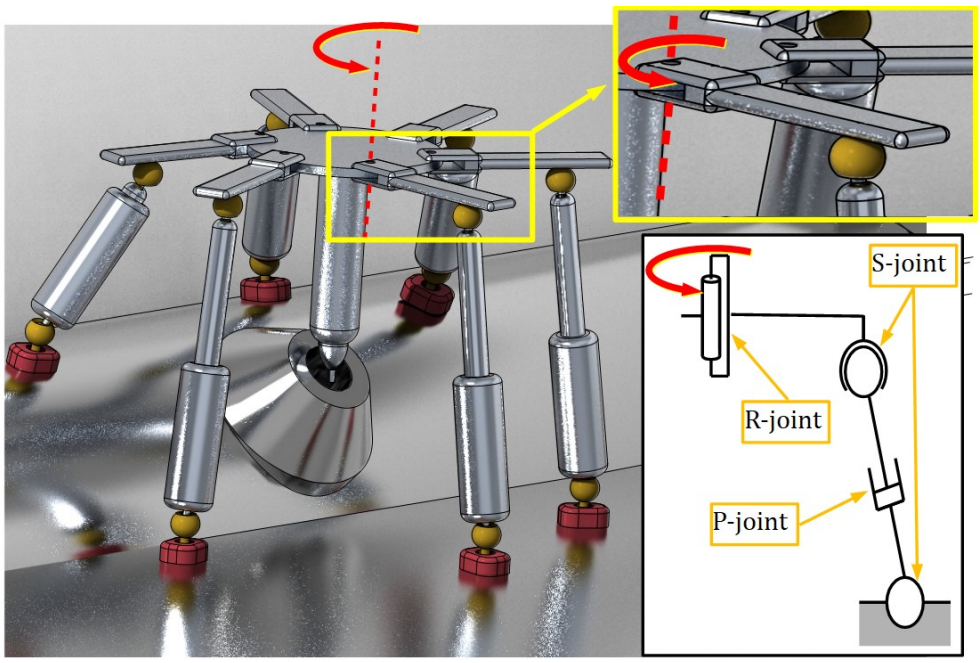


Figure 3-1. Illustration of Concept 1, configuring a revolute joint between the limbs and the moving platform.

This design permits repositioning the upper joints in configurations that are known mainly for their excellent performance in terms of stiffness, such as the Gough-Stewart configuration. Furthermore, this configuration allows adapting more symmetrical distribution of the upper joints and lower joints, which often is seen in nature to distribute the weight during the walking operations and prevent collisions between the limbs. However, when the environment presents non-flat surfaces (such as illustrated in Figure 3-1), the main factor limiting the workspace is the limb lengths and the spherical joint limits. This design could be affected by constraining the extension and contractions of the limbs and joints.

3.4.2. Concept 2

Concept 2 (Figure 3-2) configures a P-joint for each limb on the moving platform. The P-joint allows 1-DoF mobility (translation, i.e. green arrow) to displace each upper S-joint at a constant orientation linearly. This means that the radius of each joint can be modified concerning the centre of the moving platform.

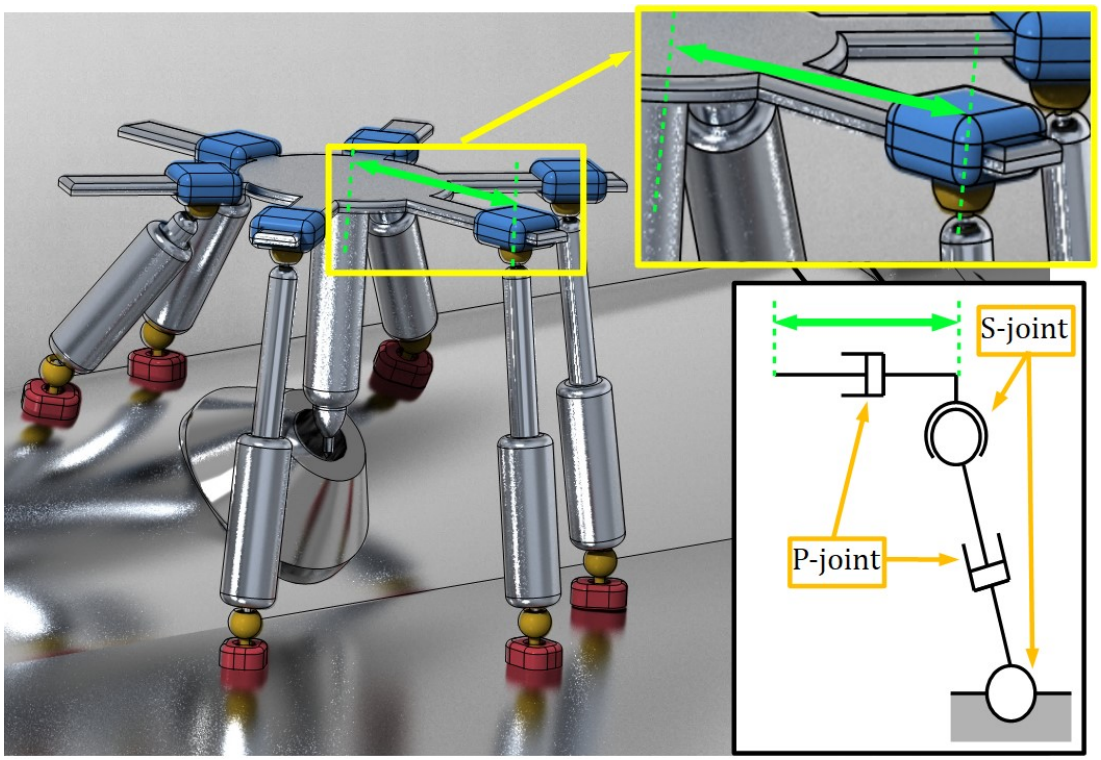


Figure 3-2. Illustration of concept 2, configuring a prismatic joint on the moving platform and each limb.

This concept intends to reduce the above limitations by displacing the location of the upper joints, along with a fixed radial orientation by using a prismatic joint. The idea relies on bringing the upper and lower joints to a reduced angle and thus improve the workspace by increasing the neutral positioning of the joints, as illustrated in Figure 3-2. However, similarly to concept 1, the main disadvantage is the limitation of the extension and contraction of the limbs.

3.4.3. Concept 3

Concept 3 (Figure 3-3) configures a Revolute Prismatic joint (RP-joint), which allows 2-DoF mobility (translation and rotation, i.e. red and green arrows). This allows rotating the S-joint around the axis of the R-joint (i.e. red dashed line) with a variable radius (i.e. green arrowed line).

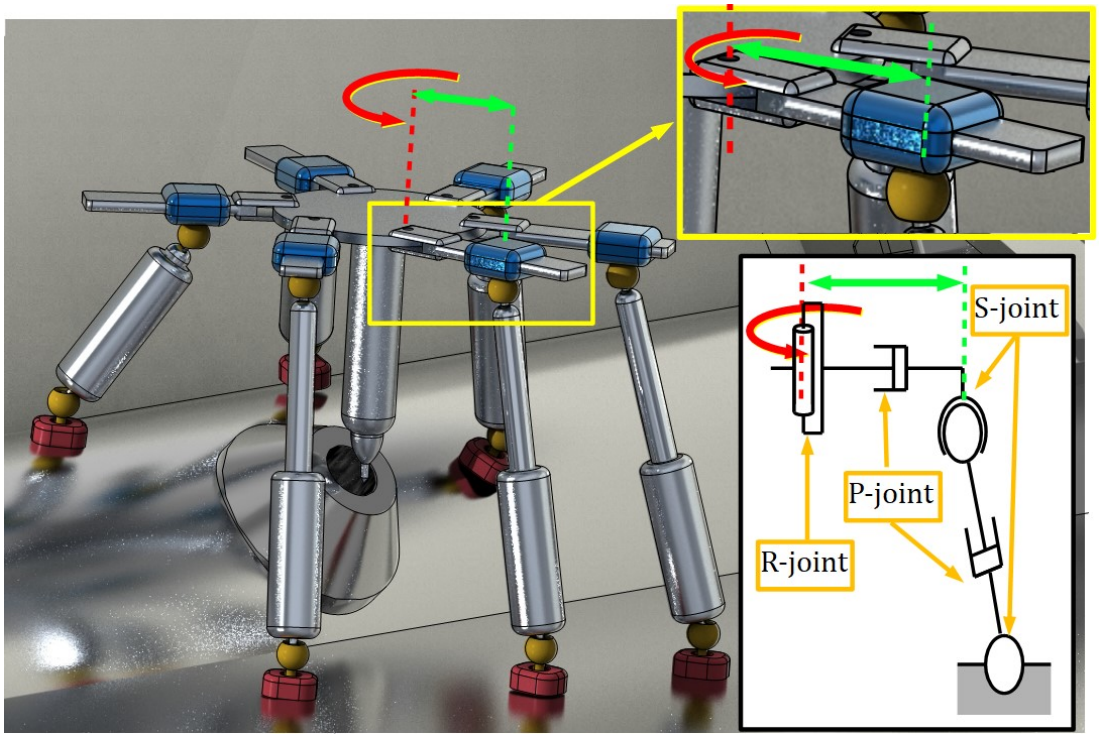


Figure 3-3. Illustration of Concept 3, configuring a revolute and a prismatic joint between the limbs and the moving platform.

This concept is targeted to combine the advantages presented by concepts 1 and 2. The capability to modify the orientations of the P-joints and modify the radial distance to the centre of the moving platform. However, the added complexity means an increase in the total weight of the RPKM proposed and an increment in cost and complexity to manufacture.

3.4.4. Concept 4

Concept 4 (Figure. 3-4) configures a Universal Prismatic joint (UP-joint), which allows 3-DoF mobility (rotation, rotation and translation, i.e. red and green arrows) to rotate and displace the S-joint around the axis of the U-joint (i.e. red dashed lines).

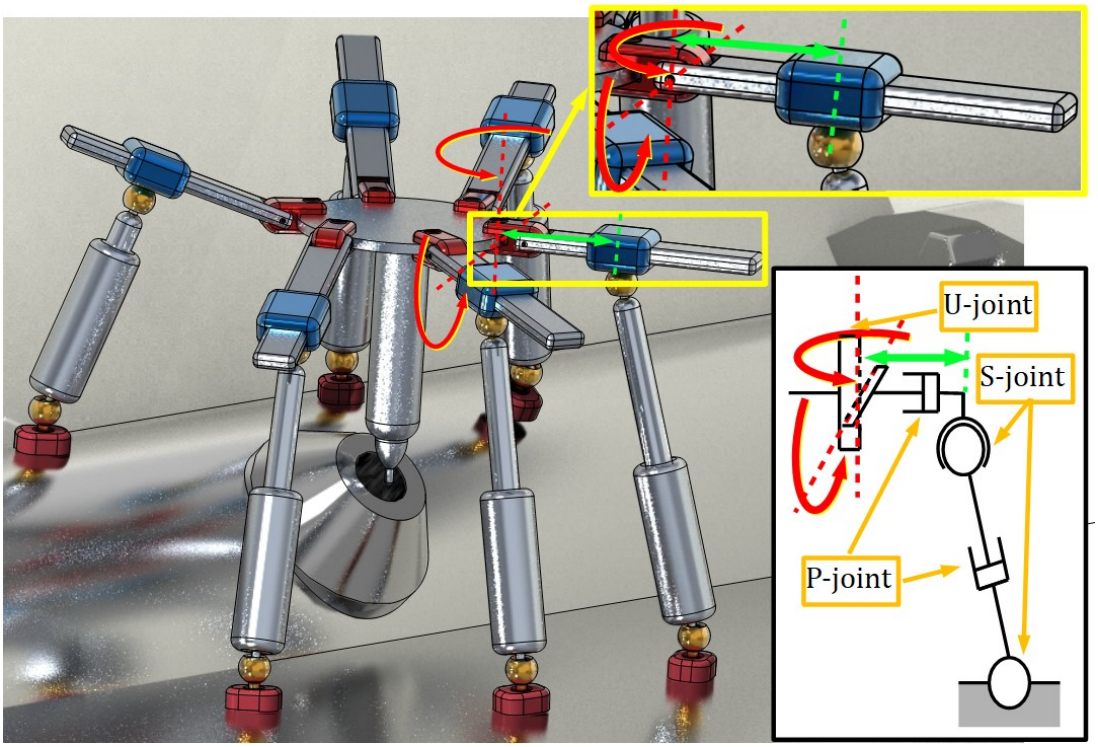


Figure. 3-4. Illustration of Concept 4, configuring a universal and a prismatic joint between the limbs and the moving platform.

Concept 4, intends to combine the capabilities of all the previous concepts, adding and adding a variable attitude of the limbs with respect to the moving platform. The idea behind this added DoF is to reduce the neutral angle of the upper spherical joints and, as such, increase the reachable workspace of the machine. More importantly, the added DoF would allow concept 4 to adapt more easily to uneven terrains, as the U-joints would allow a higher range of motion. However, similarly to concept 3, the added complexity of the RPKM has a drawback in terms of control, total weight and complexity of assemblies and cost of manufacture.

It is worth noticing that in all the proposed concepts, the lower S-joints or the feet, instead of being on a fixed base, can be placed at arbitrary positions. This capability enables the RPKMs to work as mobile 6-DoF machine tool suitable for uneven surfaces. Furthermore, it provides the ability to use the struts as limbs to perform as a walking machine. Nevertheless, these characteristics (i.e. the reconfigurable layout

of upper and lower S-joints) present the challenge of establishing the kinematic models of the proposed RPKMs for machining and walking operations. These last two conditions involve collision detection, intrinsic joint limitations and variable workspace. Additionally, singularities in the workspace must be identified and avoided to prevent the loss of control and even damage to the RPKM. Therefore, the inverse kinematics and workspace analyses of the proposed RPKMs are carried out in Chapter 4 for machining operations (considering singularity analysis and optimisation) and for walking operations in chapter 5.

3.5 Concept Summary

The comparison of the proposed concepts is presented in Table 3-1. The characteristics evaluated are the number of total joints and actuators required, the total weight of the actuators considering an average weight of possible motors commercially available. Furthermore, other characteristics are presented, such as redundancy for walking and machining. These terms refer to the minimal DoF required for the actuation of the

proposed RPKM against the total number of DoF. The total number of DoF considered for walking is regarded as the required DoF per strut to complete a full motion range to achieve a stable gait. The total DoF required per limb is regarded as 3 (two rotations and one displacement). The mass of the motors is considered based on commercially available motors, to which an average mass of 700 grams is considered. However, no other mass is considered for the other components of the reconfigurable components as this would involve several complications related to each design and even optimisations to reduce the weight. Nevertheless, the total

number of subassemblies is considered, as increasing the number of assemblies would increase the complexity of the design, and along with it, the total weight of the RPKMs.

Table 3-1. Mechanical characteristics of the family of reconfigurable PKMs proposed.

Characteristic	Conventional	Concept			
		1	2	3	4
Number of actuators required	24	30	30	36	42
Number of joints required	12	24	24	30	36
Total weight of motors (kg)	18	21	21	25.2	29.4
Degree of redundancy for walking	0	6	6	12	18
Degree of redundancy for machining	12	18	18	24	30
Number of subassemblies	14	20	20	26	26

3.6 **Reconfiguration concept selection**

Based on the previous summary and Table 3-1, Table 3-2 is presented. This table is introduced to make available a means to select between the different concepts previously proposed. This table also presents a means to select between the different characteristics for the final design of the RPKM proposed, as it assigns a value between one and four for each characteristic. The number four is assigned to the design presenting the fittest characteristic and a value of one to the worst performance. The main idea is to assign a quantitative value to each design.

Table 3-2. Concept summary

Characteristic	Conventional	Concept			
		1	2	3	4
Total weight of motors required	5	3	4	2	1
Complexity of control	5	4	4	3	1
Complexity of assembly	5	3	4	2	1
Complexity of design	5	3	4	2	1
Adaptability to complex environments	1	1	2	3	4
Cost	5	4	3	2	1
Total	26	**18**	**21**	**14**	**9**

From Table 3-2 is possible to see that the Concept 2 is scored as the fittest. Although its adaptability to complicated environments is not as high as Concept 4, the complexity of actuation and weight is highly reduced compared to Concept 4 (based on Table 3-1). Mainly this is related as the number of components and actuators are reduced. Furthermore, benefiting from the reduction of cost for its manufacture and assembly. More importantly, one of the main advantages of the PKMs is the low mass attached to the moving platform. Nevertheless, adding several motors and very complicated assemblies on the moving platform could have a negative impact on the good characteristics of PKMs (i.e. low inertia of the moving components). For this reason, even Concept 2 represents a challenge to overcome to reduce the total weight on the moving platform.

Concept 1 is the second-best scored design. Its main characteristics (total weight and complexity of control) are rated very similar to Concept 2. Nevertheless, Concept 3 merges the capabilities of Concept 1 and 2, with an increased penalty on weight and complexity. However, it is considered that Concept 2 can be merged with Concept 1 to achieve improved performance with a simplified design. The main idea is to optimise the orientation of the prismatic joints of Concept 2 in such a way that the workspace could be optimised to increase the adaptability of the proposed RPKM. Furthermore, even with the most simplified reconfigurable concept, several configurations could be adopted in other tasks such as walking, allowing the RPKM to implement forms such as those commonly found in nature. In this regard, the development of walking machines has relied on nature-inspired systems, such as those of mammals and reptiles, in the search for more efficient systems. For instance, designers have considered mammal inspired walking robots (vertically configured legs) to transport heavy loads at optimal walking speeds. Other designers have used insect-inspired configurations to traverse complicated terrains for their higher stability margins. In this regard, the number of legs, distribution, and layout plays an essential role in the performance of walking robots (e.g. speed, stability margins, actuation torques, etc.). In this regard, Concept 1 represents a clear advantage against conventional and fixed configurations PKM, especially as terrain and applications often change even in the same environment. For instance, Figure 3-5 presents tree configurations capable of passing over uneven terrain, confined spaces and inclined ground, taking advantage of the repositioning of the upper joint configuration.

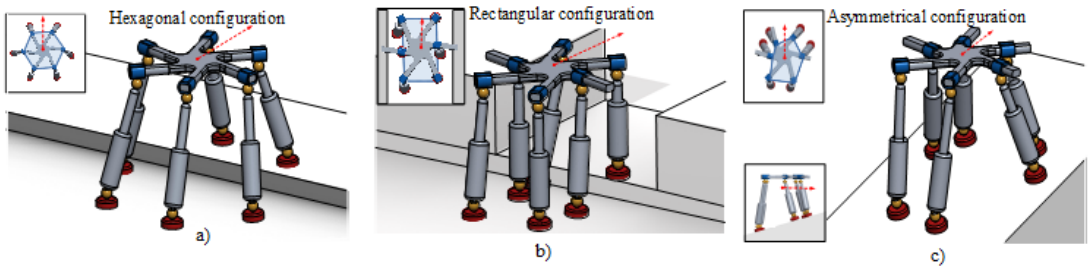


Figure 3-5. Illustration of three configurations for Concept 1: a)Hexagonal for walking on uneven ground; b) Rectangular for walking on constrained spaces; c) Asymmetrical for inclined terrain.

However, this represents a complicated task as the kinematical models must be developed, where several variables must be considered, and the most intricate design must be evaluated to create a simplified design with the most representative advantages of the family of PKMs presented in this chapter. Furthermore, these variables must be processed to allow a methodology for the optimisation of the orientations of the prismatic joints, which is related to the design of the moving platform. These models are developed and presented in chapter 4; where the kinematics and the optimisation algorithms for the design of the moving platform are introduced. Furthermore, the final design is presented in chapter 4, with an innovative design for the actuation of the prismatic joints of Concept 2. This novel design not only allows for the reconfiguration of the joints on the moving platform but further presents the advantage of reducing the total weight of the RPKM.

3.7 **Proposed overall RPKM Requirements**

The overall mechanical requirements require a PKM capable of performing 6 DoF machining operations as the conventional PKM of the Gough-Stewart type. However, the proposed RPKM must be able to self-propel itself to the place of intervention. Furthermore, the proposed RPKM must be able to adapt to different machining scenarios and different terrains to be traverse. Fort those conditions the

system must be able to adapt its kinematic architecture. To comply with the previous requirements, this chapter presented four concepts that can comply with these requirements. However, the selection and further development is based on the kinematic study presented in Chapter 4. Nevertheless, the following design requirements are presented in Table 3-3 as the intended capabilities for the proposed RPKM.

Table 3-3. Requirements for the proposed RPKM.

Characteristic	Quantity	Units
Mass of the RPKM	50	kg
Platform radius	250	mm
Platform structural thickness	10	mm
Mass of platform	5	kg
Height of RPKM	500-700	mm
Angle of spherical joints	40	degrees
Intended walking speed	200	mm/min
Maximum angle of the terrain to traverse	10	degrees

3.8 Conclusions

This chapter presented four concepts of reconfigurable parallel kinematic manipulators with the intention to increase the adaptability of PKMs in unprepared environments for manufacturing and repair. However, several challenges must be overcome; these are the development of the kinematic models that describe the concepts, the workspace analysis and a methodology for its optimisation. For this purpose Chapter 4 develops the kinematics for all this concepts. Similarly chapter 4 presents the kinematic analysis, workspace and optimisation of the orientations of

the slides. Based on these analyses the Concept 2 is presented as the most fitted design to proceed. Furthermore, in Chapter 4 the singularity avoidance and the reconfigurable capabilities of the selectec concept is developed. Nevertheless, all these analyses must be performed efficiently to reduce the time and resources required for its analysis.

Chapter 4 **Kinematic Analysis**

In robotics, the kinematic analysis studies the geometrical and spatial relations between the different components of a system. The main objective is to trace the relation between joint movements and end-effector movements. For this kinematics divides into inverse and forward. Inverse kinematics focuses on tracing the joint configuration with respect to a known position and orientation of the end-effector whilst the forward kinematics traces the position of the end-effector considering a given configuration for the joints. This chapter focuses on the inverse kinematic problem. As a class of Reconfigurable Parallel Kinematic Manipulator is introduced based on the concepts presented in Chapter 3. The analysis presented in this chapter allowed to select concept 2 as the most suitable of the family of RPKM, for this the orientation of the slides is optimised to achieve the maximum workspace, and a new methodology based on Fourier Analysis is presented to optimise the configuration of the Concept 2, taking advantage of the repositioning capabilities of Concept 2 for the upper joints on the linear slides.

4.1 **Inverse Kinematic Analysis of the class of RPKMs**

To determinate the reachable and safe to operate workspace of the proposed RPKMs, a kinematic model capable of describing the characteristics of all the proposed RPKMs is firstly established, as shown in Figure 4-1. This model is generalised to describe the reconfigurable characteristics of the upper joints and feet for any of the concepts presented in Chapter 3, as Figure 4-1 can represent any of the proposed concepts . For the purposes of kinematics, workspace and singularity analyses, the following coordinate systems are defined:

- $\{O–XYZ\}$ represents the global coordinate system, which is fixed on an unstructured environment with the positive Z-axis along the negative direction of gravity.
- $\{O_B – X_BY_BZ_B\}$ represents the local frame which is fixed on the moving platform of the RPKM. The origin of $\{O_B\}$ is located at the centre of the moving platform, and the axes are initially parallel to the ones of the $\{O\}$.

- $\{O_T - X_T Y_T Z_T\}$ represents the tool frame, where the origin of $\{O_T\}$ is fixed at the TCP (the tip of the tool) and three axes are respectively parallel to the ones of the $\{O_B\}$.
- $\{O_v - X_v Y_v Z_v\}$ represents the virtual base frame defined by three virtual points V_1, V_2 and V_3 which are respectively corresponding to the centres of A_1A_2, A_3A_4 and A_5A_6, where A_i represents the centre positions of lower S-joints in $\{O\}$. The origin of $\{O_v\}$ is at the centroid of the triangle conformed by the points V_1, V_2 and V_3. The Y_v-axis is along the direction of vector $\overrightarrow{O_v V_3}$ while the Z_V-axis is perpendicular to the plane of the triangle $V_1V_2V_3$. During the machining state of the proposed RPKM, this reference frame actually represents the ***machine coordinate system*** which is the local 'base' frame for the machining operations.

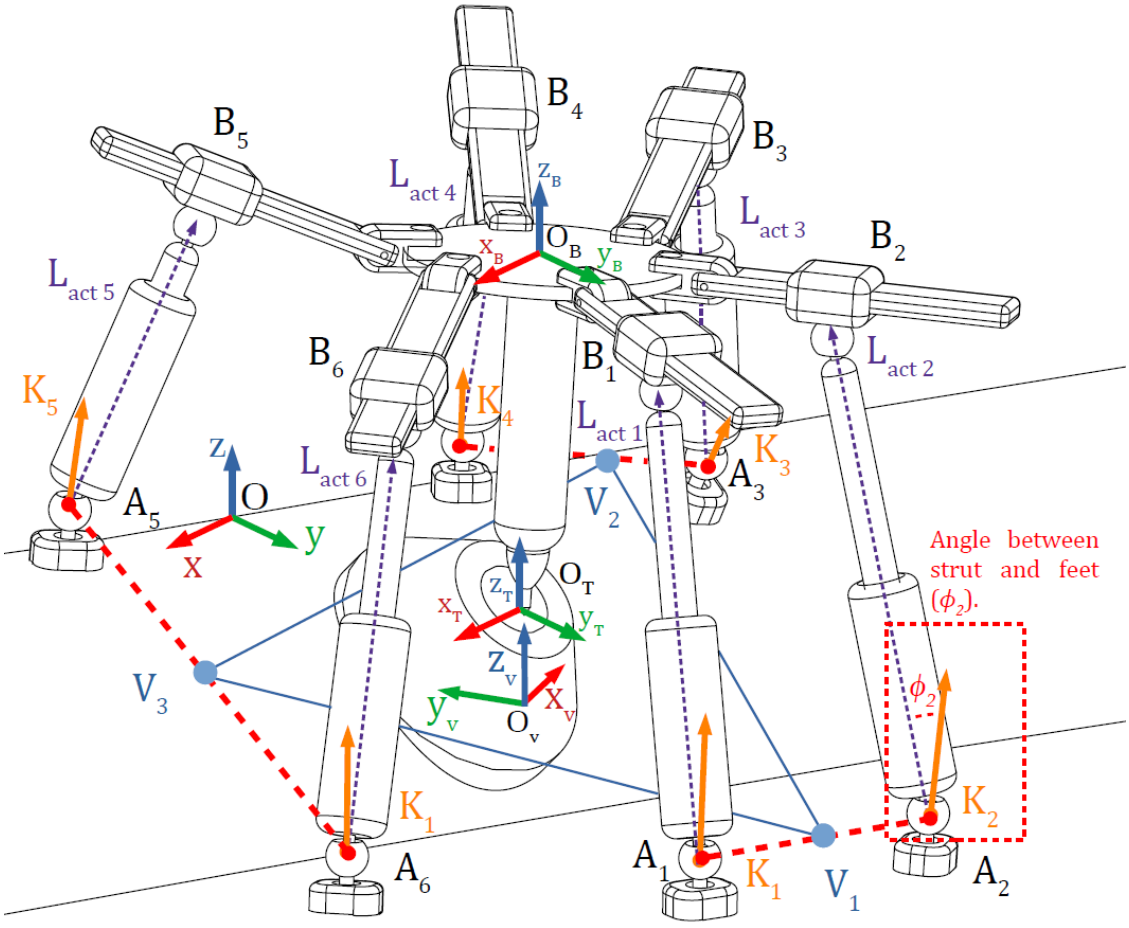


Figure 4-1. Kinematic model of the family of the proposed RPKMs.

Similarly, for the kinematic analysis a series of assumptions are listed as follows:

- The 6 limbs and linear slides are identical among them, and no defect of manufacture is considered in the analysis.

- No clearances or defects are considered for the joints (spherical, prismatic, linear, etc). So rotations are considered at the geometrical centre of each joint.
- The workspace is evaluated in discrete intervals, spaced with a parameter defined as the resolution of the analysis.
- The positions of the feet and its orientations are defined and known in the global reference frame. This means that for the theoretical analysis of the workspace no prior calibration is necessary .

For the kinematic analysis firstly, the positions of lower S-joints A_i and orientation angles A_{Ang_i} with respect to the global coordinate system $\{O\}$ can be written respectively as:

$$^{O}A_i = [X_i \quad Y_i \quad Z_i]^T \qquad \text{i=1, 2, …, 6} \tag{1}$$

$$^{O}A_{Ang_i} = [\alpha_i \quad \beta_i \quad \gamma_i]^T \tag{2}$$

According to the definition, the virtual points ($V_1 - V_3$) can be then defined as:

$$V_j = \frac{A_{2j}+A_{2j-1}}{2} \qquad \text{j=1, 2, 3} \tag{3}$$

Therefore, the machine coordinate system $\{O_v\}$ can be declared and the points A_i can be written in $\{O_v\}$ as:

$$^{O_v}A_i = {}^{O_v}R_O \cdot {}^{O}A_i \tag{4}$$

where $^{O_v}R_O$ is the rotation matrix which transforms from $\{O\}$ to $\{O_v\}$ and it defines a systematic orientation of the machine with respect to the workpiece.

The positions of the upper S-joints B_i are initially traced with respect to $\{O_T\}$ and expressed as $^{O_T}B_i$. Similarly, they can be then written in $\{O_v\}$ as:

$$^{O_v}B_i = {}^{O_v}R_{O_T} \cdot {}^{O_T}B_i + \{O_T\} \tag{5}$$

where $^{O_v}R_{O_B}$ is the rotational matrix from the tool reference system $\{O_T\}$ to the machine coordinate system $\{O_v\}$. Hence, the length of each linear actuator can be obtained by the distance between corresponding upper and lower S-joints (i.e. A_i. and B_i.) and is expressed by the norm of vector $\boldsymbol{L_{act_i}}$ as:

$$\left\| \boldsymbol{L_{act_i}} \right\| = |{}^{O_v}A_i - {}^{O_v}B_i| \tag{6}$$

Furthermore, to represent the angle between each pair of foot and linear actuator, vector $\boldsymbol{K_i}$ is defined normal to the surface of the i^{th} foot and pointing towards the moving platform with its origin at the centre of the i^{th} lower S-joint (see the orange arrows in Fig. 2). Assuming the length of $\boldsymbol{K_i}$ is defined arbitrarily. Then, the angles $\phi_i$between $\boldsymbol{L}_{act_i}$ and $\boldsymbol{K_i}$ can be calculated by:

$$\phi_i = \cos^{-1}\left(\frac{\left(\boldsymbol{L_{act_i}} \cdot \boldsymbol{K_i}\right)}{\left(\left\|\boldsymbol{L_{act_i}}\right\| \left\|\boldsymbol{K_i}\right\|\right)}\right) \tag{7}$$

A similar process is followed to obtain the angle of the upper joints. The values of $\boldsymbol{L_{act_i}}$ and $\boldsymbol{K_i}$ are tracked in order to calculate the limits of the operational range of both, the spherical joints and limbs that conform the machines proposed. Hence, a kinematic model capable of describing the locations and orientations of the components for a family of RPKMs has been established. This is of particular interest as the configurations of the upper and lower joints locations will change and adapt through the applications of the proposed family of the new RPKMs (i.e. on free-form environments and complex surfaces), as opposed to the standard PKMs that present fixed configurations. Based on this models characteristics such as reachable workspace, stiffness and singularities will be obtained and represented in later sections.

4.2 **Reachable Workspace Analysis**

As the lower joints configurations change when adapting to different scenarios, the workspace of the proposed RPMKs will change in accordance with the upper and lower joints configuration. Hence, one of the challenges of developing these RPKMs is to evaluate the reachable and safe-to-operate workspace before any operation in an effective procedure. With the aforementioned inverse kinematics for an RPKM generically described, in this section, the methodology to evaluate the workspace of the proposed family of RPKMs is presented.

The workspace analysis is of relevant importance for a RPMK as it must be performed after every reconfiguration for safe operations, in contrast to the

conventional PKMs where this process is only required during the design phase as the workspace remains constant during its operational life. Specifically, this approach considers the key component constrains and the collision between different elements in the system, which together with the kinematic model, allow a spatial search of the reachable locations of the RPKM. The main advantage of the proposed methodology is its capability to adapt to several configurations, considering those highly unsymmetrical and the capability to store the reachable locations for further analysis, which can be used to evaluate characteristics such as workspace volume and, in later sections, to the avoidance of singularities.

4.2.1. Key component constrains

To determine if a position can be reached by the proposed RPKM, two key components (i.e. P- and S-joints) are considered with their geometrical constrains, these are illustrated in Figure. 4-2 and explained as follows:

- **The P-joints:** as shown in Figure. 4-2a, the minimum and maximum lengths of the linear actuators are respectively defined as L_{min} and $L_{max,}$ and the stroke is obtained as $L_s = L_{max} - L_{min}$. $|\boldsymbol{L}_{act_i}|$ in Equation (6) are then calculated to evaluate if any of the P-joints is out of its limits and to determine if the corresponding position in the workspace is reachable.
- **The S-joints:** as shown in Figure. 4-2b, the limits for the angles of the S-joints are considered to be between 0 and θ_{Sl}, where θ_{Sl} is the maximum angle it can reach. Similarly, ϕ_i in (7) are then calculated to evaluate if any of S-joints is out of the limits and to determine if the position is reachable or not.

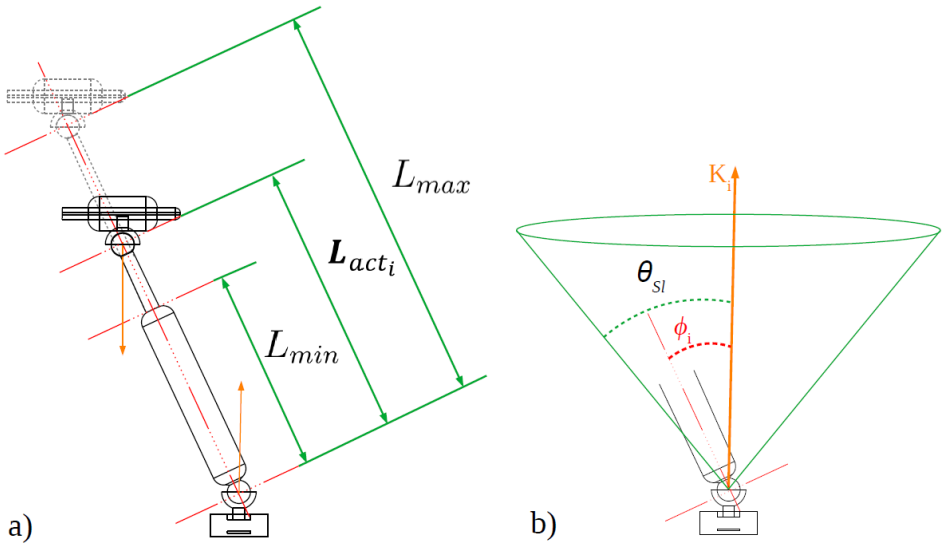


Figure. 4-2. Component constrains of: a) P-joint ($|\boldsymbol{L}_{act_i}| \in [L_{min}, L_{max}]$) and b) S-joint ($\boldsymbol{\phi_i} \in [0, \theta_{Sl}]$)).

4.2.2. Collision constraints

In this part, by using the inverse kinematics of the RPKMs the locations of the components (i.e. limbs and spindle) are traced and considering its geometrical properties (lengths and thickness) collision conditions are evaluated, preventing possible damage by impacts.

As mentioned in Section 1, to increase the adaptability of the RPKMs, the limbs can be positioned freely on the workpiece and accordingly it may lead to circumstances that the limbs operate at critical distances from each other. This may occur not only during the setup but as the task is being performed, which will significantly increase the risk of impact between the components of the machine. In conventional PKMs, collision analysis does not represent an issue as it is performed only during the design phase, given that the workspace remains the same during the operational life of the mechanism. However, it plays a significant role in the determination of the reachable workspace for an RPKM as it must be evaluated prior to any operation. For this reason, the collision analysis represents an important step to avoid any possible damage to the mechanism and still be able to operate utilising efficiently its reachable workspace. To evaluate if a collision occurs between two elements, the distances between the limbs, spindle, and slides are considered. The methodology proves to be efficient as a system of linear equations is solved instead of the methods that involve optimisation to find the distance between elements. The following assumptions and elements are defined to estimate if a collision occurs: two vectors define two elements under collision analysis, $\boldsymbol{S}$ and $\boldsymbol{L}_{act_i}$. $\boldsymbol{S}$ and $\boldsymbol{L}_{act_i}$ represent the orientation and length of each physical element of the RPKM proposed; in the example described belong, $\boldsymbol{L}_{act_i}$ stands for the vector defining one limb (orientation and physical limits) of the RPKM while S represents a vector defining the spindle of the RPKM, similarly to the limbs.

- The shortest distance between $\boldsymbol{S}$ and $\boldsymbol{L}_{act_i}$ is represented as the norm of vector $\boldsymbol{D}$, which is perpendicular to $\boldsymbol{S}$ and $\boldsymbol{L}_{act_i}$. $\boldsymbol{D}$ lies on $\boldsymbol{L}_{act_i}$ at a distance a from point A_i and on $\boldsymbol{S}$ at a distance b from O_B.

- The geometrical shapes of the elements are simplified to be cylinders where the radius is determined as the half of diameter of the thickest part.
- The collision occurs when the distance $|\boldsymbol{D}|$ is smaller or equal to the sum of the radiuses of the two elements under analysis.
- The scenarios considered for possible collisions are the distances between spindle and limbs, adjacent limbs and adjacent slides, as shown in Figure. *4-3*a.

By referring to Figure. *4-3* and the above assumptions. The vector $\boldsymbol{D}$ is expressed as:

$$\boldsymbol{D} = \left(\boldsymbol{A_i} + a\boldsymbol{L_{act_i}}\right) - \left(\boldsymbol{O_V} + b\boldsymbol{S}\right) \tag{8}$$

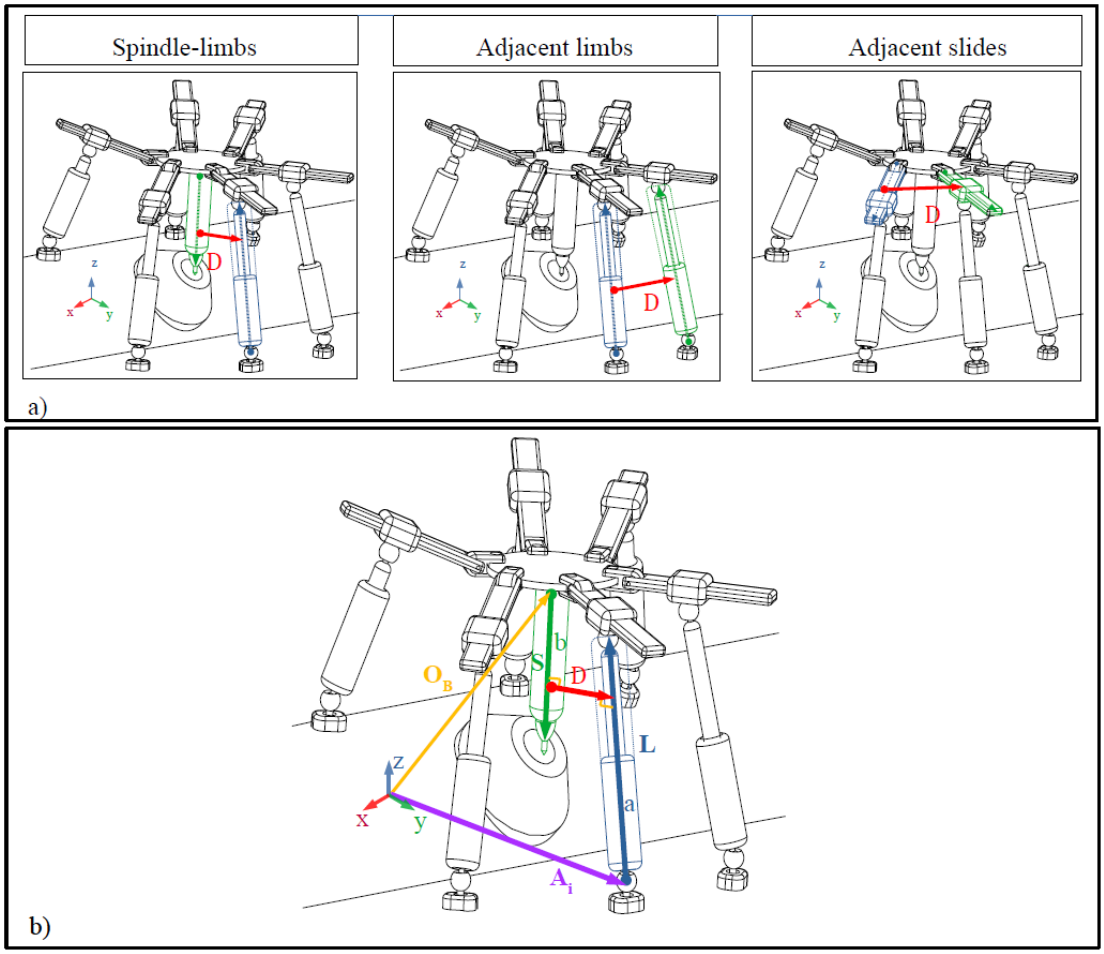


Figure. 4-3 Illustrations for collision analysis: a) scenarios of possible impacts between elements of the RPKM; b) Zoom of the scenario for one limb and the spindle of an RPKM.

Multiplying Equation (8) by $\boldsymbol{L}$ and $\boldsymbol{S}$:

$$\boldsymbol{L_{act_i}} \cdot \boldsymbol{D} = \boldsymbol{L_{act_i}} \cdot \left(\boldsymbol{A_i} + a\boldsymbol{L_{act_i}}\right) - \boldsymbol{L_{act_i}} \cdot \left(\boldsymbol{O_V} + b\boldsymbol{S}\right) \tag{9}$$

$$\boldsymbol{S} \cdot \boldsymbol{D} = \boldsymbol{S} \cdot \left(\boldsymbol{A_i} + \boldsymbol{L_{act_i}}\, a\right) - \boldsymbol{S} \cdot (\boldsymbol{O_V} + b\boldsymbol{S}) \tag{10}$$

As $\boldsymbol{L}$ and $\boldsymbol{S}$ are orthogonal to $\boldsymbol{D}$:

$$\boldsymbol{L_{act_i}} \cdot (\boldsymbol{A_i} - \boldsymbol{O_V}) + \left(\boldsymbol{L_{act_i}} \cdot \boldsymbol{L_{act_i}}\right)a - \left(\boldsymbol{L_{act_i}} \cdot \boldsymbol{L_{act_i}}\right)b = 0 \tag{11}$$

$$\boldsymbol{S} \cdot (\boldsymbol{A_i} - \boldsymbol{O_V}) + \left(\boldsymbol{S} \cdot \boldsymbol{L_{act_i}}\right)a - (\boldsymbol{S} \cdot \boldsymbol{S})b = 0 \tag{12}$$

Solving the systems of equations for a and b it is obtained that:

$$a = \frac{\left(\boldsymbol{L_{act_i}} \cdot \boldsymbol{S}\right)[\boldsymbol{S} \cdot (\boldsymbol{A_i} - \boldsymbol{O_V})] - (\boldsymbol{S} \cdot \boldsymbol{S})\left[\boldsymbol{L_{act_i}} \cdot (\boldsymbol{A_i} - \boldsymbol{O_V})\right]}{(\boldsymbol{S} \cdot \boldsymbol{S})\left(\boldsymbol{L_{act_i}} \cdot \boldsymbol{L_{act_i}}\right) - (\boldsymbol{S} \cdot \boldsymbol{S})^2} \tag{13}$$

$$b = \frac{\left(\boldsymbol{L_{act_i}} \cdot \boldsymbol{L_{act_i}}\right)[\boldsymbol{S} \cdot (\boldsymbol{A_i} - \boldsymbol{O_V})] - \left(\boldsymbol{S} \cdot \boldsymbol{L_{act_i}}\right)\left[\boldsymbol{L_{act_i}} \cdot (\boldsymbol{A_i} - \boldsymbol{O_V})\right]}{(\boldsymbol{S} \cdot \boldsymbol{S})\left(\boldsymbol{L_{act_i}} \cdot \boldsymbol{L_{act_i}}\right) - (\boldsymbol{S} \cdot \boldsymbol{S})^2} \tag{14}$$

By substituting Equations. (13) and (14) into Equation (8) the norm of $\boldsymbol{D}$ can be calculated to compare it with the sum of the radiuses of the two elements under analysis, which determines if a collision occurs or not. This process is iterated for other elements under the risk of a collision such as adjacent slides, adjacent limbs, etc. Similarly, *Figure. 4-4* describes the process to evaluate if a collision occurs in any configuration proposed for the RPKM. Later on this chapter this strategy is combined in the workspace analysis to evaluate the different possible collisions, and to prevent possible collisions in the workspace.

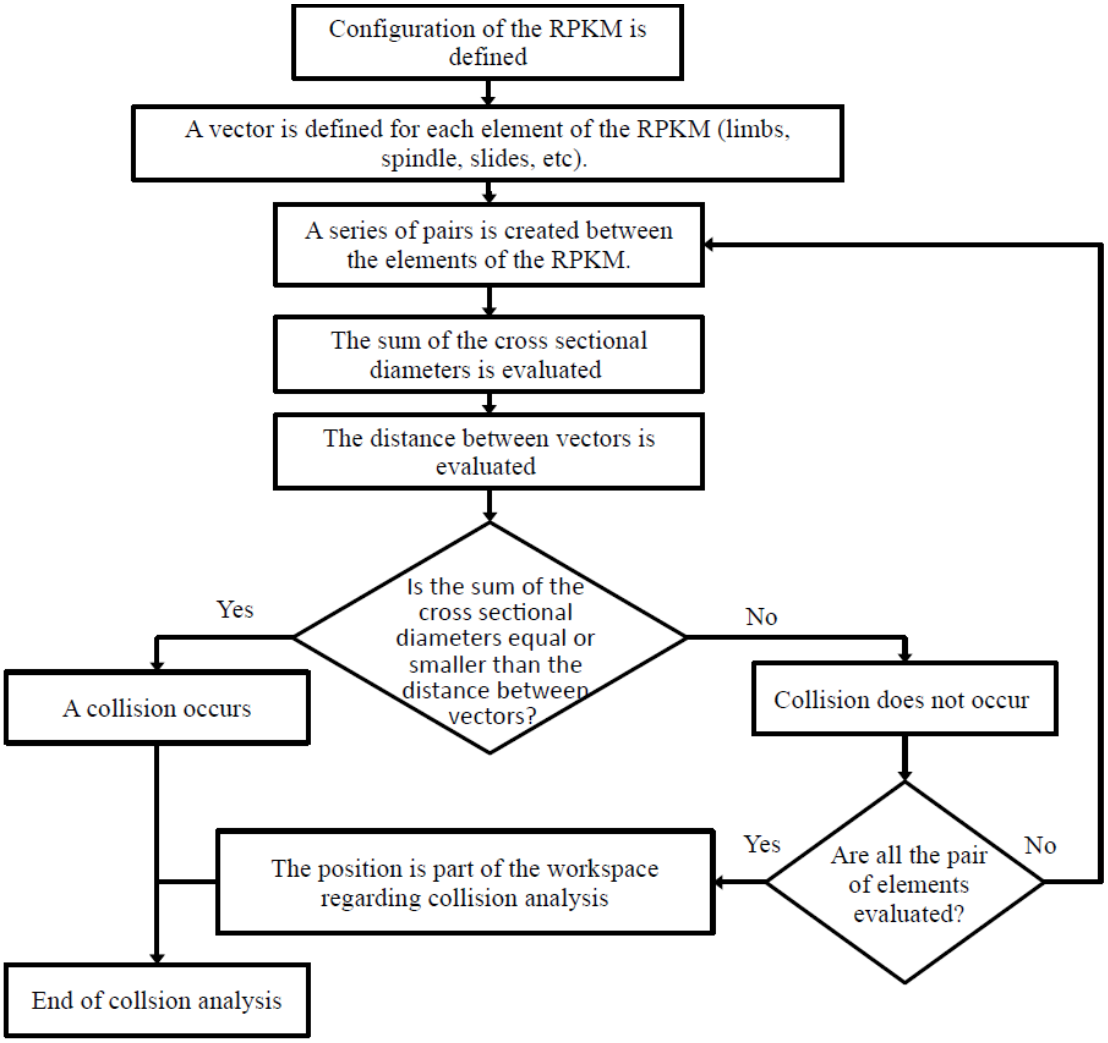


Figure. 4-4. Flow diagram to evaluate possible collision for a given configuration.

4.2.3. Workspace

Initially, the configuration of the lower S-joints (points A_i in Figure 4-1) is declared, then several positions for the TCP are proposed and if the criteria related to the constraints of the key components and collisions between different mechanical elements are met the positions are saved. The main difference to other methodologies [100] is that there is no need to declare large probabilistic zones or predefined shapes and with this the reduction of the locations to evaluate. The algorithm performs two major processes for the search of reachable locations:

1. **The lateral search:** is firstly carried out inside planes (see Figure. *4-5*a) where in each plane a polar vector is defined to propose positions for analysis and then to identify the reachable limits (see Figure. *4-5*b). The main advantage of this

method is its capability to obtain and save the information of the workspace to further use it in the singularity analysis. If the geometrical limits and collision conditions are satisfied, the position (blue spot in Figure. *4-5*) is stored as part of the reachable workspace and the norm of the polar vector increases (continuous orange arrow), this increments are defined by the resolution for the analysis. If a condition fails, the position (red spot in Figure. *4-5*b)) is removed and the reachable limit on this vector is identified. Then the orientation of the polar vector is changed in the anti-clockwise direction and its norm set to the resolution value to start the search in the new orientation (dashed orange arrow in Figure. *4-5*b). When this plane is fully swept, the centroid of the plane is calculated and projected to the next plane where the lateral search starts again. This process divides the search into the planes above and below the plane $x_v y_v$.

2. **The height limit search:** is then targeted to find the top and bottom planes reachable by the TCP. By comparing the number of positions reachable in each plane, the top/bottom planes are defined where only single element exists (see Figure. *4-5*a) and if the number is less than one, then the search for reachable elements stops.

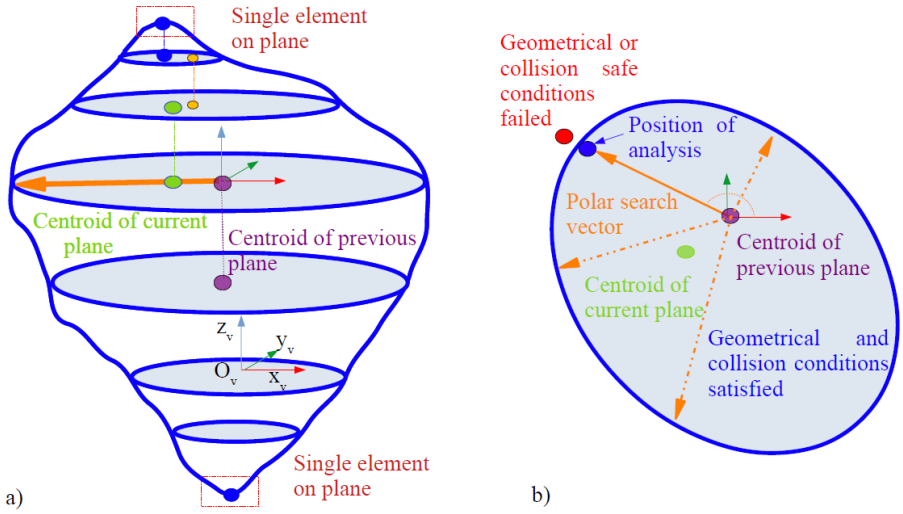


Figure. 4-5 Illustration of the limit search for the workspace. a) The search is performed dividing the space into planes; the centroid of each plane is the starting point for the search in the next plane. b) Illustration of the polar search on each plane.

The full process to evaluate the workspace is presented in Figure 4-6, where the flow diagram for the evaluation of the workspace is presented.

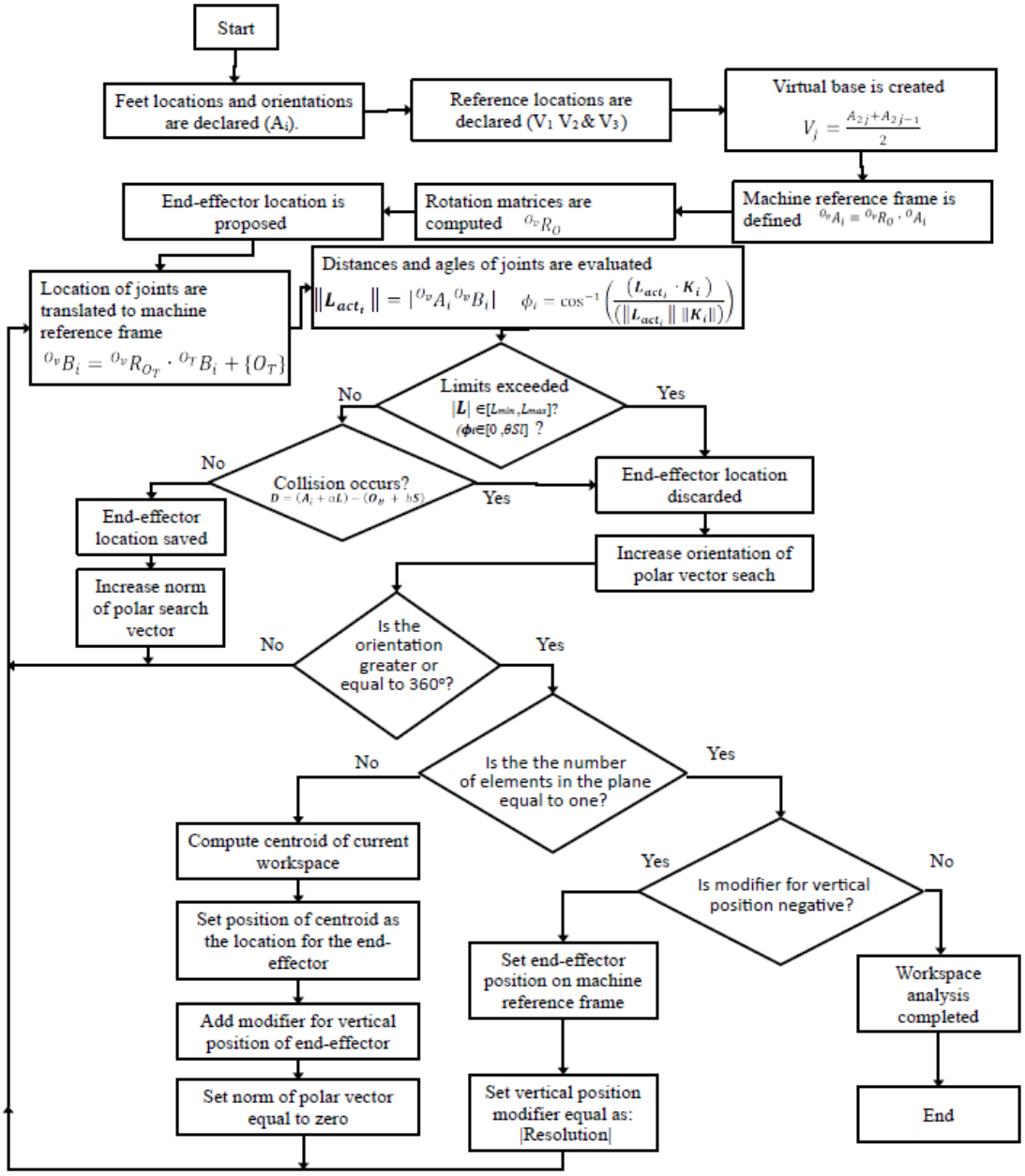


Figure 4-6. Flow diagram to evaluate the reachable workspace.

To evaluate the proposed methodology above, a case study is presented based on a highly non-symmetrical configuration of the RPKM, where the lower joints A_i are placed randomly (Figure. 4-7b) with different heights (Figure. 4-7c), the upper joints B_i are located at different positions on the slides (Figure. 4-7b), as well as the slides oriented with different angles from the corresponding hexagon edges of the moving

platform (Figure. 4-7b) and different tilt angles with respect to the moving platform plane (Figure. 4-7c).

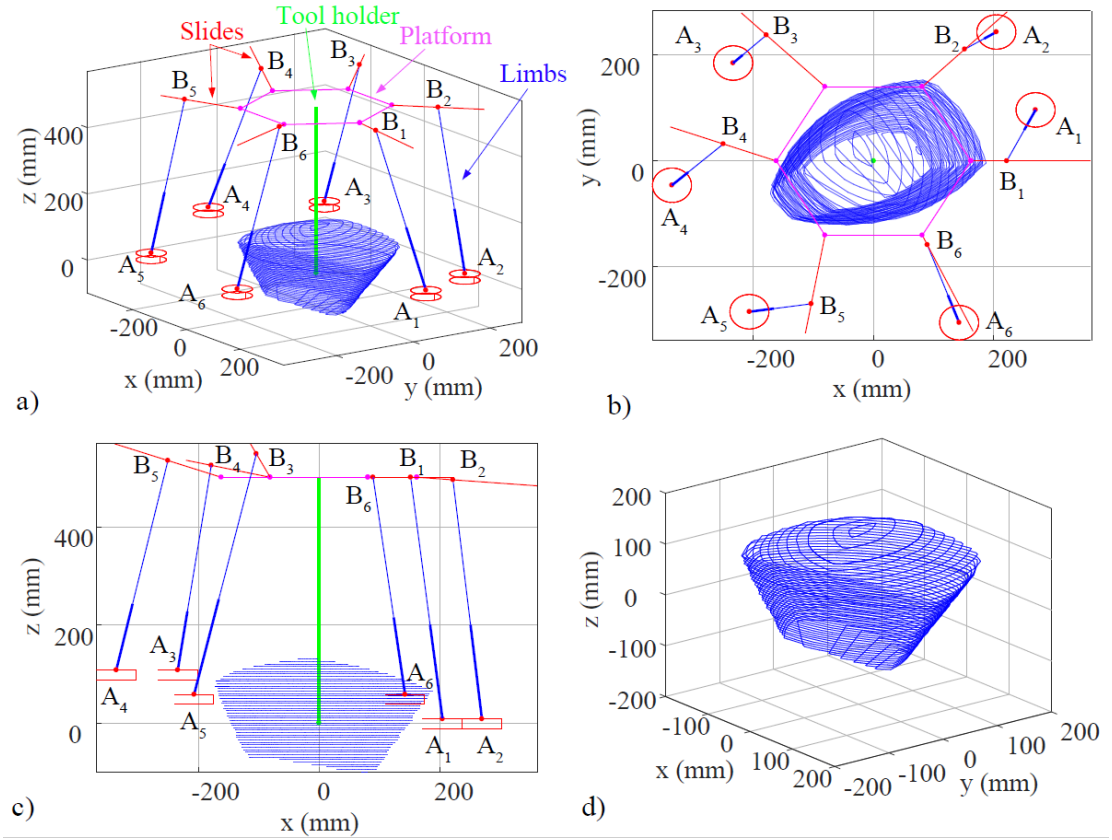


Figure. 4-7. A case study on the workspace analysis of the proposed RPKM under a highly asymmetrical configuration where feet are placed at uneven heights and slides orientation are unsymmetrically distributed and tilted with respect to the moving platform in: (a) a 3D view, (b) xy plane, (c) xz plane and (d) a 3D view with detailed workspace.

The reachable workspace analysis is of particular interest as it will define the paths that can be performed by the TCP. Thanks to the reconfigurability of the proposed concepts of the RPKMs, the reachable workspace can be modified to better adapt to the desired operation, which can overcome one of the main disadvantages of the conventional PKMs, i.e. the fixed and non-adaptive workspace. However, so far, the workspace analysis has been analysed considering only the geometrical and collision constraints imposed by the mechanical elements of the RPKM. In the following section the process to adapt the configuration of the RPKM to avoid singularities in the workspace is presented.

Although the models presented in this section are capable of representing and obtaining the workspace for the four concepts presented in Chapter 3, Table 3-2represents the most suitable concept in terms of optimised performance against complexity of design (considering the final number of components, actuators and assemblies required). For these reason the analysis of workspace and design focuses on Concept 2. Which allows the upper spherical joints to displace along a series of slides (as presented in Figure 4-8). However, concept 3 presents the capability to reorient the slides to increase the performance. Based on this idea, it is considered that the concept 2 can be optimised to produce larger workspaces for different configurations by considering a fixed orientation of the linear slides. This means that the optimal angle between the slides and the radial direction must be identified, which results a challenging task as several variables (e.g. feet positioning, stroke of actuators, collusion conditions, slides orientation, upper joints position) are identified and non-direct functions representing the workspace analysis.

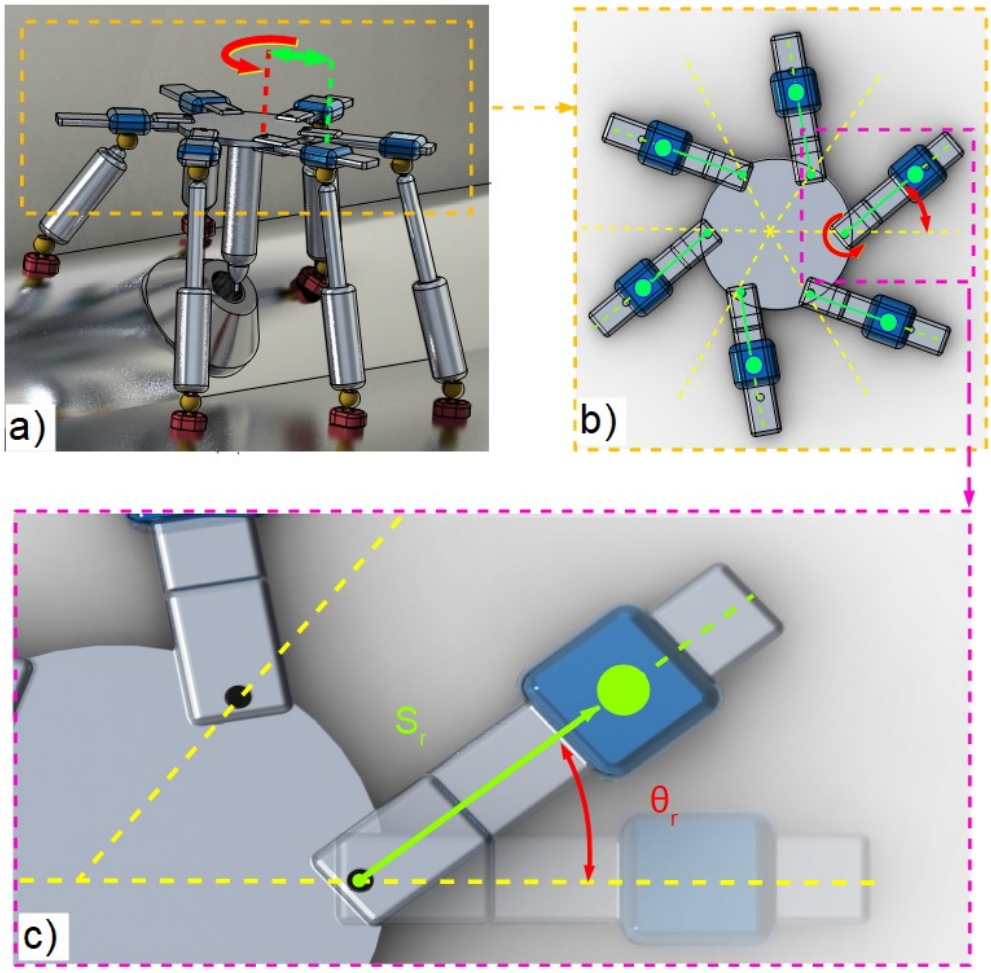


Figure 4-8. Illustration of RPKM based on Concept 2. a) The RPKM on uneven surfaces with a symmetrical configuration; b) Top view of the platform. c) Zoom to one of the slides showing the orientation and position of the slide.

However, the orientation of the slides for each slide is considered to be identical, and the position of the joint over the slides can be independently adjusted. Meaning that for each configurations there exist 10^6 possible configurations, considering incremental steps of 10% for each slide. Considering the high amount of possible configurations a standard configuration is selected. Then the orientation of the slides is incremented between cero degrees and 60 degrees.

The proposed method to optimise the design of the platform proposes a random configuration of the two characteristics to be optimised, and then evaluates the performance of the group with the proposed characteristics. Once the performance is evaluated, the method selects the fittest elements in the population and adds new elements with the combinations of the previous fittest elements. To avoid possible

local maxima, random modifications are included in the new group. This process is iterated until recursive results are found. In order to evaluate the effectiveness of the method followed, and arbitrary configuration of the hexapod is declared and the orientation and position of the upper joints are evaluated over its operational configurations. The results show the greatest working space to occur when the orientation of the slides is at 0 degrees with respect to the radial direction, and to occur at 100 percent the length of the slide, this is to the furthest position from the platform centre. The proposed methodology gave the results presented in Figure 4-9. Once the method has been validated, the algorithm is used to provide results with unsymmetrical configurations of the slides. As the RPKM proposed is intended to achieve a high number of possible configurations, two sets of 20 random configurations are proposed. These configurations consider different locations for the base of each leg within the reachable limits of the feet/ lower joints. This means that each limit is projected into an area reachable by each foot.

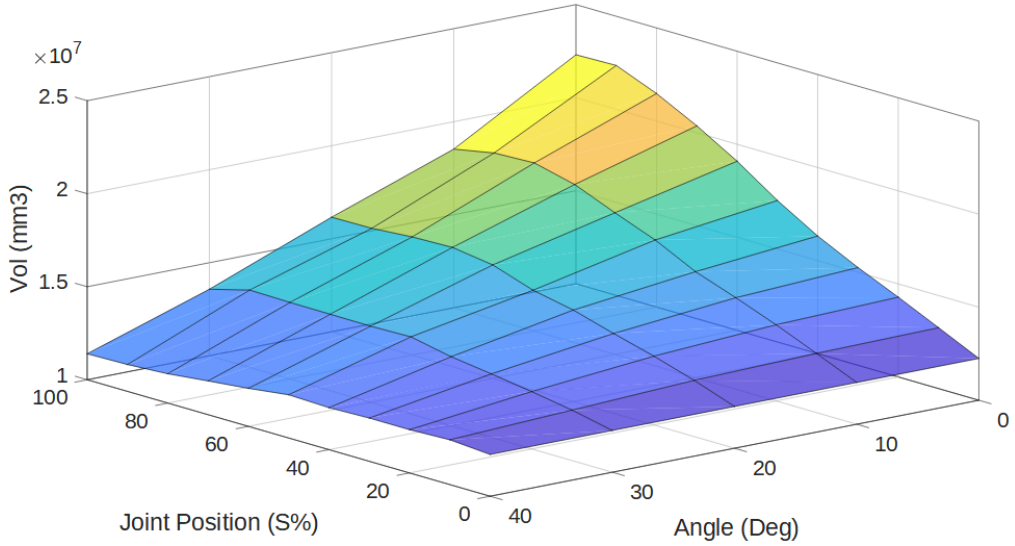


Figure 4-9. Workspace volume dependant of slide position and orientation of slide for Concept 2 presented in Chapter 3.

The proposed methodology is executed, the configurations with the biggest volume of the workspace are saved through the analysis and the results show a clear trend to achieve the maximum workspace. Two sets of random configurations are proposed;

set 1 considers the maximum angle for the central point to lay with in +- 15 degrees of the central position of each limbs, while the set 2 considers the maximum possible angle being +- 30 degrees, For the two sets of proposed configurations, the results show that the maximum workspace is achieved when the slides are oriented at the radial direction and at the maximum position on the slides (see Figure 4-10 blue and green dots). However, there is also possible observe that there are some results where the works is valuated as null (red dots in Figure 4-10). These is results are obtained when the feet are close or out of the limits imposed for the limbs and the spherical joints, and the algorithm detects that none of the conditions to reach the workspace are achieved, then the workspace methodology is not able to evolve on the search space and finally these configurations are discarded.

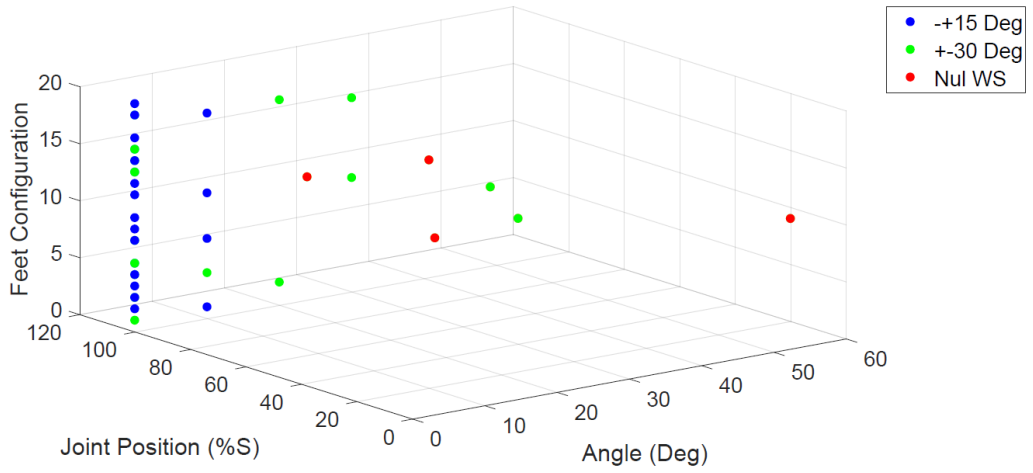


Figure 4-10. Results of maximum workspace volume considering slide orientation and joint position on slide for Concept 2 presented in Chapter 3.

More importantly this methodology allows to select a subset of Concept 2, this is the slides are considered to change their orientation angle to maximise the workspace of the proposed RPKM. This represents that Concept 1 is selected to become the design of the proposed RPKM, ensuring that the maximum workspace can be achieved with Concept 1 and thus reducing the number of components required for its construction and operation.

4.3 Singularity Analysis and Optimisation

Compiling the workspace of the RPKM could be regarded as a routine exercise. Nevertheless, there is still needed to rapidly search for singularities after each reconfiguration that may be present in the reachable workspace of the TCP and these instabilities will result in loss of control and possible damage to the RPKM. To prevent these undesired conditions after each reconfiguration, a new method is proposed to estimate the presence of singularities based on the Fourier transform, where the main frequencies conforming the Jacobian determinant are extracted for different TCP orientations in the workspace. It is noted that with the conventional PKMs the singularity analysis is conducted during the design phase, and the zones where singularities exist are discarded, resulting in a reduced workspace and limiting the applications for PKMs. However, an RPKM by repositioning the upper and lower joins is assumed to be capable of adapting itself to meet the task requirements and avoid instabilities. To validate this, a machining operation is proposed as a case study in this section, where the singularities in the operation path are traced and, using genetic algorithms, the upper joints locations are optimised to be able to comply with the required operation by avoiding the unstable patterns. The method proposed presents as the main advantage in reducing the computational burden of analysing the full workspace and is capable of presenting a new configuration free of singularities.

4.3.1. Singularity analysis

To ensure the RPKM operates out of unstable conditions, the singularity analysis is performed along a path followed by the TCP. A new method based on Fourier transform is proposed to extract the amplitude and main frequencies from the Jacobian as presented in the following subsections.

Jacobian surface and Jacobian profile

This subsection presents the methodology to estimate the Jacobian (although based on classical derivations) introduces a new approach to estimate singularities and its behaviour with special attention to the TCP. The Jacobian is calculated based on the method presented in [101], where the Jacobian is formulated by a velocity-closure

equation for each limb and then the equations are differentiated with respect to time. These equations are assembled and expressed in a matrix form.

As the vectors associated to the upper (B_i) are related to the position and orientation of the TCP, the Jacobian will change not only as different elements of the workspace are approached but also with the orientation at which these are approached. In this case, each position of interest inside the workspace can be considered as approached with respect to two angles:

- α represents the tilt angle between Z_v- and Z_T-axes.
- β represents the angle of the direction at which the element is approached with respect to $\{O_v\}$.

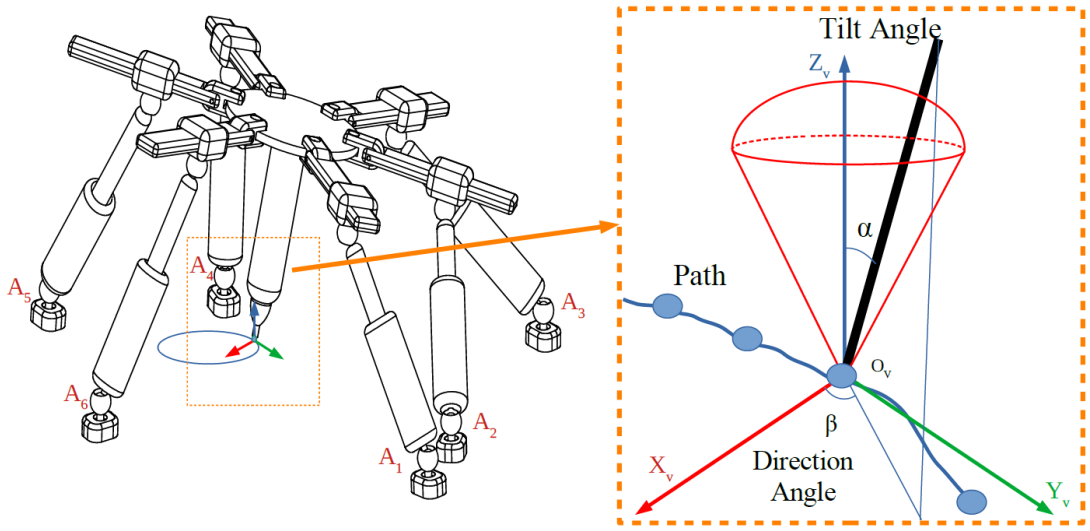


Figure. 4-11. Illustration of TCP approaching an element of the workspace with a direction angle α and tilt angle β.

The direct kinematic singularity is considered to be present when the Jacobian determinant is equal to zero. In order to estimate if singularities exist in a particular configuration, the Jacobian determinant is calculated by considering the corresponding element inside the workspace and the approaching angles α and β. As a case study, Figure. 4-12 represents the Jacobian analysis for one element of the reachable workspace with the configuration indicated in Figure. 4-12b. In Figure.

4-12a, the variation of Jacobian determinant is presented as a surface (later referred as the Jacobian surface) with the approaching tilt and direction angles among the ranges of [0, 0.25π] and [0, 2π], respectively.

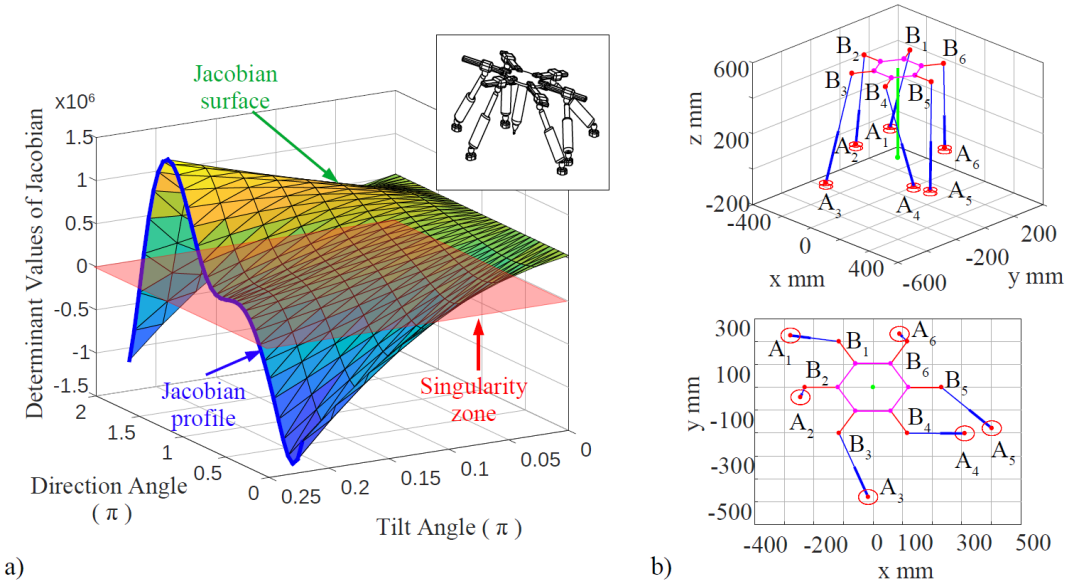


Figure. 4-12. A case study on singularity analysis for an element of the workspace. a) variation of the Jacobian determinant; b) configuration of the RPKM in both isometric and top views.

In Figure. 4-12a it is shown that the Jacobian determinant may result to zero (singularity zone) not only depending on the position but also on the approaching angles. Furthermore, it is noted that the Jacobian determinant follows a sinusoid pattern along the direction angle at constant tilt angles (e.g. blue curve in Figure. 4-12a) and this pattern amplifies as the tilt angle increases. For this reason, the profile of the surface (i.e. sinusoid pattern) that represents the highest rate of change of the Jacobian Determinant is selected for its analysis. This is named as the Jacobian profile in the following sections. As aforementioned, there may be task which require the RPKM to operate in conditions that would lead to singularities (Jacobian equal to zero). However, the upper joint layout could be modified, changing the relations between $\boldsymbol{B_i}$ and the TCP, to reach them in a singular-free condition and comply with the desired orientation. Therefore, a novel methodology is proposed to track and modify the behaviour of the singularities based on the Jacobian profile in the following subsection.

Jacobian Profile Analysis

In this subsection, the Jacobian determinant is analysed based on the Fourier analysis where the Jacobian profile is decomposed to extract the subcomponents in terms of amplitudes, frequencies and phases. This study is relevant as in later sections is used to optimise the configuration (i.e. position of upper joints on the moving platform) of the RPMs proposed to avoid singularities in the operation to perform.

In order to optimise the behaviour of the proposed RPKM, the shape of the Jacobian surface is traced using the Fourier transform. As stated by the Fourier theorem, any signal stationary in time can be represented by the sum of a series of different sinusoid waves. It is proposed to simplify the shape of this surface such that the singularities are predictable in a reasonable manner. For this case the harmonics of the fundamental frequency or sinusoids of higher values conforming the singularity surface would increase the complexity of these surfaces and increase the conditions that lead to unstable configurations.

Spectrum Analysis

Consider the signal represented in Figure 4-13. This signal is composed of the sum of five sinusoid waves as expressed in Equation 22.

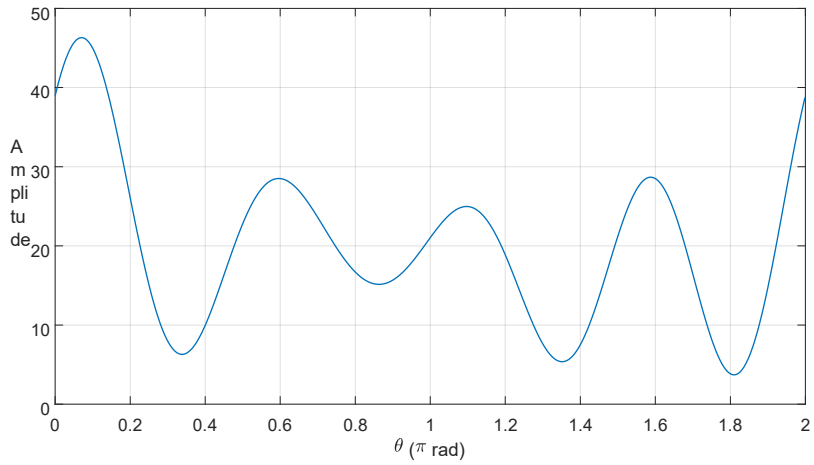


Figure 4-13. Signal composed by five sinusoid waves.

$$S_{5s} = 20 + 4\,sin(\theta + 0.78) + 4\,sin(2\theta + 1.57) + 5\,sin(3\theta + 0.78) + 12\,sin(4\theta + 0.52) + 3sin(5\theta + 1.04) \quad (15)$$

Assuming that the waves composing S_{5s} are unknown, by implementing the Fourier transform, the amplitude and frequency of each sub-wave could be obtained. As Fourier series state if $S_{5s}(\theta)$ is a periodic function , according to [102] its Fourier series representation is given by:

$$S(\theta) = a_0 + \sum_{n=1}^{\infty} (a_n \cos(n\omega_n\theta) + b_n \sin(n\omega_n\theta)) \tag{16}$$

Where:

- a_n and b_n are the amplitude coefficients.
- ω_n is the frequency at which each wave n operates.

If the frequency of interest is sampled at a constant interval $\Delta\theta$ for a period T, the solution can be expressed as the sum of a series of sinusoid functions and is expressed as:

$$S(\theta) = a_0 + \sum_{n=1}^{\infty} (c_n \sin(n\omega_n\theta + \varphi_n) \tag{17}$$

Where:

- a_0 and c_n are the amplitude coefficients of each wave.
- ω_n is the fundamental frequency, assuming that the rest of the frequencies are multiples of the fundamental frequency.
- φ_n are the phase coefficients.

When the methodology proposed is used, the coefficient of the waves conforming S_{5s} are obtained. These result are the summary of the spectrum analysis displayed in Figure 4-14 and Figure 4-15.

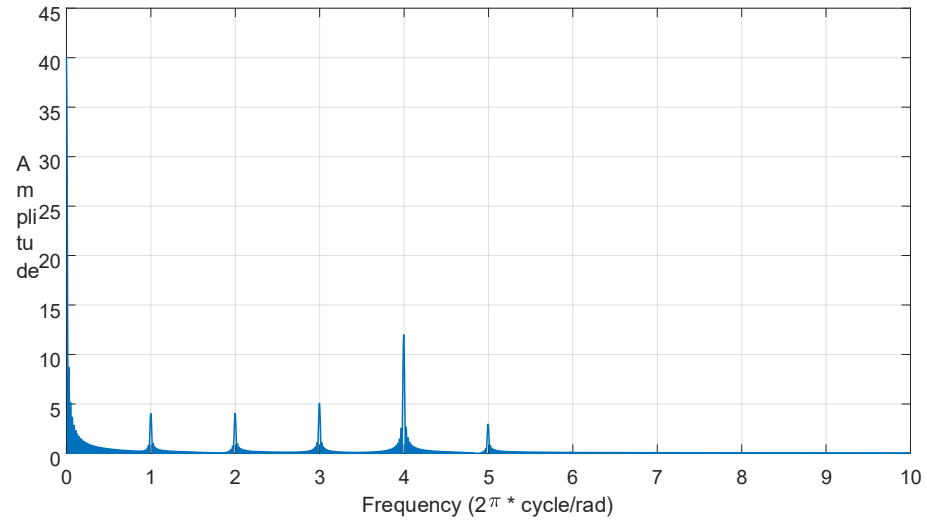


Figure 4-14. Sctrum analysis of amplitude coefficients.

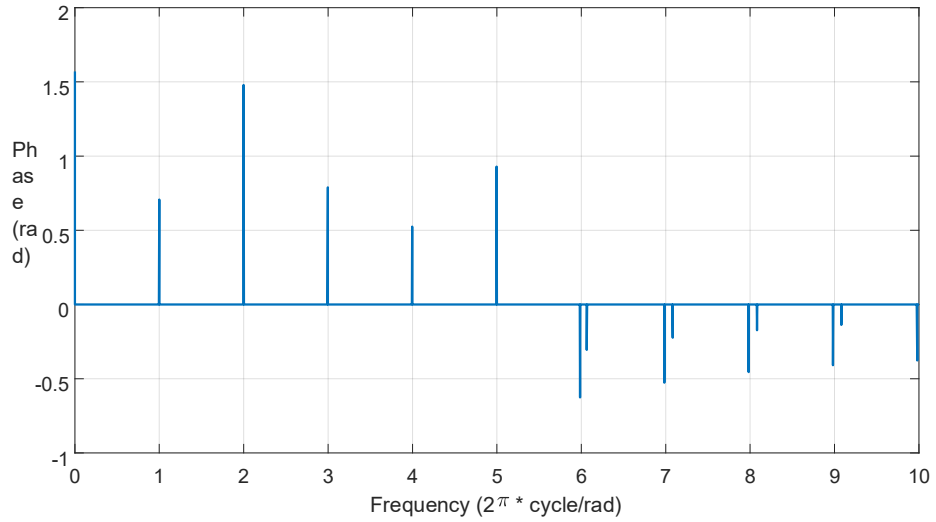


Figure 4-15. Spectrum analysis of phase coefficients.

By applying Equation (20) with the parameters of Figure 4-14 and Figure 4-15 the signal presented in Figure 4-13 can be reconstructed , as the information of each wave conforming the signal is known in the range of interest. As the scope of this chapter is to trace the behaviour of the singularities in the workspace of the RPKM, the employed algorithms are based on commercial software (such as FFT functions in Matlab). This allows reducing the computing burden as several configurations have to be studied and combined with the proposed kinematic models.

Spectrum Analysis: Jacobian Profile

Within the obtained Jacobian surface (see Figure. 4-12 and Figure. 4-16a), the Jacobian profile is extracted at the tilt angle of 0.25π, as shown in Figure. 4-16. By performing the Fourier analysis, as shown in Figure. 4-16c, it can be noted that it is conformed mainly by a constant value (A_0), the fundamental frequency and the next five harmonics of it (Figure. 4-16c and Table 4-1. Figure. 4-16d represents the phase angles at which the different harmonics are operating in the system. This process to analyse the Jacobian profile by the use of the Fourier analysis is represented in Figure 4-17 and will be referred as the Dominant Frequency Analysis (DFA).

n	A_n	$Frequency_n\,(cycle/2\pi)$	ϕ_n *(rad)*
0	256856.24	0	1.57
1	1503983.74	1	3.65
2	1119921.59	2	-1.56
3	397104.23	3	-0.26
4	144210.95	4	-1.08
5	65318.47	5	-0.42
6	10926.08	6	2.45

Table 4-1 Main harmonics of the selected Jacobian profile in Figure 15.

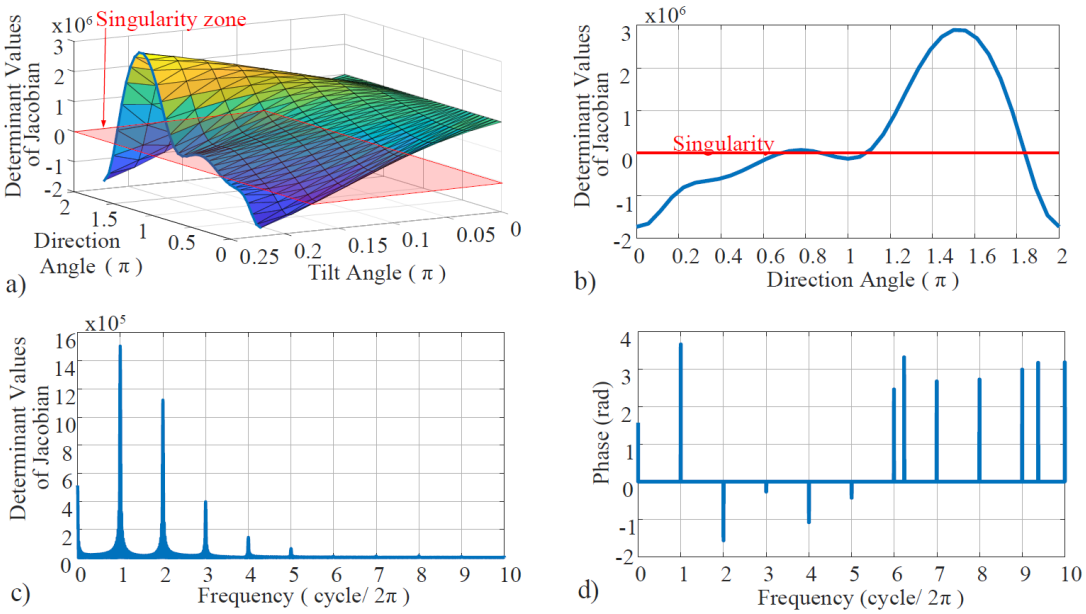


Figure. 4-16. a) Spectrum analysis results of Jacobian profile for an element of WS: (a) Jacobian determinant surface; b) Jacobian profile at tilt angle of 0.25π; c) amplitude vs frequency; d) phase vs frequency.

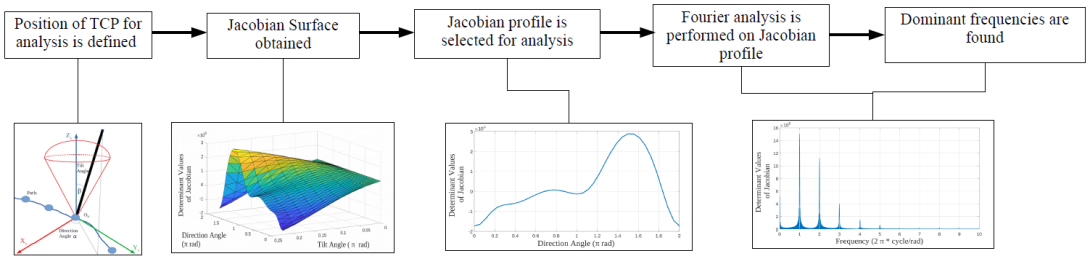


Figure 4-17. Flowchart for the DFA of the Jacobian for a given TCP position.

In order to validate the proposed spectrum analysis through DFA, a reconstructed profile is obtained using the information extracted from the DFA (Figure 4-17**).** Then both profiles are plotted (Figure. 4-18) and the error along both profiles is then calculated to be 2.21% based on a normalised percentage root mean square difference (NPRD) [103].

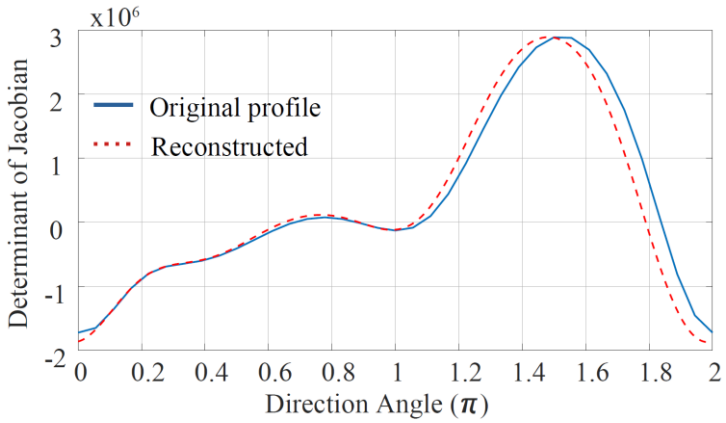


Figure. 4-18. Comparison between the original Jacobian profile and reconstructed one by DFA.

With this validation it is proved that the information extracted from the DFA is capable to accurately represent the Jacobian related to the configuration of the RPKM. Then this information is used to optimise the positions of the upper joints on the platform in the following subsection.

4.3.2. Singularity Optimisation of the RPKM

Although the singularity of a 6-DOF PM is impossible to be graphically represented, as the locus is a six-dimensional hypersurface, in this paper the singularity behaviour is presented at each element of interest inside the workspace. However, the procedure is observed to be high source consuming to analyse the full workspace, given that a great number of iterations are required for each element. For this reason, a novel method is proposed in this section to represent the Jacobian surface based on the Fourier transform and to obtain a singularity-free path for the TCP which is achieved by optimising the upper joint location of the proposed RPKM. An optimisation strategy based on Genetic Algorithms (GA) [104] is developed to select the shape of the singularities surface to one not crossing the zero value. Lower dominant frequencies are weighted to elevate the fitness and avoid singularities. With this, a simplified shape of the Jacobian surface is obtained and therefore the unstable configurations are avoided. First, the method proposes a population with random layouts of the upper joints, then computes the DFA (Figure 4-17), selects the elements with the best performance, creates a crossover of the characteristics of the best elements and includes mutations to the new elements of the generation being

created. This process is iterated in several generations where a maximum number is established as the limit of generations, this process is illustrated in Figure 4-19.

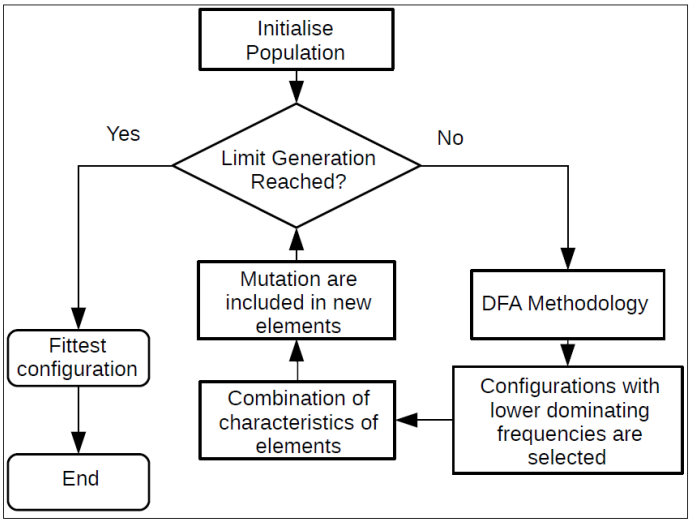


Figure 4-19. Flowchart for the configuration optimisation to avoid unstable configurations.

As a case study, a configuration of the proposed RPKM is studied with the lower joints accommodated in a random manner (Figure. 4-12b) and the upper joint locations are optimised according to the method described previously. The result from the optimisation using GA shows that the configuration of the upper joints allows increasing the performance of the machine proposed. Figure. 4-20a-b show the Jacobian determinant values after the optimisation of the locations for the upper joints and there is no pattern close to the critical value of zero (singularity). Furthermore, observing the frequency analysis (Figure. 4-20c) the first frequency (A_0) has become dominant, influencing the pattern of the Jacobian, displacing it over the zero value and preventing the singularities (compared to Figure. 4-16a).

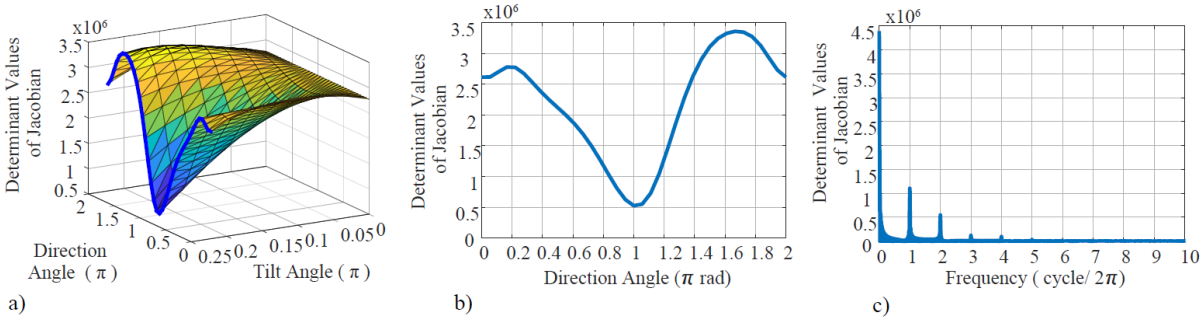


Figure. 4-20. Results after optimisation using GA for: a) Jacobian surface for an WS element; b) Jacobian profile at tilt angle of 0.25π; c) frequency vs Jacobian.

In order to validate the proposed method, a machining tool path is proposed for the TCP (Figure. 4-21), which is a circular with an inclination angle of 0.25π and conformed by 360 elements with a diameter of 32 mm. The centre of the path is considered to lay on the machine origin. This path is selected such that the mechanism under analysis has to perform high tilt angle operations with different approach angles to the required positions, which increase the possibilities to find singularities in the planned task.

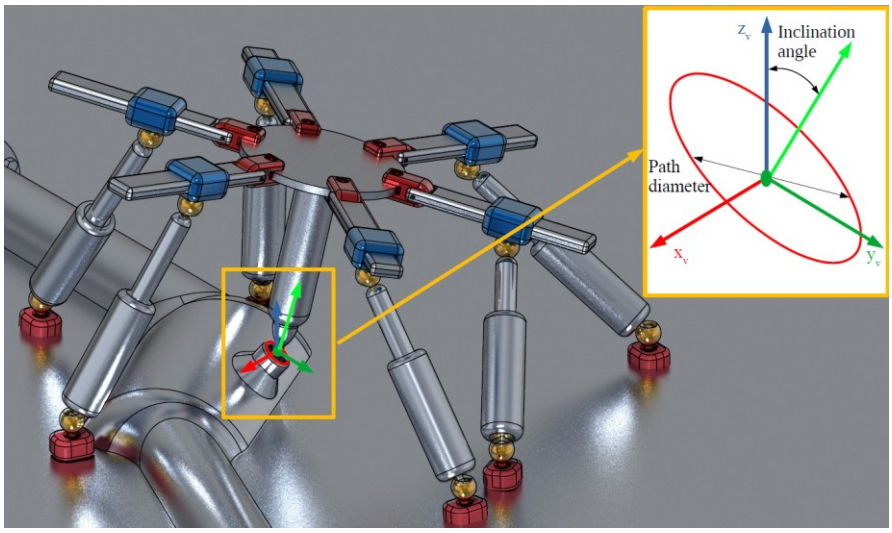


Figure. 4-21. A case study for a proposed path considering a circular trajectory with an inclination of 0.25 π

First, a random configuration is proposed for the upper joints. Then the location of the upper joints is optimised using GA with the same location of the lower feet. Therefore, the influence on the behaviour of the singularities relies only on the upper joints. Figure. 4-22a presents the behaviour of the machine in a non-optimal

configuration for the task previously proposed while Figure. 4-22b shows the values for the determinant of the mechanism in an optimal configuration.

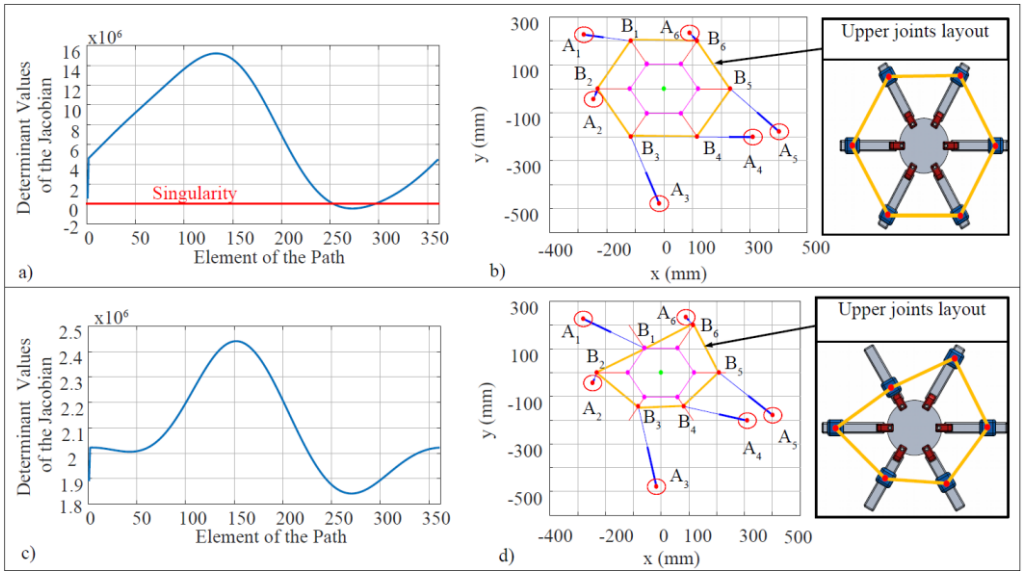


Figure. 4-22. Element of planned path against the determinant value of the Jacobian. a) Non optimised configuration Jacobian values; b) non optimised joints layout; c) optimised configuration Jacobian values; d) optimised joints layout.

After the proposed methodology selects the optimal configuration (Figure. 4-22d), the behaviour of the machine is singular-free (Figure. 4-22c). It is possible to conclude that after this optimisation the RPKM is capable to comply with the required task, avoiding unstable configurations and preventing loss of control or damage to the mechanism caused by singularities. Besides, a Fourier-based methodology has been presented to efficiently analyse and decompose the Jacobian of the proposed RPKM. This methodology allows to trace the sub-components of the Jacobian determinant and presents the capability to predict unstable configurations. Furthermore, this strategy is used to reconfigure the upper joints layout to avoid singular conditions and comply with the operation to perform (e.g. drilling, milling, etc) within non-conventional environments such as for repair and manufacture. This optimisation is achieved using genetic algorithms where the lower frequency waves are weighted to propose an optimised stability pattern, which is then used to consider the fittest from the population.

4.3.3. Validation of singularity analysis and optimisation

In Section 4.3.3, the configuration of the proposed RPKM has been optimised to produce a path free of singularities, which relates to the Jacobian of the system. As it is difficult to validate the Jacobian of a physical system, the stiffness of the RPKM is calculated to make an indirect validation, since the stiffness of a manipulator can be easily measured from simulation. If a singular configuration is present in the workspace the stiffness of the system becomes null. Furthermore, the numerical results obtained by the Jacobian stiffness model is then compared with the simulated results from a commercial Finite Element Analysis (FEA) software, for this the same configuration presented in Section 4.3.1 is considered in both analyses.

The Jacobian of the RPKM is challenging to be determined and validated in any form of direct simulation, but is related to the stiffness of the system. Therefore, it is necessary to connect the characteristics of the stiffness by means of two different approaches. In this section the modelling of the stiffness of the RPKM is introduced. This comparison is evaluated on an analytical methodology of the stiffness, later a finite element analysis based on a commercial software is presented to validate the results obtained and compare the stiffness by both methods. Firstly, the stiffness matrix of a parallel manipulator [101] can be obtained based on the Jacobian as:

$$K = J^T K_l J \tag{18}$$

where K_l represents the diagonal matrix for the stiffness of the limbs and J represents the Jacobian matrix. By considering the limbs acting as link elements, the only possible deformation is along the length direction. Assuming that the stiffness of each link element is considered to be identical as k, Equation. (18) can be then simplified as:

$$K = k J^T J \tag{19}$$

Furthermore, the displacement and rotation, ΔX, of the end-effector at a PKM produced by the applied forces and moments, F, can be obtained as:

$$\Delta X = K^{-1} F \tag{20}$$

In addition, an FEA model is established in the ANSYS APDL® environment as shown in Figure. 4-23. As several configurations must be analysed to perform the desired tool path of the proposed RPKM, the computational burden and characteristics of the key elements in the FEA model are defined as follows:

- The limbs are considered to perform as link elements with a constant stiffness k.
- The lower joints are constrained of any possible displacement.
- The upper joints are connected to the end-effector by rigid elements.

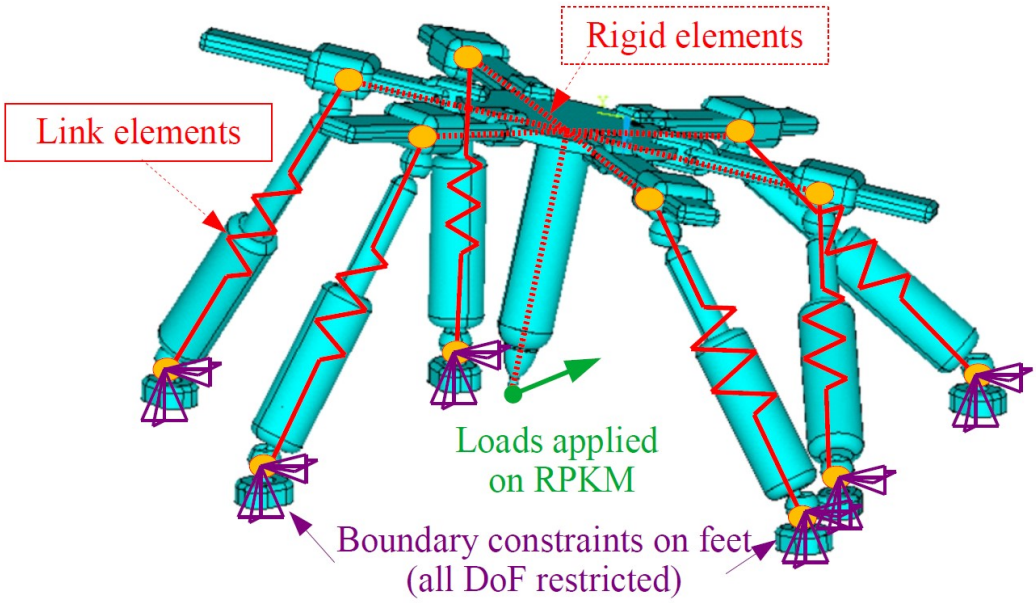


Figure. 4-23. An FEA model used to evaluate the stiffness of the proposed RPKM.

The stiffness of the proposed RPKM is presented by means of the numerical results which are calculated by the Jacobian-based stiffness model from Equation. (20), and the simulated results that are obtained by the FEA. Both methods consider the same load conditions and setup configuration for the comparison. To obtain a scalar value that permits to evaluate the global stiffness of the RPKM, the norms of ΔX and F are obtained and used to estimate a global value for the models proposed; these are compared with the results obtained by FEA. This comparison starts by estimating the stiffness of the RPKM by both methods, with normalised values to allow it to be independent from the scalar k.

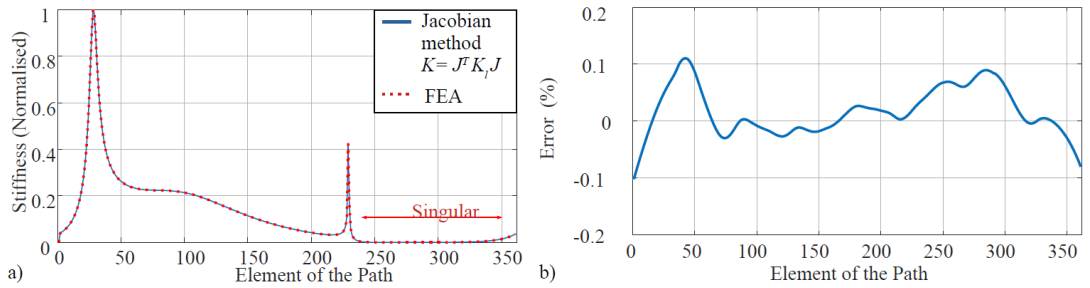


Figure. 4-24. Stiffness of the RPKM when conducting a circular path in Fig. 14a: a) Jacobian stiffness model vs FEA-based model; b) percentage of error between both models.

In order to validate the proposed methodology for singularity optimisation, the same non-optimised and optimised configurations of the RPKMs and the tool path in Section 3.2 are applied to perform stiffness analysis and the results are presented in Figure. 4-24 and Figure. 4-25.

Figure. 4-24 shows a good correlation between the stiffness values obtained by the FEA-based and the Jacobian-based models, where the absolute error can be calculated as smaller than 0.1% (see Figure. 4-24b). It can be noted that the non-optimised configuration leads to instabilities between the elements 250-350 along the predefined tool path as the stiffness becomes to zero, which is similar to the singularity results shown in Fig. 14a.

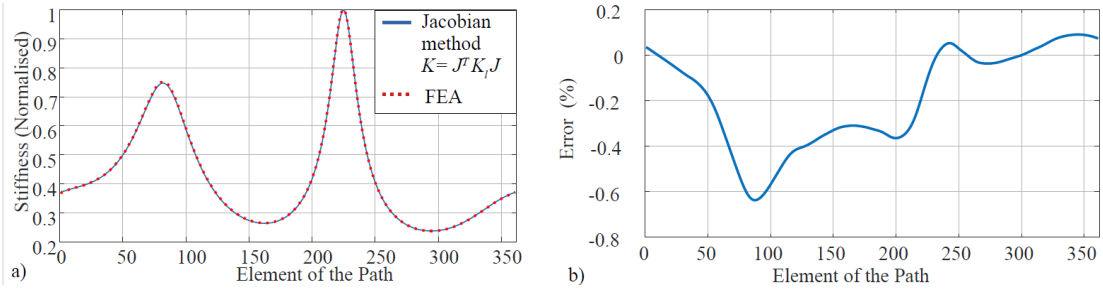


Figure. 4-25. Stiffness of the RPKM when conducting a circular path after an optimisation; a) Jacobian stiffness model vs FEA-based model; b) percentage of error between both models.

The stiffness of the RPKM is then evaluated between both models with the optimised configuration obtained in Section 4.3.2. In Figure. 4-25, it can be noted that the value of the global stiffness is greater than zero for all the elements of the path proposed. It

can be indicated that after the optimisation the unstable configurations are not present in the path. Furthermore, the proposed optimisation methodology is validated to be an effective and efficient approach to reconfigure the proposed RPKMs to adapt to the place of intervention with singularity-free configuration.

4.4 Conclusions

This chapter reports on the concept of a new class of reconfigurable parallel kinematic manipulators. Based on the kinematics and workspace analysis the Concept 2 presented in Chapter 3 is selected to continue with the design. Concept 2 is considered as a RPKM able to:

a) Adapt and operate on non-conventional sites of manufacture and repairmen, thanks to the repositioning of the upper joints on the moving platform and the free positioning of the lower joints, the RPKM can modify its workspace and be positioned on non-flat surfaces. To safely operate in the versatile workspace the kinematic and workspace analysis has been carried out, considering the limitations and possible collisions between its mechanical components.

b) Prove the versatility of the reconfigurable parallel manipulators not only to modify the workspace but for the avoidance of singularities. To overcome the presence of singularities inside the versatile workspace a novel methodology based on the Fourier analysis has been introduced which can reduce the computation time compared to conventional methods. In this analysis the Jacobian has been decomposed to identify its subcomponents and use them to detect singular configurations and later for its avoidance by optimisation.

c) Open the opportunity for developing future portable machine tools by utilising the reconfigurable capabilities of RPKMs, as the necessary tools for its analysis have

been provided in this chapter (i.e. workspace analysis, singularities identification and optimisation). Therefore, designers can use this paper as a reference to further design of RPKMs.

Chapter 5 **Design**

This chapter focuses on the description of the design of the proposed RPKM as based on Concept 2, initially presented in Chapter 3. Furthermore, the design presented in this chapter is based on the results obtained in chapter 4. The systems integrating the RPKM are described to increase the adaptability to machining and walking operations. More importantly, the design is focused on a reconfigurable strategy to enhance the RPKM adaptability and exploit different configurations to extract the most advantageous structures. First, the RPKM design is presented based on the reconfiguration mechanism on the moving platform. The reconfiguration design is proposed based on six identical clutches relying on Shape Memory Alloy (SMA) and a system of wire rope and pulleys.

5.1 **Conceptual design**

In Figure 5-1, a conceptual design of the proposed RPKM is presented as converted from the conventional Gough-Stewart platform by removing the fixed base (to free six feet) and integrating the moving platform with a repositioning mechanism. More specifically, the repositioning mechanism consists of six identical clutches and a rope-pulley mechanism driven by a single motor (see Figure 5-1b). Each clutch connects a limb to the moving platform. The limbs are composed of a series of joints in a spherical-prismatic-spherical (SPS) configuration. The upper S-joint of each limb is fixed with a clutch, allowing to reposition the limbs layout on the moving platform(see Figure 5-1c). Furthermore, in contrast to conventional PKMs, removing the lower fixed base provides the flexibility to directly adapt to the intervention site. Furthermore, removing the fixed base also confers the walking capability under

challenging conditions, such as uneven surfaces, constrained spaces and slopes. Figure 5-1d-f proposes the RPKM with three configurations to traverse over uneven terrain, walk on narrow paths and walk on inclined surfaces.

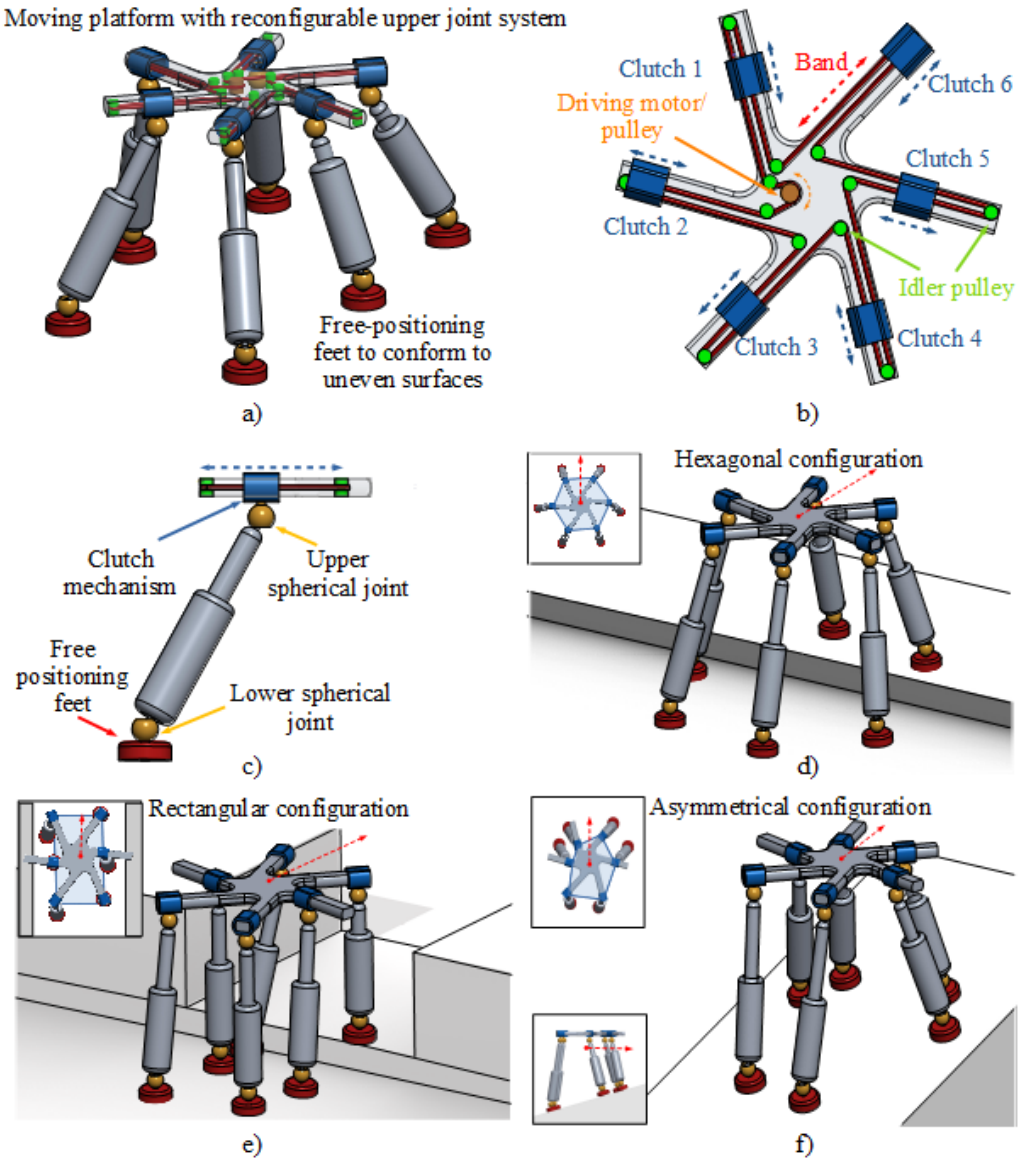


Figure 5-1. Illustration of the proposed RPKWM design.

However, to achieve a practical design of the proposed RPKM, three main challenges need to be addressed:

1. **Optimising the layout of clutches on the moving platform.** For this, a symmetric layout has been decided with each clutch and slide positioned along the radial direction of the moving platform. This is based on the maximum workspace analysis presented in Chapter 4, as the intention is to increase the machining capabilities over more significant volumes.
2. **Switching the upper S-joints between passive and active modes.** The upper spherical joints are required to act as passive when the system is in machining mode, while each joint is required to be active during the walking operations. A dual-mode tendon-driven upper S-joint has been adopted to design the limbs as presented in [87]. This design allows each upper S-joint to switch between passive and active modes by releasing and tensioning three tendons. The S-joint is in active mode when three tendons are tensioned and in passive mode with released tendons.
3. **Actuate efficiently and compactly the clutches for relocating the upper joints.** This challenge comes after the limitations of conventional mechanisms representing heavy and bulky designs with several motors and transmission systems, especially as six clutches need to be implemented on the moving platform. Therefore, a novel repositioning clutch system is required.

The next sections describe the design implemented to tackle these challenges.

5.2 **Design overview**

As shown in Figure 5-2, the proposed RPKM is based on an architecture with six limbs (each with 3-DoF) that are connected to a moving platform by a novel repositioning system appointed in this document as Smart Actuation System (SAS). Furthermore, in contrast to conventional PKMs, the lower fixed base has been removed, and the positioning of the limbs on the moving platform is reconfigurable. Removing the lower base provides flexibility to place the RPKM directly on the intervention site and to use the limbs to walk on different surfaces.

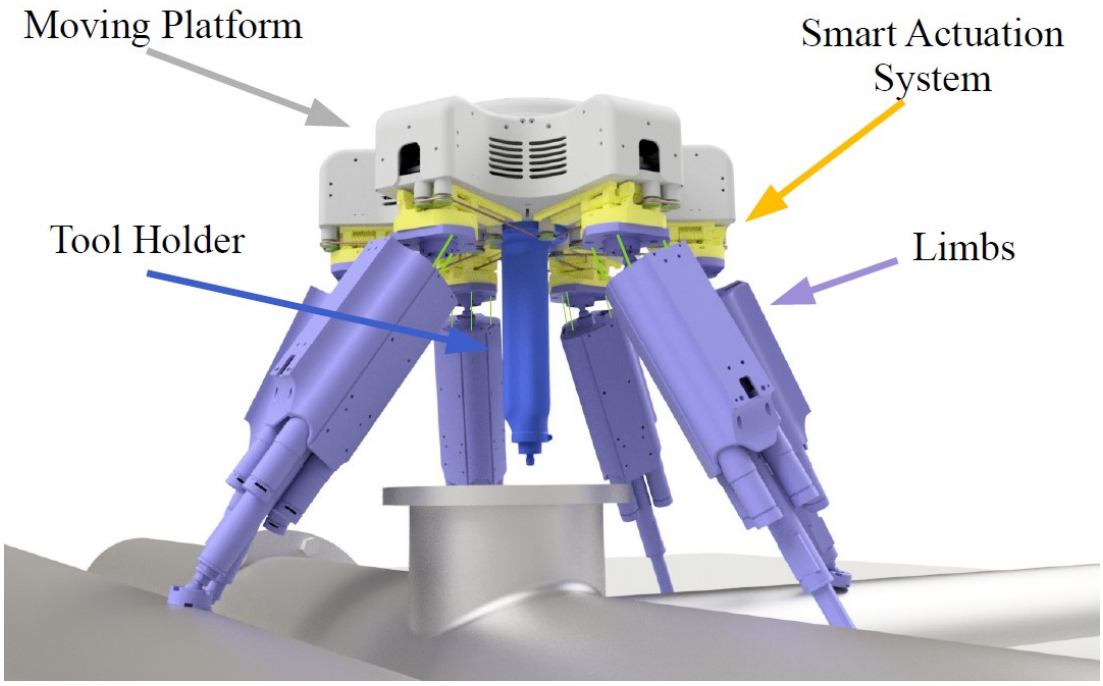


Figure 5-2 Reconfigurable Parallel Kinematic Manipulator. The illustration presents the capability of the RPKM to place its limbs on complicated to operate environments for in-situ repair.

The design has integrated three central systems to achieve optimised capabilities for walking and machining. These systems are six 3-DoF limbs, six 1 DoF Smart Actuation Systems (based on smart memory alloy), and a moving platform containing the electronics for automation. Further, the design considered a tool holder to comply with inspection, manufacturing and repair operations with different devices (i.e. spindle, probes, etc.). A detailed description of each subsystem is presented in the next sections. Furthermore, the design is planned to incorporate six magnetic feet, capable to actuate in passive and active modes. In active mode each foot is capable to resist a sheer force of 490 N, making them ideal for machining operations in locations with ferromagnetic surfaces. However, this part of the work is under development, and this thesis will not describe fully its design and operation as the work relates to the research which under development.

5.3 **Platform Design**

The platform design considered the integration of the limbs and the repositioning system for the upper joints. Furthermore, the platform is designed to contain and protect the electronic systems of the RPKM for increasing its autonomy in the future. Nevertheless, for the tests and analysis performed, the system is provided with electrical power from an external power supply. In the future, the system can be integrated with independent batteries to increase the autonomy and remote operation of the RPKM.

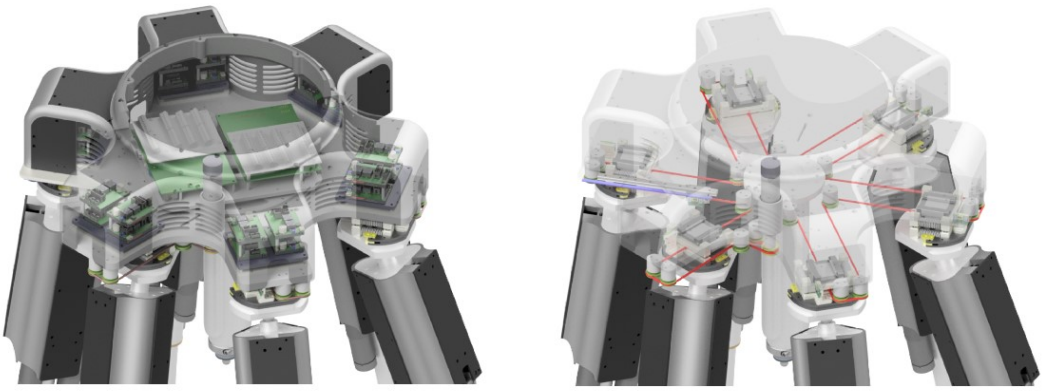


Figure 5-3. Illustration of the platform design, the design considered: a) the integration of the electronics on the platform to increase autonomy. b) Integration of the SAS clutch system on the platform for improved performance.

5.4 **Smart Actuation System**

The Smart Actuation System is based on the concept initially proposed in [105] and . [106]. However, the system presented in [105] was a model intended as a prove of concept and several modification had to be included. This modifications required the system to be able to withstand an opposing force of 31 N, and capable to reposition individually or simultaneously 6 joints. Similarly, the SAS incorporated a reference system, for tracking the location of the joint between the two ends of a closed loop wire-rope. More details are provided later in this chapter will be described.

Aimed to reposition six clutches individually with a single motor, the SAS is proposed consisting of six identical Shape Memory Alloy (SMA) clutches, six linear slides, a series of pulleys, a wire-rope band and a single motor for its actuation, as shown in Figure 5-4, where:

- Each SMA-clutch mechanism is integrated with a linear slide to position the corresponding upper S-joint along the radial direction (blue dashed arrow) of the moving platform.
- A wire-rope band (red component) that passes through all the SMA clutches.
- A series of idler pulleys (green components) that guide the wire-rope band.
- A DC motor with a driving pulley that actuates the wire-rope band (orange component).
- A knot referencing mechanism that traces the position of the knot of the wire-rope to prevent blockages.

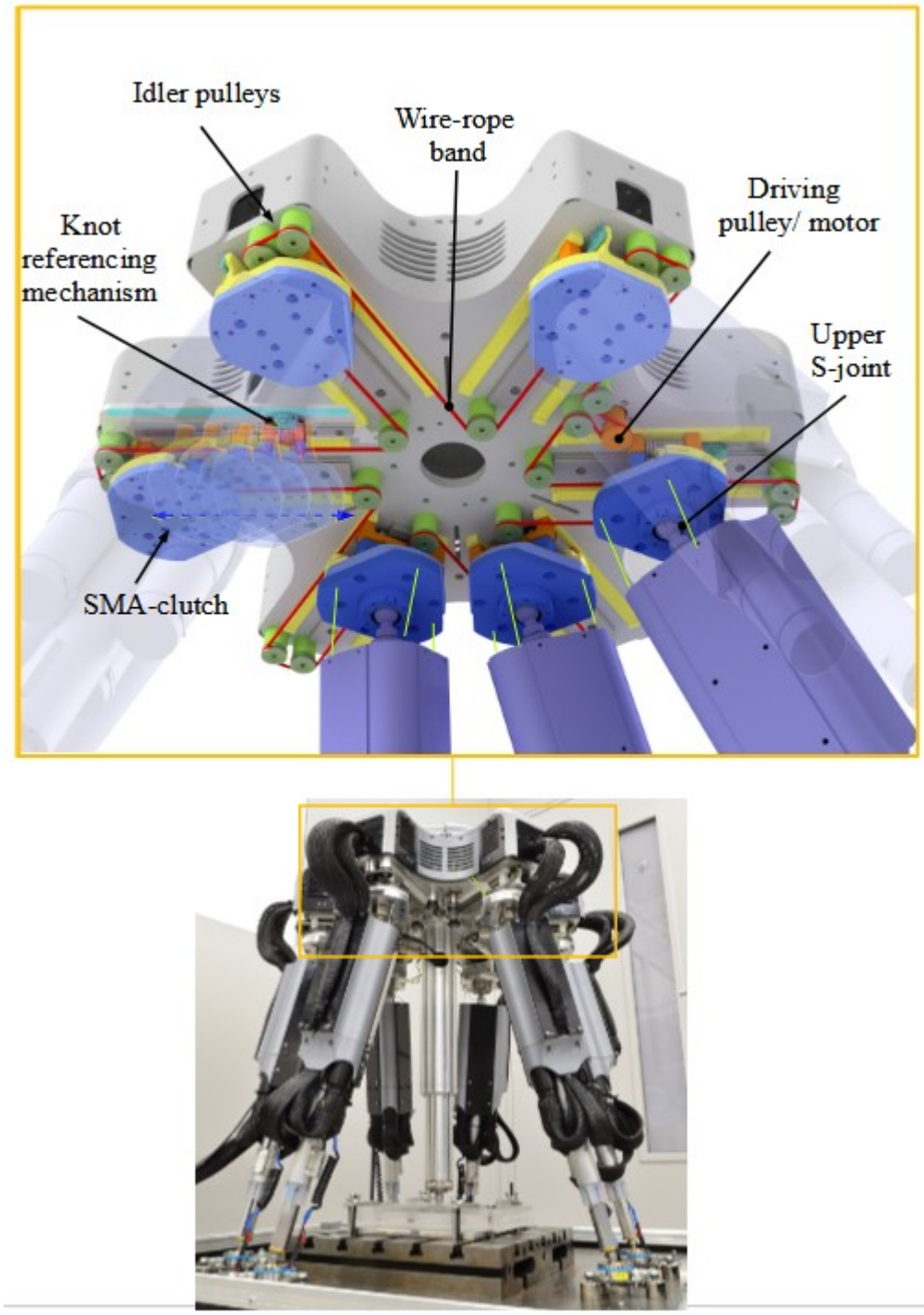


Figure 5-4. Illustration of the proposed RPKM design over a scenario with uneven surfaces: a driving pulley/motor (orange) actuates a wire-rope band to reposition six upper S-joints.

The main advantage of integrating these systems relies on the SMA clutches, which allow repositioning six limbs on the moving platform with a single motor. In

contrast, conventional actuation packages would require a motor and several accessories (i.e. gearboxes, spindles, guides) for each limb, adding up to the total weight of the RPKM. More importantly, the reduction of the components needed for the repositioning allows reducing the total mass on the moving platform. Reducing the weight on the moving platform is of high importance for the performance of the RPKM, as the inertial forces are reduced during machining and walking operations. SMAs are known for their capability to exert a high wrench compared to their volume [107]. This characteristic has allowed the creation of lightweight miniaturised systems incorporating SMAs in their design (when compared to electromechanical, hydraulic, and pneumatic actuators). Furthermore, successful applications of SMAs in the aerospace industry [108] and medical devices [109] have shown their advantages in metamorphic and intelligent structures as compact and lightweight devices. For these reasons, SMAs are considered in this thesis for the development of a novel repositioning system.

5.4.1. SMA-clutch mechanism

The SMA-clutch design (Figure 5-5) is composed of a pair of shift pads, a pair of braking pads, an SMA wire, an encoder, and a linear guide. By powering on/off the SMA wire with electrical power, the SMA-clutch mechanism can perform the engagement (Figure 5-6a) and disengagement (Figure 5-6b) between the shift and braking pads to lock its position. When the SMA wire is active, the shift pads release the braking pads(Figure 3b) and grasp (Figure 3c) the wire-rope band simultaneously, allowing its repositioning by moving the wire-rope band. The wire-rope band passes through the centre of each clutch and forms a closed-loop pattern on the moving platform. Furthermore, The band movement is actuated by a single motor, which permits the positioning of the six clutches connected to the limbs, as

shown in Figure 5-4. Therefore, by powering on/off the SMA wire and collaboratively actuating the wire-rope band, the proposed SMA-clutch mechanism can be utilised to reposition six joints on the moving platform along with each slide.



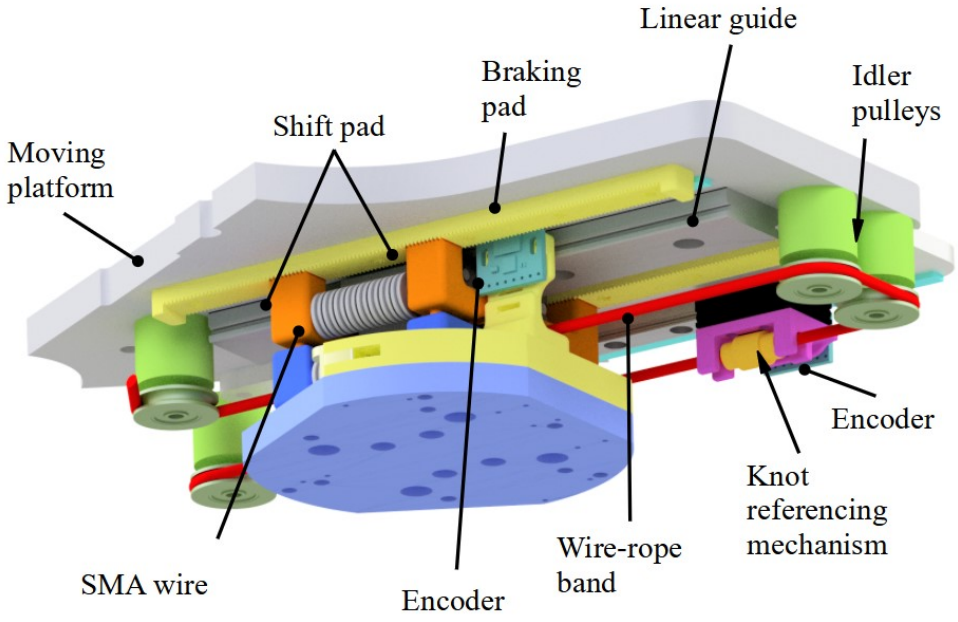


Figure 5-5. Illustration of the SMA-clutch with its main components.

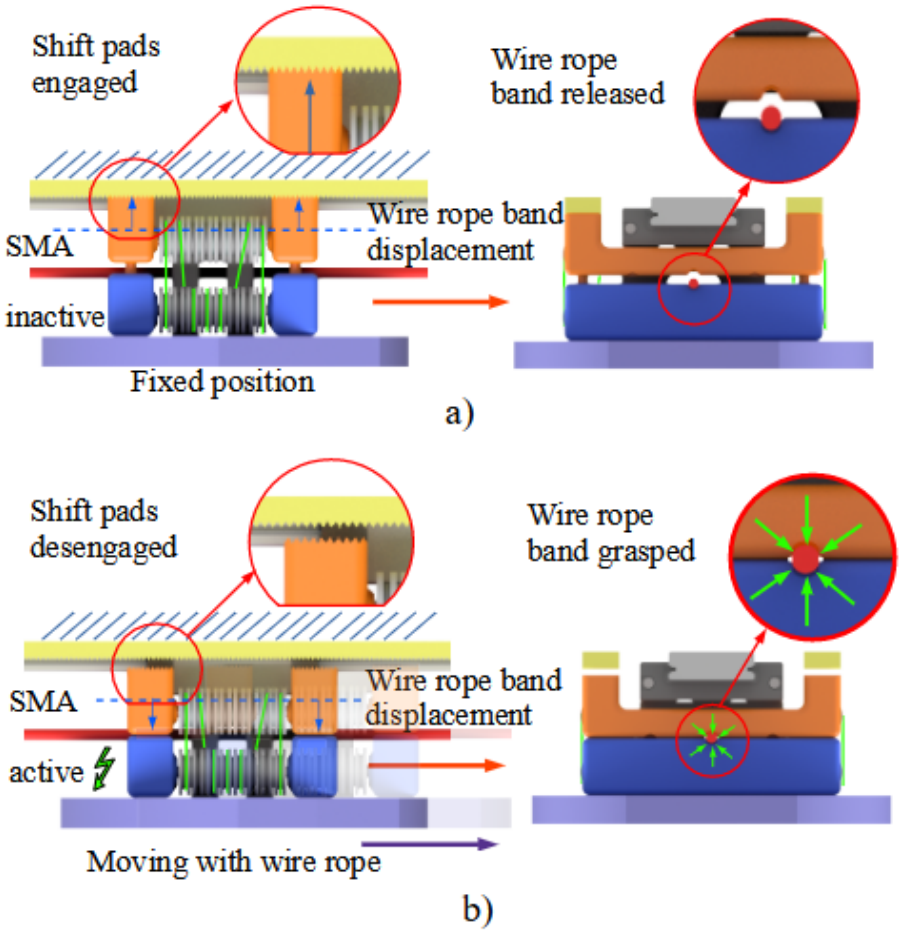


Figure 5-6. Illustration of the SMA-clutch with its working modes; a) SMA inactive, the shift pads are engaged, the position is locked; b) SMA active, the sift pads grasp the wire-rope band, displacement follows the wire-rope band actuation.

5.4.2. SMA wire characterisation

According to [110], more than 20 000 patents have been issued on applications involving SMAs in their design. The reason motivating these applications relies on the capability of SMA to reduce the complexity of conventional actuation systems (hydraulic, pneumatic, electric motors). However, the available products developed with SMA actuation have been considerably limited as better methodologies to achieve the desired performance need to be developed

To ensure that the SMA clutch is able to produce the required grasping force during its operational life, a series of tests have been performed to obtain the actuation forces exerted and select the most suitable working conditions for the SMA. The main parameters to define are the actuation force, the current and the restoring force (pre-stress conditions) to operate the SMA. The last two parameters are essential, as providing high current values to the SMA can damage it prematurely. On the opposite condition, providing a low current reduces the actuation forces and increases the response time of the SMA wire. Similarly, not delivering the right pre-stress force can lead to the reduced operational life of the SMA wire.

For these reasons, a test rig has been designed and implemented to obtain the parameters to operate the SMA wire optimally. As shown in Figure 5-7, the design consists of three sliders mounted on a rail with two connectors and an encoder per slide, three limiting and adjustable blocks, an SMA wire, an FPGA, one Arduino, a wattmeter and a motor controller.

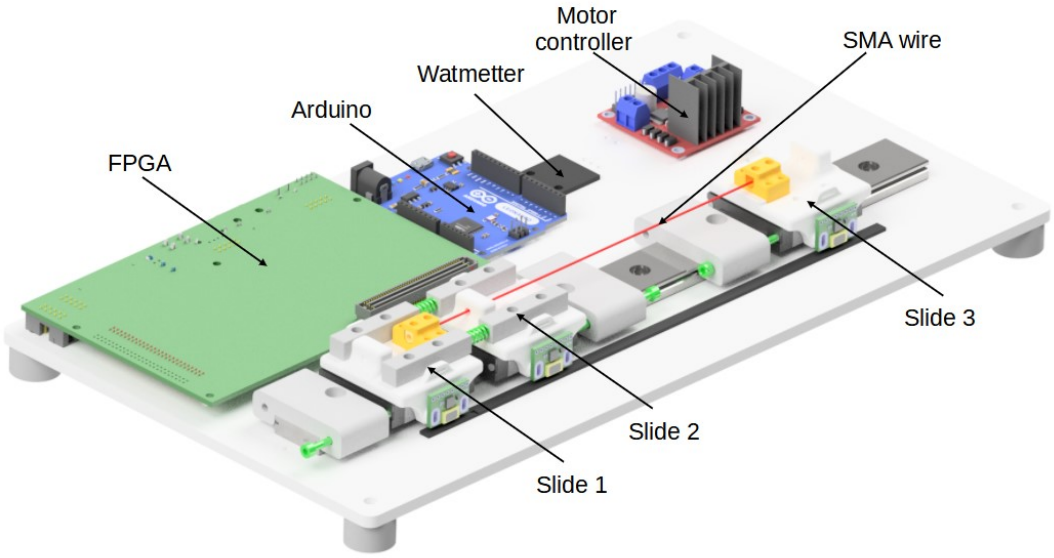


Figure 5-7 Illustration of the test rig for the characterisation of the SMA wire with the main components.

As shown in Figure 5-8, the SMA wire is connected to slides 1 and 3, while slides 1 and 2 are connected by means of a pair of springs. These springs are preloaded by limiting the maximum distance between slides 1 and 2. Two bolts attached to the limit blocks control the distance between slides 1 and 2. The force exerted by the springs is directly transmitted to the SMA wire, providing the necessary restoring force when the SMA is cooling down. Once the electrical power is provided, the SMA heats up and thus, slides 1 and 2 are brought together; the relative displacement of the three slides is traced by the encoders and recorded by the FPGA. The FPGA also provides the necessary outputs signals to control the electrical power by means of the motor controller. The Arduino is used to read the values from the Wattmeter and send the read values to the FPGA.

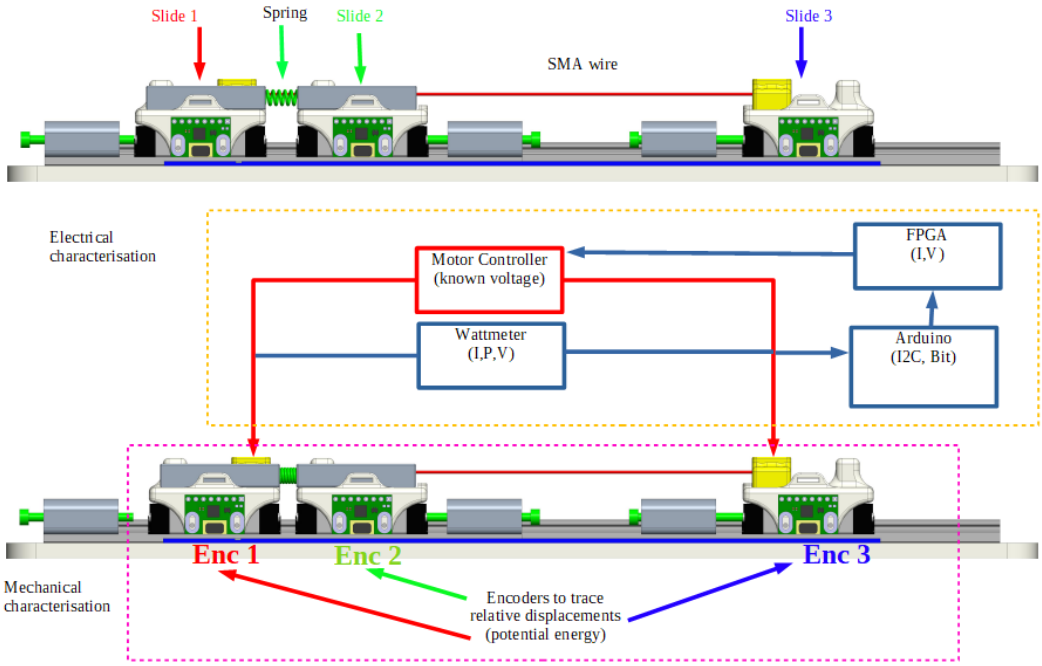


Figure 5-8. Illustration of the mechanical and electrical connections for the test rig.

More importantly, this test rig allows characterising the SMA in terms of its mechanical and electrical performances. Several tests have been performed, providing different pre-stress values to the SMA wire with different currents and voltage values.

Pre-load value (N)	Current (A)	Pre-stress Value (MPa)
1	0.25-1.5	8.0675
2	0.25-1.5	16.135
3	0.25-1.5	24.202
4	0.25-1.5	32.27
6	0.25-1.5	48.405
8	0.25-1.5	64.54

The maximum value for the preload is limited to 8N as this force relates to the maximum stress that the SMA-wire can resist before getting damaged. Similarly, it has been observed that providing currents higher than 1.5 Amps damaged the SMA wire, and thus the maximum value is limited to 1.5 A. Each test considers the maximum force exerted by the SMA wire, the time to reach a steady-state (in terms of the force) and the time required to cool down (when the SMA wire reaches a neutral state). This information is extracted from the displacements of the encoders and relates the forces and displacements on the SMA wire when the system is preloaded from 1 to 8 N and at a range of 0.25-1.5 Amps. This information is illustrated in Figure 5-9 for the case of 1N of preload, 0.25 Amps .

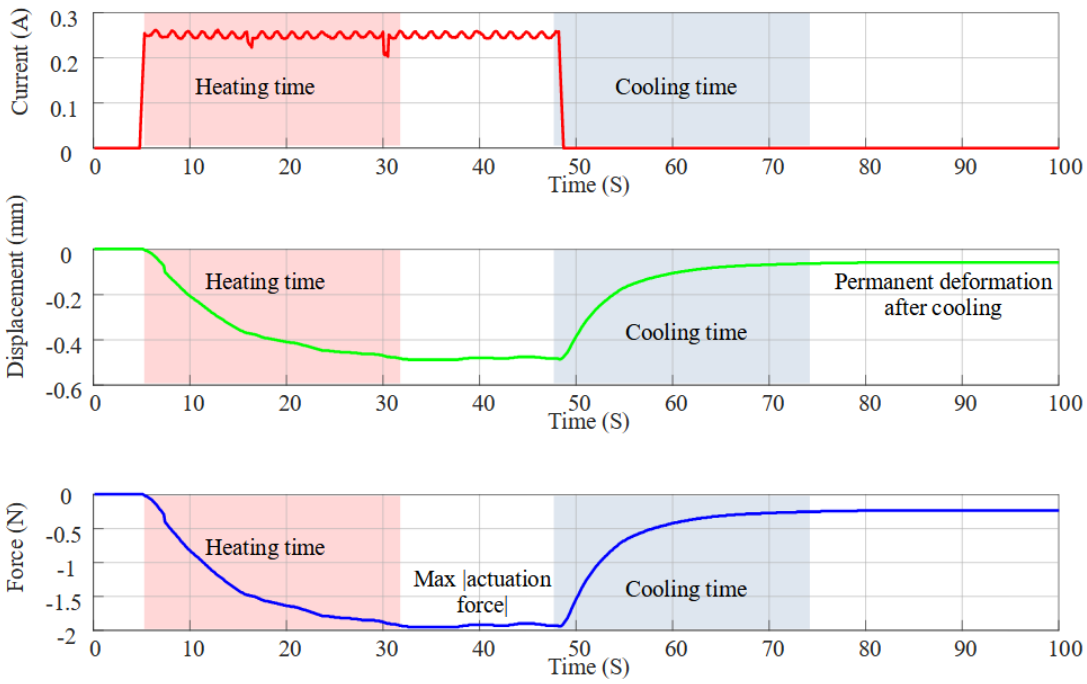


Figure 5-9. Relation between force time and current provided.

More importantly, the information extracted from these tests is compiled in Figure 5-10. Although the maximum force is achieved when the system is powered with 1.5 Amps, although the 1.5 Amps showed to damage the SMA wire in iterative tests. For this reason, the operational current is established to be at 1.2 Amps.

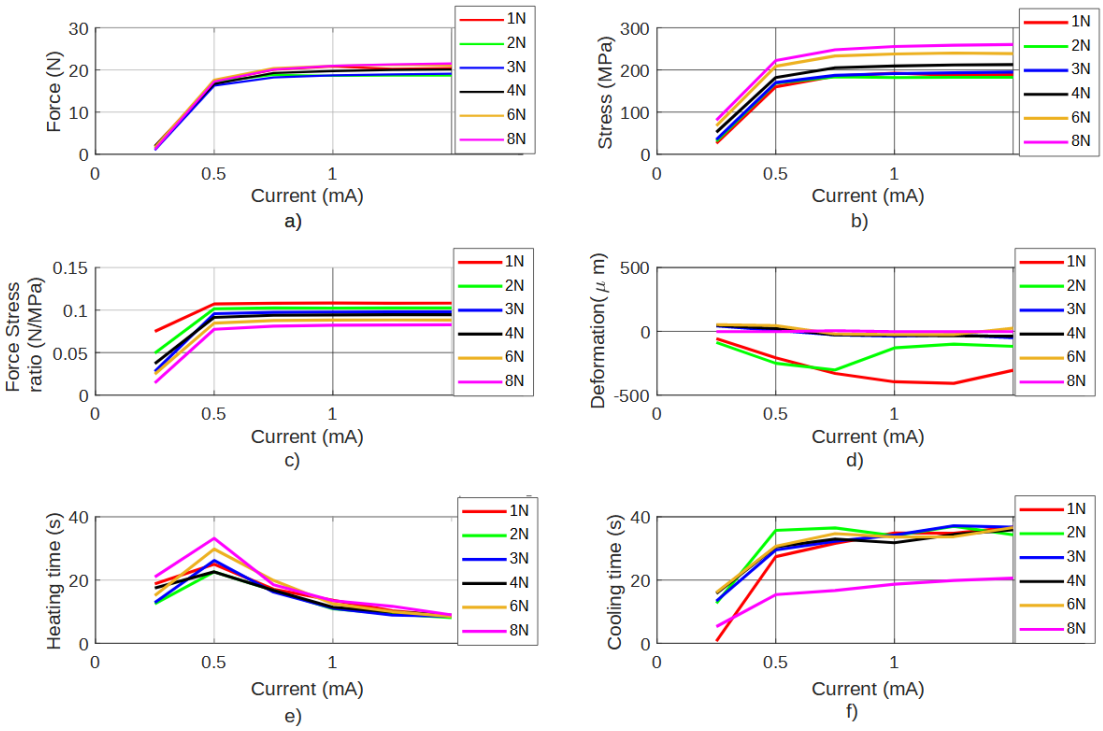


Figure 5-10. Characterisation of SMA wire. a) force vs current; b) Cooling time vs current; c) Heating time vs current; d) Efficiency vs current.

The information presented in Figure 5-10 is used to create a table with the fittest characteristics of the SMA for the clutch. This table ponders the best performance with different operational conditions. The attributes of Force/stress ratio, final deformation, heating time and cooling time are rated from 4 to 1 (considering 4 as the fittest). Similarly, the performance of each preload is rated from 1 to 6, rating as 6 the best performance and with 1 the worst performance. These ratings are considered at 1.5 Amps for each preload condition.

Table 5-1. Pondering table for the working conditions of the SMA wire.

Importance rating	4	3	2	1
Preload	**Force**	**Final Deformation**	**Heating time**	**Cooling time**
8 N	1	6	1	6
6 N	2	5	5	3
4 N	3	4	2	4
3 N	4	3	3	1
2 N	5	2	6	5
1 N	6	1	4	2

Preload	**Force/Stress**	**Final Deformation**	**Heating time**	**Cooling Time**	**Total Score**
8 N	4	18	2	6	30
6 N	8	15	10	3	36
4 N	12	12	4	4	32
3 N	16	9	6	1	32
2 N	20	6	12	5	43
1 N	24	3	8	2	37

From Table 5-1, the preload of 2 N is selected to be implemented in the design of the SMA clutch. Although in the initial test, a maximum deformation of 100 microns is registered for the preload of 2 N, it proved to be neglectable in the clutch mechanism. However, an iterative test considering hysteresis effects should provide

a deeper understanding of the system for longer operational life cycles. Nevertheless, this is considered out of the scope of this thesis and is proposed as future work. Figure 5-11 shows the complete clutch mechanism with the implemented SMA wire around the system and the springs used to pretension it.

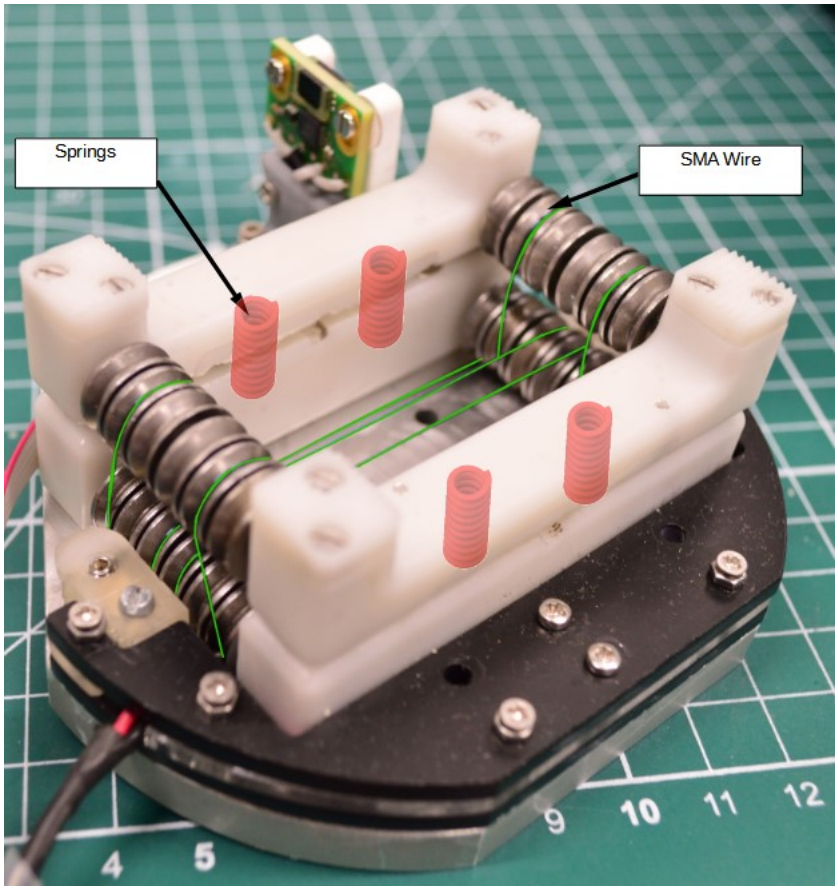


Figure 5-11. Illustration of the clutch mechanism highlighting the SMA wire and the springs for the pretension of the SMA wire.

The preload of 2 N is implemented by compressing four springs of know stiffness. The system is provided with 1.25 Amps when the clutch is actuated as there is no significant force variation between 1.5 Amp and 1.25 Amps (considering 18.6 N for both cases as based on Figure 5-10). Furthermore, the operational life of the clutch is extended as the current is reduced from 1.5 Amps to 1.25 Amps (as overheating is prevented). The total force exerted by the clutch mechanism is computed based on

the loops created by the SMA wire and the force exerted by the springs (F_k), which is considered constant (at the grasping location of the wire-rope band) and equal to 32 N, the equilibrium equation on the system expressed as:

$$F_{t\,SMA} + F_k = 0 \tag{1}$$

Where $F_{t\,SMA}$ is the total force exerted by the SMA wire and relates to the vectors defining the loops in the system. This relation is expressed by Eq. 2 and considers $F_{SMA} = 18.6\,N$. Table 5-2 presents the vectors defining each loop of the SMA and the force exerted by the SMA.

$$F_{t\,SMA} = F_{SMA} \sum_{i=1}^{8} \widehat{\boldsymbol{V}}_{\boldsymbol{Loop\ i}} \tag{2}$$

Table 5-2. Coordinates and unit vectors for SMA wire.

F_{SMA} **20 N**	**Start Position**			**End Position**			**Unit vector components** $(\widehat{\boldsymbol{V}}_{\boldsymbol{Loop\ i}})$		
Loop	**X**	**Y**	**Z**	**X**	**Y**	**Z**	**X**	**Y**	**Z**
1	13	25.15	24	10.5	25.15	6.5	-0.14	0.00	-0.99
2	13	34.95	24	13	34.95	6.5	0.00	0.00	-1.00
3	-13	25.15	24	-10.5	25.15	6.5	0.14	0.00	-0.99
4	-13	34.95	24	-13	34.95	6.5	0.00	0.00	-1.00
5	-13	-25.15	24	-10.5	-25.15	6.5	0.14	0.00	-0.99
6	-13	-34.95	24	-13	-34.95	6.5	0.00	0.00	-1.00
7	13	-25.15	24	10.5	-25.15	6.5	-0.14	0.00	-0.99
8	13	-34.95	24	13	-34.95	6.5	0.00	0.00	-1.00

	$\sum_{i=1}^{8} \hat{V}_{Loop\ i}$	0	0	-7.96

Based on Eq. 1 and 2, the force exerted by the SMA wire is 148 N. However, the real grasping force for the system depends on the friction between the shift pads and the wire-rope band. For this, the static friction coefficient is considered 0.3. (based on literature for PVC on Polioximethyl). As the clutch comprises a pair of pads grasping the wire rope band, the total friction coefficient is 0.6. Representing that the maximum grasping force to oppose a sliding force for the system is 89 N (9 Kg). This is later validated when the system is tested with several loads (2-98 N), as shown in Figure 5-12. However, the maximum force that the clutch mechanism can resist is 74 N (7.2 kg) before the wire-rope band starts to slide. This difference is related to possible variations of the real current provided to the system and possible losses due to friction on the components of the grasping pads.

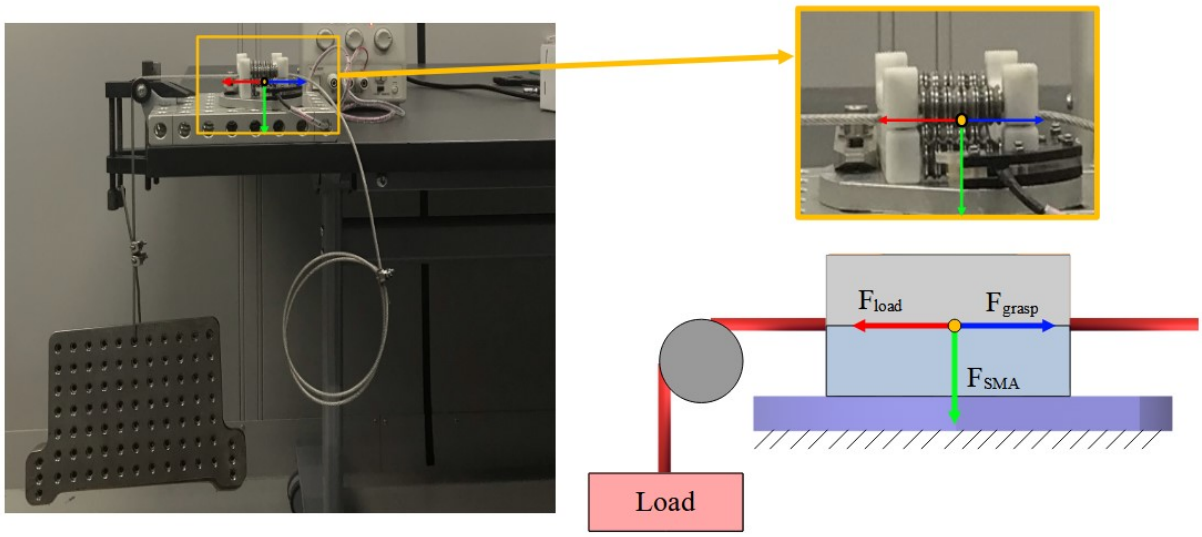


Figure 5-12. Testing of the cutch mechanism to validate the grasping force exerted on the wire rope.

Based on the datasheet provided by the manufacturer of the linear slides, 5.3 N are required to reposition each clutch, this value is below the grasping force exerted by the clutch mechanism and proved to be adequate to reposition each limb when the platform is normal to the direction of the gravitational force. This also represents that the force exerted on the wire-rope can reach a value of 31.8 N if the six clutches are operated simultaneously. Furthermore, the system has to be pre-tensioned prior to operation. Accordingly, this implies that the load capacity of the band needs to be capable to withstand more than 31.8N.

5.4.3. Knot Referencing Mechanism

Another challenge that had to be resolved is related to the wire-rope band by considering the load capability and deformations. Generally, a standard solution of rubber bands is applied in similar band-pulley systems, but with load restrictions smaller than 9 N. However, in the proposed design, the wire-rope band must resist a load of 5.3 N for a single clutch mechanism (plus the pre-tensioning of the system) to operate without significant deformations. Furthermore, it is required that the system can operate several clutches simultaneously (exceeding the maximum 9 N for rubber bands when two clutches are operated simultaneously). As a result, a steel-cored wire solution had to be implemented, requiring clips or a knot connection of the wire-rope ends. However, the diameter of the clips/ knots are larger (compared with the band diameter), which prevents them from passing through the clutch mechanism. Therefore, a knot referencing mechanism is proposed to track the knot position and ensure the wire-rope band actuation in the operational range, as shown in Figure 5-6. By integrating a linear encoder, the knot referencing mechanism can

identify or even relocate the position of the knot, which allows the SMA-clutches repositioning without any blockage by the knot.

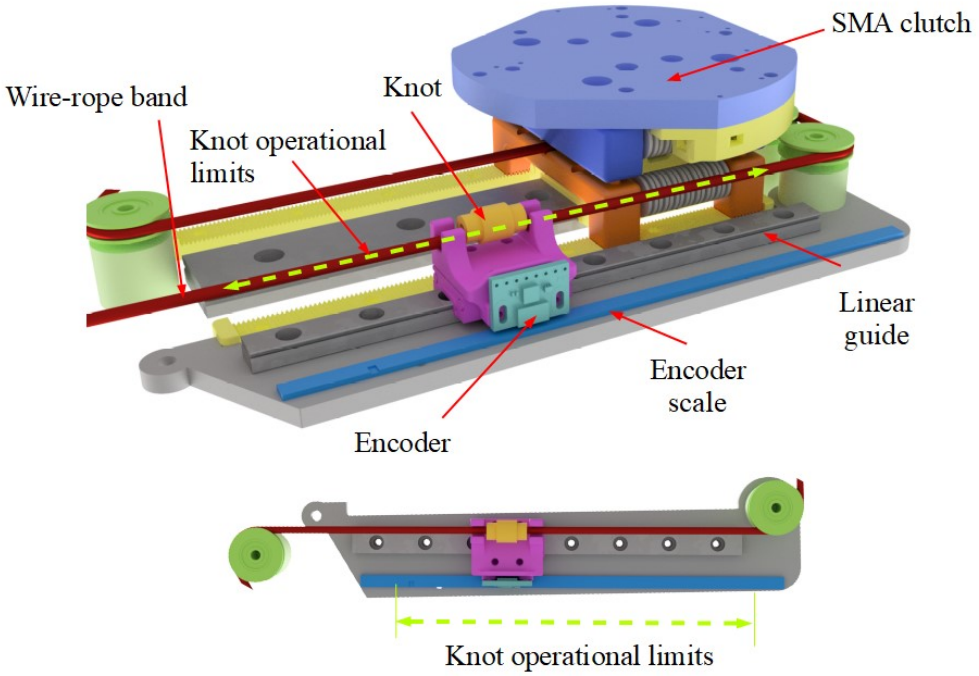


Figure 5-13. Illustration of knot referencing system.

5.5 **Limbs**

The design of the limbs is based on the concept presented in [111] as this system allows to control 3-DoFs (two rotations and one translation), which conforms to the required movements for the proposed RPKM. More importantly, this system achieves an active and passive mode. The active mode controls the orientation of each limb by adjusting the distance between two plates connected by a spherical joint (shown in Figure 5-14). In the passive mode, the tendons are slagged, and the limbs operate as in a conventional Gough Stewart platform. However, to accurately control the positioning of each limb for the design used in this thesis, this section

proposes a kinematic model to accurately control the orientation of each limb. These models are later used in the walking process presented in the next chapter.

For the kinematic model, a local coordinate system, $\{O_s\text{- } X_sY_sZ_s\}$, is declared at the centre of the upper spherical joint, where the x_s-axis is declared to point into the direction of tendon 1, and the z_l axis is considered to be normal to the surface of the upper plate. Then the two angles defining the orientation of each limb are defined $\theta_1 \; and \; \theta_2$ being respectably defined as the direction and tilt angles. A vector **n** is declared, with magnitude equal to one and direction equal to $\theta_1 - 90$ degrees is declared and constrained on the plane y_sx_s. The vector **n** serves as the reference where the rotation of the leg is declared to occur. Another coordinate system is declared on the limb $\{O_l\}$, the axis z_l is parallel to the length of the limb and the x_l positive axis points into the direction of motor 1. A vector called **L** is considered to represent the foot of each limb (starting at the origin of O_l and pointing to the feet of the limb).

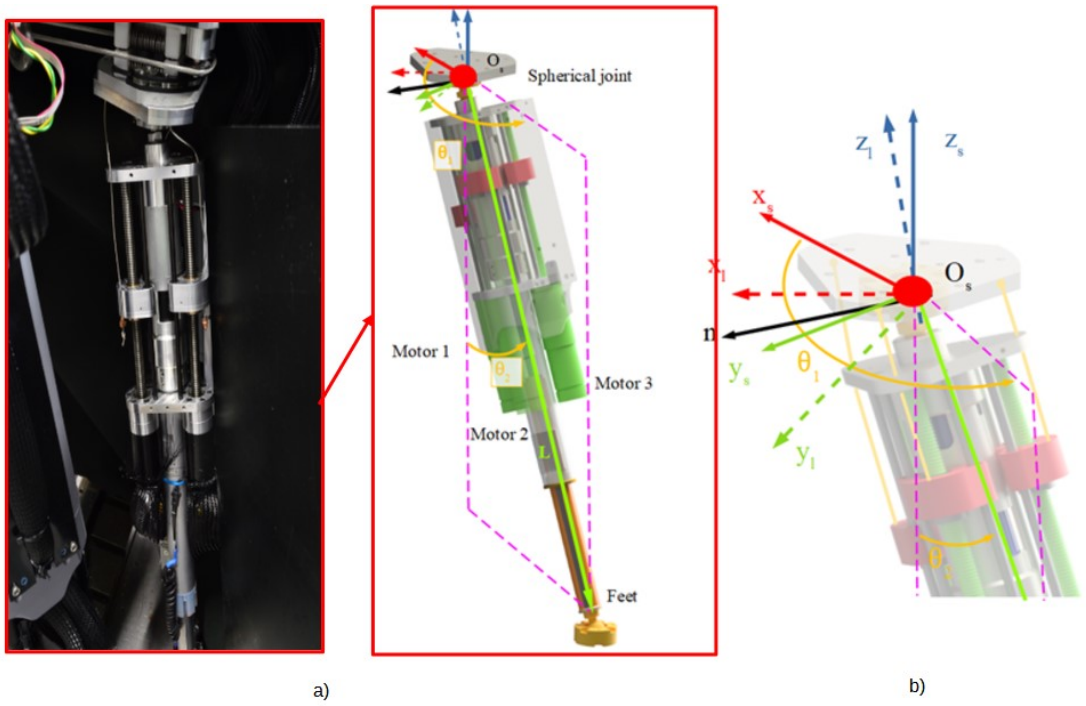


Figure 5-14. Illustration of the limbs. a) Actuation package of the S-joints; b) main reference frames for the actuation of the S-joint.

The rotation of the limb is considered to occur around **n**, in the direction of θ_1 with an angular amplitude of θ_2 as shown in Figure 5-14. Then the positions of interest are traced back to O_s, these elements are the tendon guides ($\boldsymbol{Tl_i}$) on the lower plate of the limb and the tendon guides in the upper plate of the limbs. The equation that relates the position of $\boldsymbol{T_i}$ into $\{O_s\}$ is:

$$^{Os}T_i = {}^{Os}R_{Ol}[\,{}^{Ol}Tl_i] \qquad (21)$$

Where ${}^{Os}R_{Ol}$ is the rotation matrix from the limbs reference frame to the S-joint reference frame. Then the distance between the upper and the lower tendon guides is calculated as the norm of the vector connecting both positions for the tendon guides and is expressed as:

$$T_{length_i} = ||{}^{O}Tl_i - {}^{O}Tu_i|| \quad (22)$$

The nominal length of each tendon $T_{nominal}$ (when the limb is at $\theta_2 = 0$) is compared against the required length to actuate the limb into the required orientations T_{length_i}. This is the subtraction of the T_{length_i} minus the $T_{nominal}$. A similar approach is followed to provide the actuation between two non-neutral positions (θ_1 and θ_2 different to zero.)

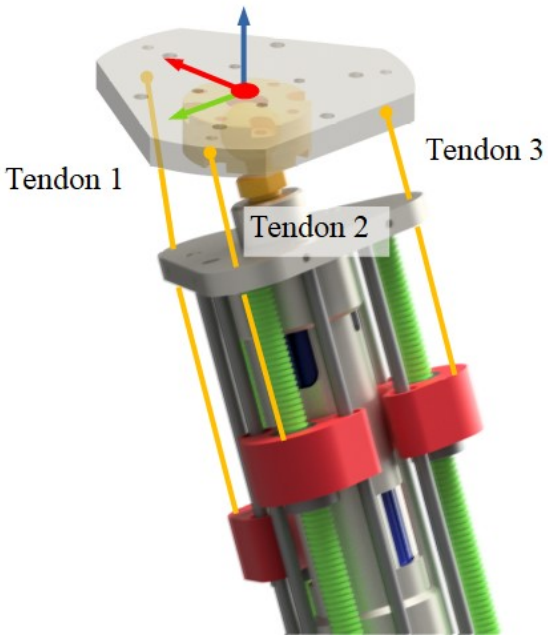


Figure 5-15 Illustration of the design and components of the 3-DoF limbs.

This represents that the S-joint can be actuated in 360º for θ_1, and from 0 to 30º for θ_2 which corresponds to the maximum operational limits of the S-joints. Similarly to achive the different actuation angles, the tendons must modify the relative distances between the upper and lower plates. The required variation of the length for each tendon is represented in Figure 5-16.

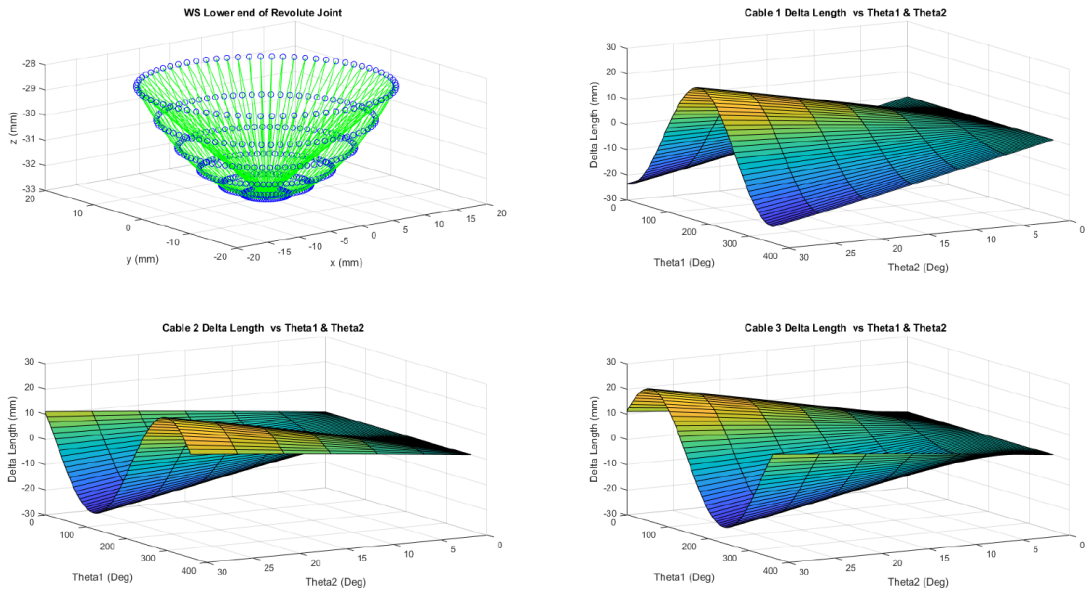


Figure 5-16. Required variation of length toto operate the S-Joint within the operational limits. a) Plot of the centre of the lower end of the S-joint. Required delta length for: b) Tendon 1; c) Tendon 2; d) Tendon 3

Furthermore, the plots presented in Figure 5-16 allow to evaluate the required operational range of the tendons, so the limbs can be operated as a dual-mode S-joint. The S-joints is considered passive when the tendons are slagged and active when the tendons are brought to tension.

To evaluate the effectiveness of the proposed models, a test implementing a motion tracking system is carried out. This validation considers the actuation of a limb between 0º and 20 º for the θ_2 (amplitude angle). In comparison, θ_1 (direction angle) is set to be modified between 180º and 90º with steps of 30º. The validation is performed using a commercial motion tracking system (Vicon). Four cameras are placed around a frame supporting one limb, and several markers are placed around the limb (as shown in Figure 5-17), then the desired orientations are actuated for the limb, and the movement is recorded. The results of this experiment are presented in Figure 5-17 and compelled in Table 5-3.

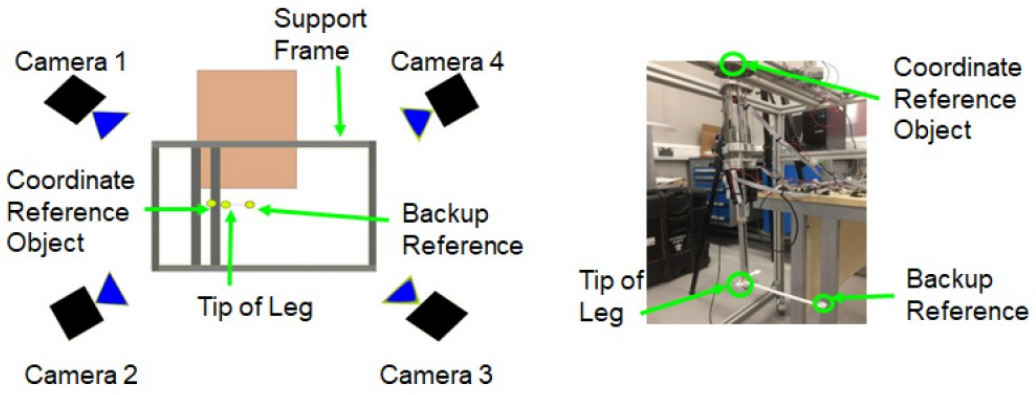


Figure 5-17. Illustration of the test set-up for the actuation validation.

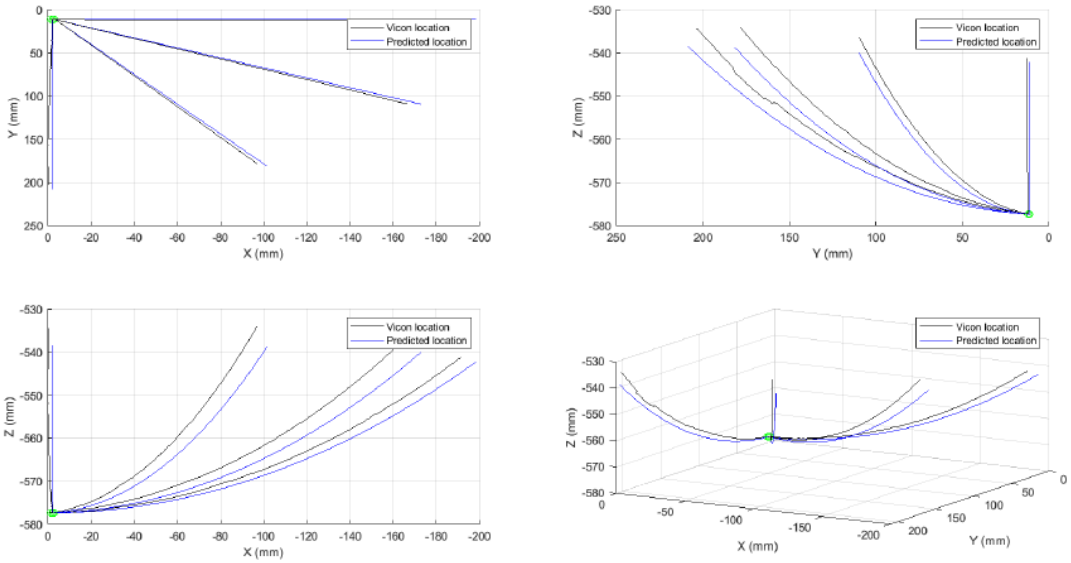


Figure 5-18. Trajectories recorded from the motion tracking system.

Table 5-3. Error calculated from tracking motion system and estimated trajectories from kinematics.

Direction Angle	Error (%)	Error(%)
180	0.23	0.19
150	0.47	1.61
120	0.48	1.99
90	0.45	1.87

Table 5-3 shows that no significant deviations occur in any actuated position, as the errors remain smaller than 2%. And thus the model presented in this section is implemented in future sections of the walking process.

5.6 Conclusions

This chapter presented the design of a novel RPKM based on the analysis and optimisation presented in Chapter 4. Several subsystems have been integrated into the design. One of the central systems is the SAS which offers a compact and lightweight design compared to conventional systems. Furthermore, to achieve practical use of SMAs, the characterisation of the SMA has been performed in this chapter. Similarly, the design of a 3-DoF mechanism for the limbs has been implemented as based on [99]. Moreover, the kinematics for the actuation of this mechanism is further developed in this chapter. This methodology is applied in later chapters to perform the walking task of the RPKM.

Chapter 6 **Gait Analysis**

In this chapter, the kinematic model for walking on different ground conditions with different configurations is introduced. Four configurations are proposed and tested on three different inclination terrains to account for the variation of the stability margins. Furthermore, to determine the optimal configurations of the proposed RPKM for walking on different conditions, the stability margins, maximum steps and forces exerted on the components are compared. The main advantage of the model is its capability to consider different configurations for the RPKM (the location of the upper joints is modified) considering different terrain conditions to enhance the performance in terms of stability and displacement characteristics (e.g. speed of displacement, positioning error, etc.).

6.1 **Kinematics and stability analysis**

In this section, a kinematics model and different ground conditions are presented for the gait analysis. This model is required independently from the kinematic analysis presented in Chapter 4, as the analysis in Chapter 4 is focused on machining operations. However the analysis presented in this chapter focuses on the walking kinematics and considers the reconfigurable capabilities of the RPKM proposed for stable and optimal gaits against different ground conditions (e.g. flat terrain, inclined terrain, different walking directions, low friction surfaces). Similarly the parameters computed in this chapter are focused on the walking capabilities of the RPKM and differ from those required for machining operations. Furthermore, two configurations, namely Insect and hexagonal, are presented in later sections to walk in different gait conditions. In addition, a third configuration allows changing the walking direction without the need to turn the RPKM.

6.1.1. Singularity Analysis

Although the singularity analysis is an important part of the analysis for any PKM, this analysis is discarded in this chapter. The main reason relies on the mechanical design of the proposed RPKM. As presented in Chapter 5, each limb is capable of operate in passive and active modes. For walking operations each limb is required to operate in active mode, and therefore the orientation of each limb is controlled by three tendons, providing the required constrain conditions to safely operate during the walking task, even in configuration that would be considered singular in conventional PKMs. However, this chapter focuses on the stability during walking, considering the forces required to tip-over the RPKM, as well as the analysis of the forces that could lead the tendons of each limb to fail.

6.1.2. Coordinate systems

For the kinematics of the walking process, gait and displacements, a scheme of the proposed RPKM on the walking surface is shown in Figure 6-1. This new reference frames are required to facilitate the analysis of the walking process, and using the reference frames defined in Chapter 4 would complicate the analysis as Chapter 4 is focused on the kinematics for machining operations. For these reasons the following coordinate systems are defined:

- $\{O - XYZ\}$ represents the global coordinate system with the -Z-axis along the direction of gravity.
- $\{O_G - X_G Y_G Z_G\}$ represents the ground frame, where the X_G- and Y_G-axes lie on the plane defined by the ground surface. The X_G-axis is along the elevation gradient.
- $\{O_H - X_H Y_H Z_H\}$ represents the local frame fixed on the moving platform of the proposed RPKM, where O_H is at the centre of the moving platform. The X_H-axis

points from O_H towards the $\boldsymbol{B_4}$, and the Y_H-axis points to the central location between the $\boldsymbol{B_5}$ and $\boldsymbol{B_6}$.

- $\{O_{B_i}$ - $X_{B_i}Y_{B_i}Z_{B_i}\}$ represents the local coordinate system at the i^{th} upper joints, where O_{B_i} is located at the centre of the i^{th} upper S-joint (B_i), with the X_{B_i}-axis pointing towards O_H and Z_{B_i}-axis parallel to Z_H-axis. Moreover, the O_{B_i} is located on the X_HY_H plane, and the distance between O_{B_i} and O_H is defined as the motion parameter c_i and controlled by the SAS.

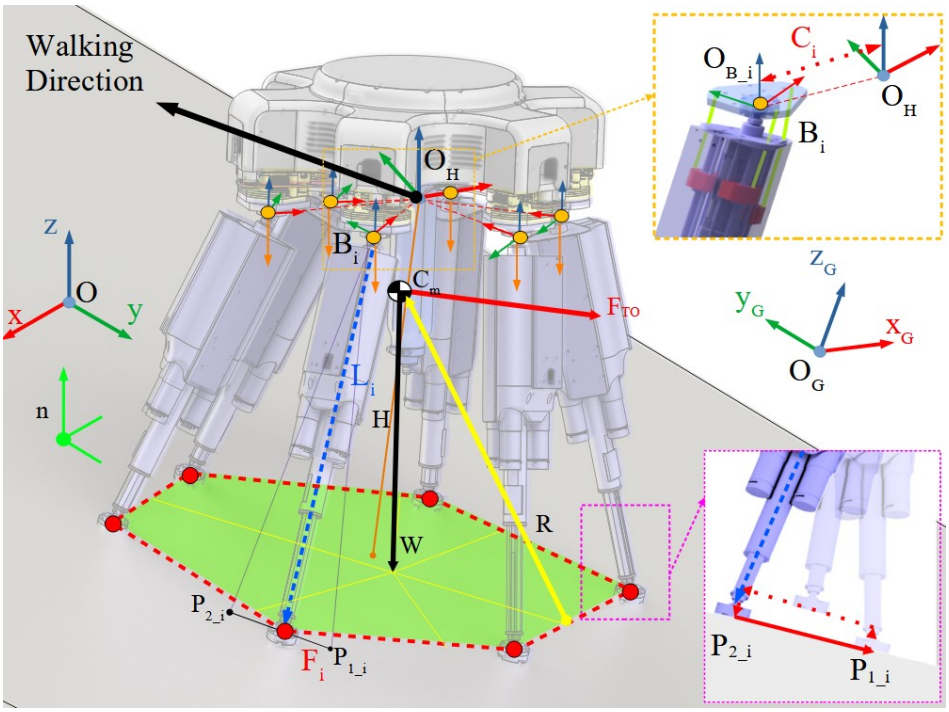


Figure 6-1. Schematic of the RPKM on an inclined surface considering the pitch, yaw and roll angles for the kinematic model in the gait analysis.

6.1.3. Kinematic Analysis

The analysis starts defining the locations that describe the plane comforming the ground. For convenience, four elements are considered to define the limits of the ground. These locations are defined in $\{O_G\}$ of the ground as:

$$^{O_G}G_j = \left[x_j\ y_j\ z_j\right]^T \quad j = 1,2 \ldots 4. \tag{23}$$

Then the position and orientation of the ground is defined in the global frame $\{O_G\}$ as:

$$^{O}G_i = {}^{O}R_{O_G}\,{}^{O_G}G_i + O_G \tag{24}$$

The rotation angles between these two frames are first the rotation of *{O_G}* around the Z_G axis and then a rotation around the Y_G axis, which defines the slope of the ground against the global frame. Later the positions of the ground $^{O}G_1$ to $^{O}G_3$ are used to calculate a parametric equation of a plane forming the ground. Then the plane defining the position is given as:

$$\boldsymbol{n} \cdot \boldsymbol{P_{int}} = \boldsymbol{n} \cdot \boldsymbol{P_0} \tag{25}$$

Where **n** is a vector normal to the ground plane, $\boldsymbol{P_{int}}$ is a vector from the origin O_G to the position of interest on the plane and $\boldsymbol{P_0}$ is a vector pointing from the origin O_G to a position know to lay on the plane. Then *{O_H}* is defined to lie at a distance *H* from the ground plane (along with the vector **n,** orange line in Fig. 9). Then the locations of the upper joints are defined, laying on the O_H-X_HY_H plane at a distance C_i from the centre of the platform, O_H (detailed view in Fig. 9).The SAS clutch mechanism controls the distance C_i and is later used to enhance the performance in terms of stability. The position of each upper joint is translated from the $\{O_H\}$ to $\{O\}$ as:

$$^{O}B_i = {}^{O}R_{O_H}\,{}^{O_H}B_i + O_{HGr} \tag{26}$$

Nevertheless, as different angles of roll, pitch and yaw are considered for the RPKM one complication is raised, the distances from the upper joints to the ground are

unequal among themselves. This complication has to consider possible interactions between the feet and the ground in non-tangential conditions; this means that the limbs feet must be traced to prevent undesired contact/collisions and to remain at a constant distance from the ground (Figure 6-2a). More importantly, further requirements must be studied:

- The limbs must be lifted from the ground in the direction and magnitude of the walking conditions maintaining a safe distance from the ground (Figure 6-2a), this distance is defined arbitrarily.
- The limb must remain in contact with the ground and displace backwards (from the walking direction) to produce the displacement of the platform (Figure 6-2b).

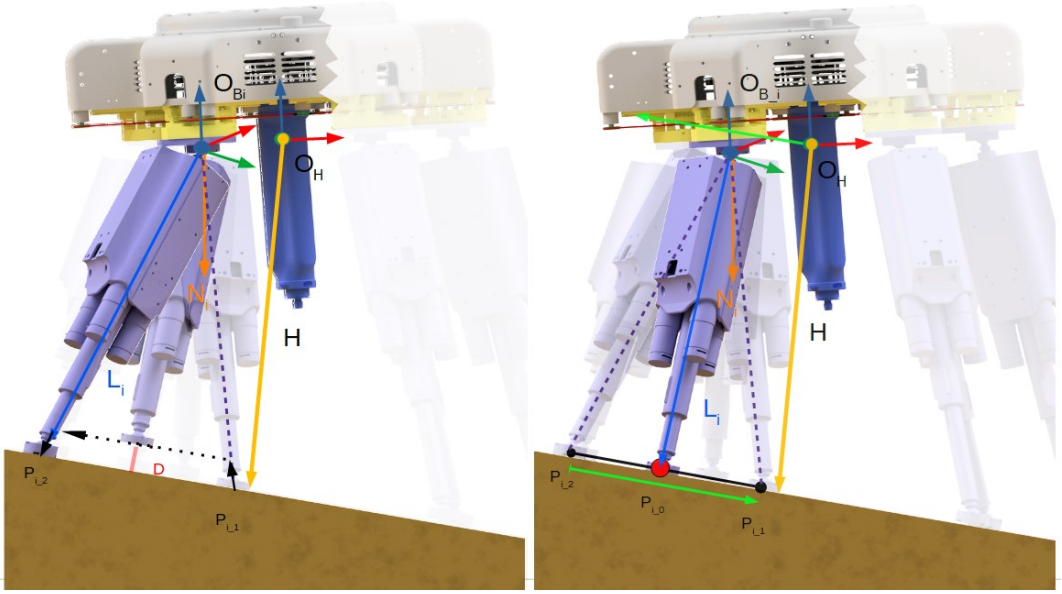


Figure 6-2. a) Illustration representing the repositioning of a limb without contacting the ground; b) limbs interacting with the ground to produce the displacement of the platform.

A five-step methodology is proposed to solve the interaction between the ground and the feet. The steps considered in the proposed methodology are listed as follows (and illustrated in Figure 6-3Figure 6-3):

Step 1. A vector P_v leaving from each upper joint B_i is declared into the neutral position of the limb (along -Z). With a parametric equation defined as:

$$P_v(t, B_i) = B_i + t_v \boldsymbol{N_v} \qquad (27)$$

Where $\boldsymbol{N_v}$ represents an arbitrary vector in the direction of -Z, and t_v represents a coeficient for $\boldsymbol{N_v}$ to intersect the ground plane.

Step 2. The location of the intersection between each neutral vector and the plane is computed. The location of each intersection serves as a reference position for each limb; its norm serves to trace the attitude of the RPKM against the ground (pitch and roll angles). The intersection is found when the Eqs. (25) and (27)are solved simultaneously, expressed as:

$$t_v = \frac{\boldsymbol{n} \cdot \boldsymbol{P_0} - \boldsymbol{n} \cdot \boldsymbol{B_i}}{\boldsymbol{n} \cdot \boldsymbol{N_v}} \tag{28}$$

Step 3. Another vector is computed to identify the current position of each foot with respect to the neutral position. This vector serves to identify the location of each foot on the ground. This vector is described to lay on the ground plane and to point from the neutral projection of the upper joint into the projection of the corresponding slide on the ground. This vector is defined as:

$$P_i = \boldsymbol{P_n} + A\, \boldsymbol{N_{slide}} \tag{29}$$

Step 4. Two positions are declared to perform the gaits of each foot P_{i_1} and P_{i_2}. This vector lays on the ground plane and points into the direction of walking, P_{i_1} and P_{i_2} , half step forward and half step backwards, respectively. This condition is imposed, so the limbs perform a full step between the displacement from $P_{i_1}$and P_{i_2}.

$$P_{i_1} = \boldsymbol{P_i} + \frac{Step_{amp} \boldsymbol{W_{Direction}}}{\mathbf{2}} \tag{30}$$

$$P_{i_2} = \boldsymbol{P_i} - \frac{Step_{amp}\boldsymbol{W_{Direction}}}{\mathbf{2}} \qquad (31)$$

Step 5. An interpolation is generated between P_{i_1} and P_{i_2}. Several points are generated between these two locations to be used for the actuation of the limbs. These elements serve as paths which the limbs follow to perform the gaits.

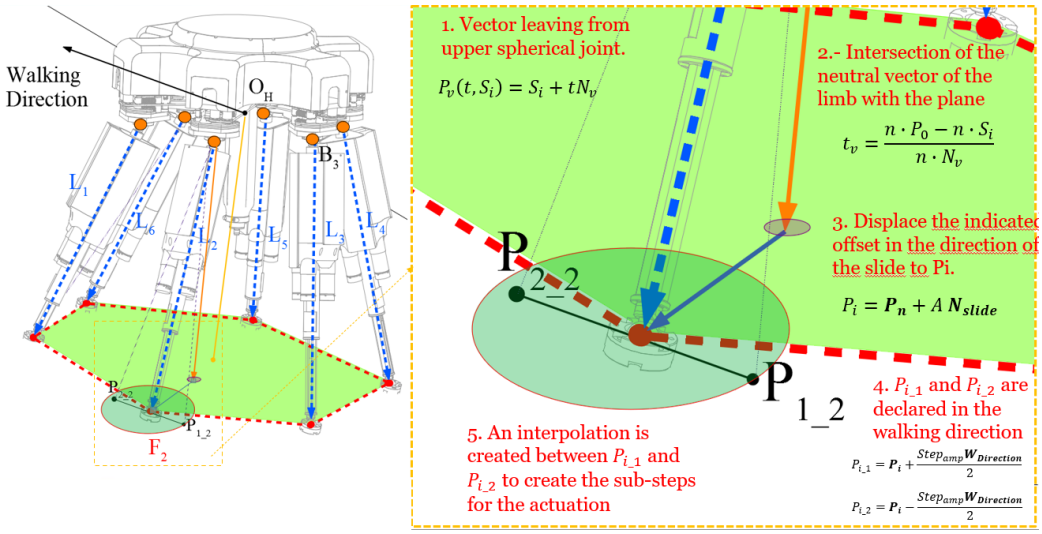


Figure 6-3. Illustration of the methodology for interaction between the feet and the ground in the gait analysis.

Once the starting locations of the lower joints have been identified, the process for the walking can begin. For this, each limb must move between P_{i_1} and P_{i_2} in iterative motions. This means that each leg must be lifted from P_{i_1} to P_{i_2}, make contact with P_{i_2} on the ground and then move all the limbs together backwards making contact with the ground to produce the displacement of the RPKM (as indicated in Figure 6-4). Furthermore, P_{i_1} to P_{i_2}, must be translated to each of the centres of the upper spherical joints to create the actuations for the tendons on each

limb as presented in Chapter 5. For this P_{i_1} to P_{i_2} are used to compute the values of each limb, and then the required actuations are computed based on equations 21-22. These movements must be coordinated in groups, where one group swings the limbs in the air to P_{i_2}, while the others support the RPKM on the ground. This grouping can be performed similarly to those found in nature, such as the gaits of ants [112] that walk in tripod groups; or those of metachronal or wave gaits [113]. For this reason the tripod and wave gaits are considered for the walking analysis. In the tripod gait, the limbs are divided in two groups named G1 and G2, while G2 supports the RPKM the G1 is repositioned, then G2 support the hexapod while the is repositioned, then both groups maintain contact with the group while the platform is moved forward to effectuate the displacement of the hexapod. This process is iterated as necessary to produce the desired displacement of the platform. three limbs are lifted from the group and repositioned to P1, while the rest. Furthermore, these movements must be effectuated considering the different positions and possible collisions occurring between the limbs and its components, to effectuate the collision analysis this models consider the analysis proposed in [114].

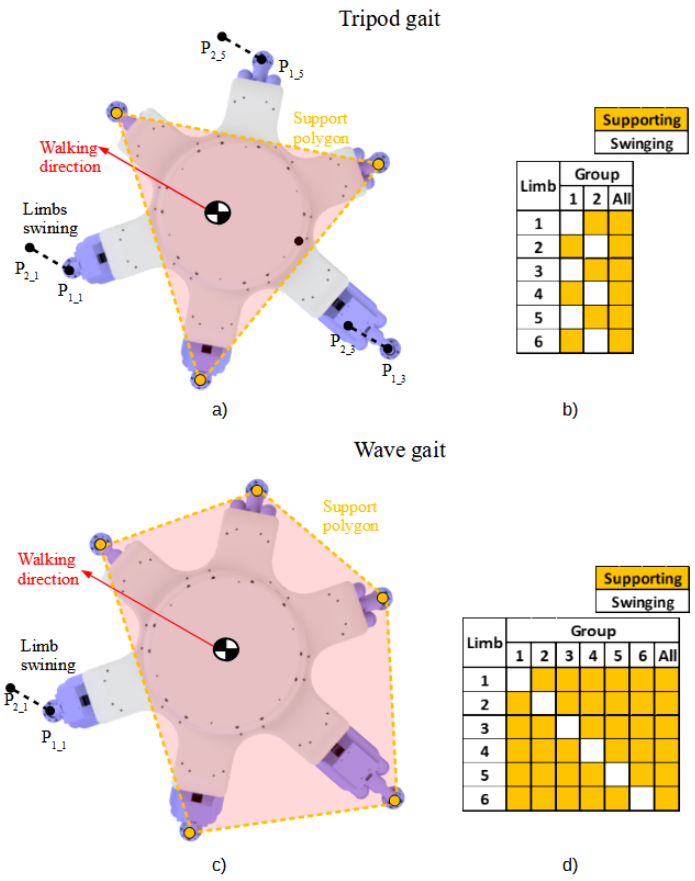


Figure 6-4. Schematic of selected gaits. a) Tripod gait: Limbs 1, 3 and 5 being swung between P_{i_1} to P_{i_2}, limbs 2, 5 and 6 supporting the RPKM. b) Table of the tripod gait. Metachronal gait: a) Limb 1, swung between P_{i_1} to P_{i_2}, limbs 2 to 6 supporting the RPKM. b) Table of the metachronal gait.

More importantly, this must be done in such a form that the limbs remain in contact with the ground to form a support polygon. Moreover, the projection of the centre of mass of the RPKM must remain inside this polygon. This is directly connected to the stability of the RPKM during the walking operations, and some authors consider these parameters as the static stability margins. However, this criteria neglects the effect of the vertical position of the centre of mass, where a higher position will have a negative impact on stability. To include these conditions, the smallest distance is

considered as the critical condition for the stability margin and then evaluates the force required to tip-over the RPKM, finally this value is divided by the total weight of the RPKM. This allows to provide positive coefficients for stable conditions; as the value of the coefficients approach to zero the system is considered as more instable and if negative values are present the system is considered to be in an unstable configuration. This is represented in Figure 6-5 and is expressed by Eq. 13.

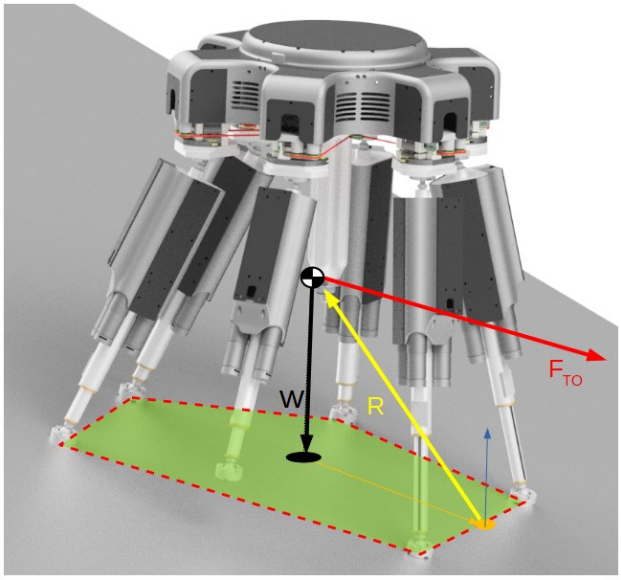


Figure 6-5. Illustration of the stability criteria considered for the walking analysis.

$$\sum M_a = (R \times W) + (R \times F_{TO}) = 0 \qquad (13)$$

Where R is the distance to the centre of mass, W represents the weight of the RPKM and F_{TO} represents the force required to tip-over the RPKM. More importantly, this criterion allows evaluating the stability of the RPKM proposed in different configurations over different conditions for the ground (i.e. inclined ground) taking in consideration the vertical location of the centre of mass.

6.1.4. Comparing the different walking configurations

As the RPKM proposed can modify its upper joint configuration, different layouts can be arranged to increase the performance of the RPKM over different walking conditions (i.e. low friction surfaces, slopes, obstacle avoidance). However, four configurations are considered in this paper:

1. Symmetrical hexagonal (Sym-Hex):

Considers a symmetric configuration, distributing the six limbs evenly around the centre of the moving platform, allowing an increased size of the support polygon with a cost on the maximum step size and reduced distance to the ground, as shown in Figure 6-6.

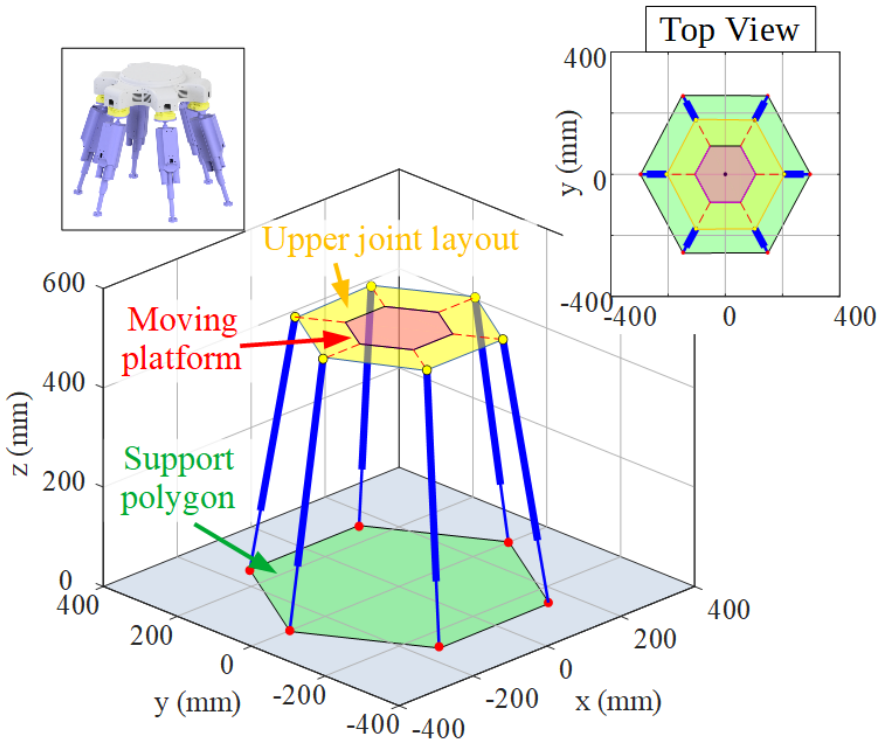


Figure 6-6. Illustration of the RPKM with insect configuration Insect.

2. Insect:

Arranges the upper joints aligned in two rows, which faces the direction of displacement. Some of the more prominent characteristics are the capability to avoid obstacles, as the limbs can remain in a straight position, allowing each limb to retract to the minimum length and create the furthest distance to the ground. Furthermore, as the limbs are grouped in two rows, the space required for walking is reduced, allowing it to pass over narrow locations, as shown in Figure 6-7.

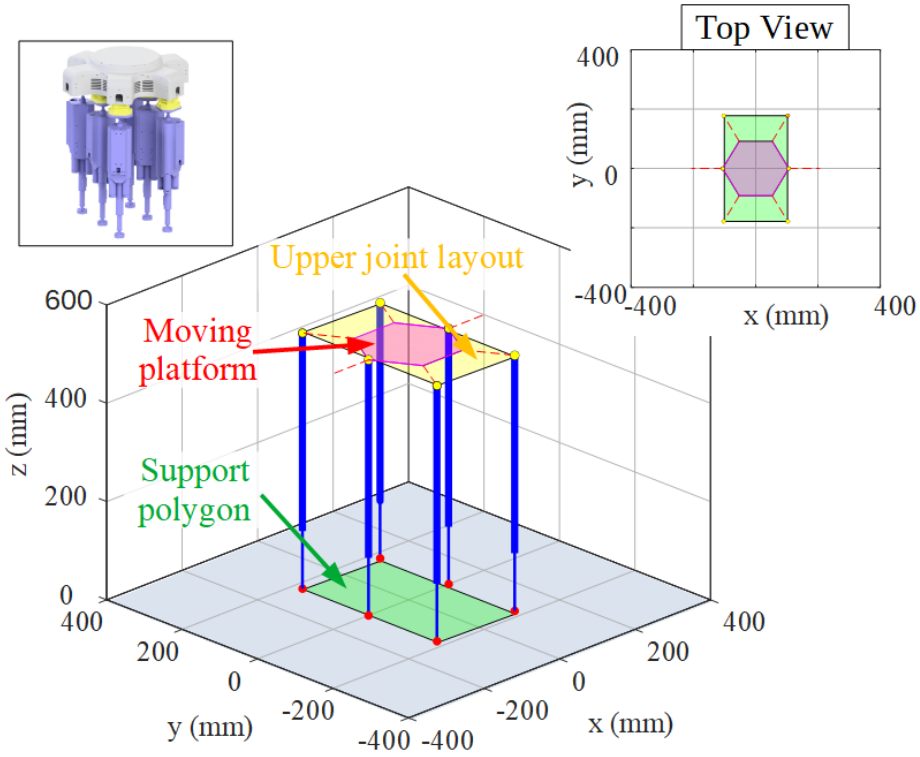


Figure 6-7. Illustration of the RPKM with Insect configuration.

3. Gough-Stewart (G-S):

Considers the upper joints in a hexagonal configuration, while the lower joints are arranged closer to each other in pairs (Figure 6-8). This configuration is well known in PKMs, as this allows to achieve high accuracy and to be support high forces compared to its own weight [115]. Furthermore, this configuration achieves higher stability as the support polygon is increased, compared to the insect configuration.

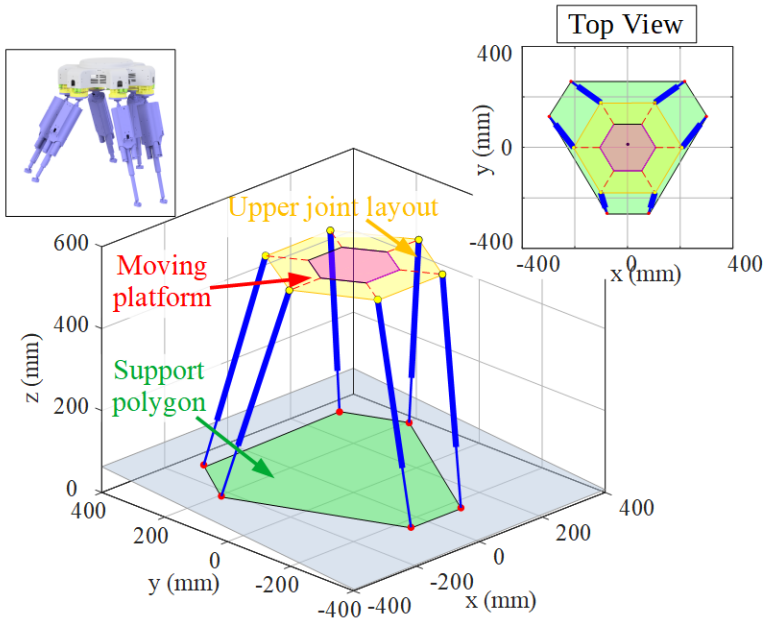


Figure 6-8. Illustration of the RPKM with G-S configuration.

4. Asymmetrical hexagonal (Asy-Hex):

Considers an asymmetric configuration, distributing the six limbs unevenly around the centre of the moving platform, allowing to utilise more efficiently the workspace of each limb on inclined surfaces Figure 6-9. However, this configuration is only presented when terrain at higher angles is required to be traversed. The reason to implement this configuration in such condition is based on the fact that more symmetric configurations are better suited for low angle inclinations of the terrain. The explanations of this conditions are explained later in this chapter.

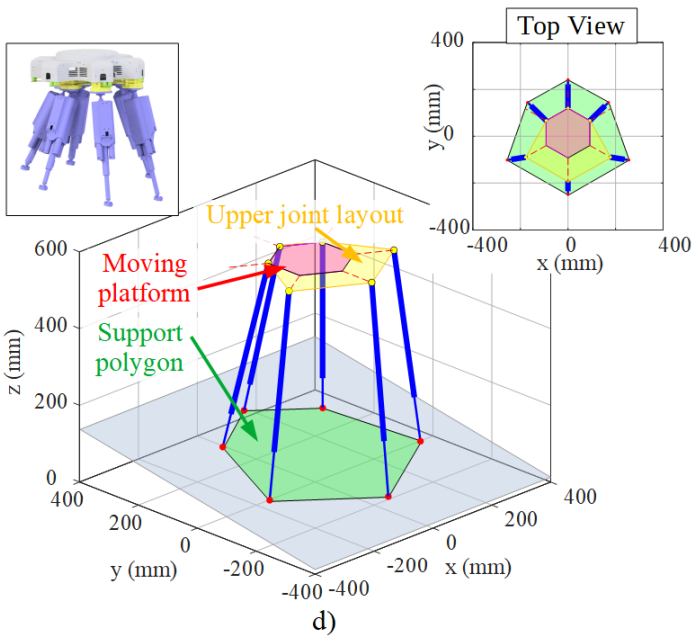


Figure 6-9. Illustration of the RPKM with Asy-Hex configuration.

More importantly, the advantages of a RPKM are presented when these configurations are compared in different terrain conditions. The next subsections present the capabilities of each configuration considering different inclinations on the terrain (i.e. no inclination, inclined at 4 and 10 degrees).

6.2 **Force Analysis**

The proposed RPKM is capable of repositioning its joints to adopt different configurations; however, as seen in nature, insects modify their gaits to take advantage of their morphology to improve their performance under the conditions to traverse various terrains. This section develops the force analysis for the RPKM, with special attention on the critical components (i.e. tendons that actuate the upper

joints). Furthermore, this analysis is later used to proposed the most feasible gait for each configuration.

To understand the influence of different configurations over the components in the proposed RPKM, an FEA model is created in the ANSYS APDL environment. This model bases on the kinematic models developed in section 6.1 and is designed in a parametric condition to trace the reaction forces on the feet and tendons of the RPKM. More importantly, the walking process is divided into a finite number of sub-steps. In this way, a full walking cycle can be characterised to select the most feasible configurations for walking in terms of the forces exerted on the components. To reduce the computational burden, the FEA model is defined as follows:

- The limbs are considered to perform as beam elements.
- The upper joints are connected to the centre of the platform by rigid elements.
- The mass of each limb is concentrated at its centre of mass.
- The mass of the platform is considered to be concentrated at its centre of mass.
- The feet supporting the RPKM are constrained of all translational displacements.

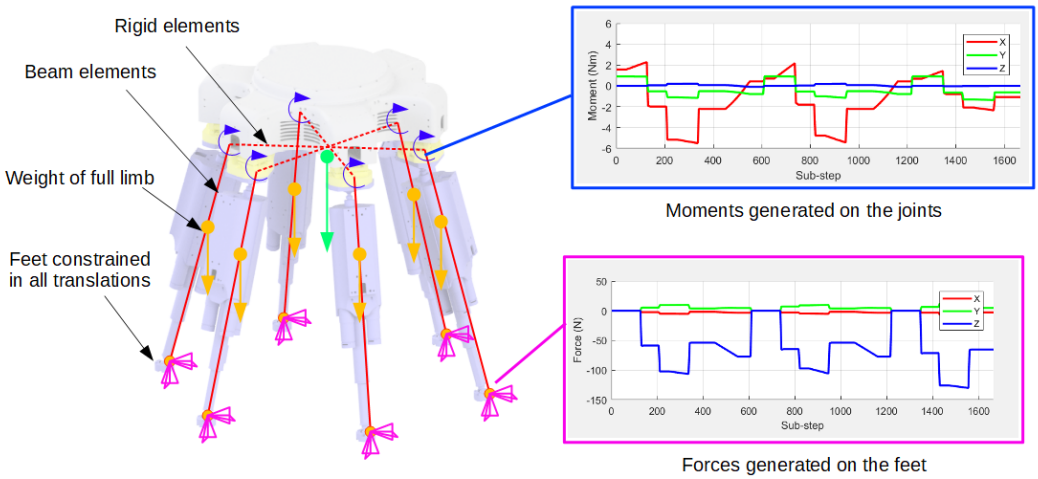


Figure 6-10. Illustration of the FEA, the end result is the reaction forces on the feet and the moments exerted on the upper joints.

More importantly, the reaction forces and moments obtained from the FEA model are used to evaluate the tensile forces on the tendons that actuate each limb. This is of relevant importance as the tendons are the most critical component in the limbs, constraining and preventing to deviate to undesired positions. Furthermore, if the limbs deviate significantly from the desire position, the walking process would fail. For this reason, a static model of the limbs is implemented.

The equilibrium conditions to evaluate the system are the moments generated by the tendons and the moments created by the weight of each limb, and the reaction forces of the feet for the centre of the joints.

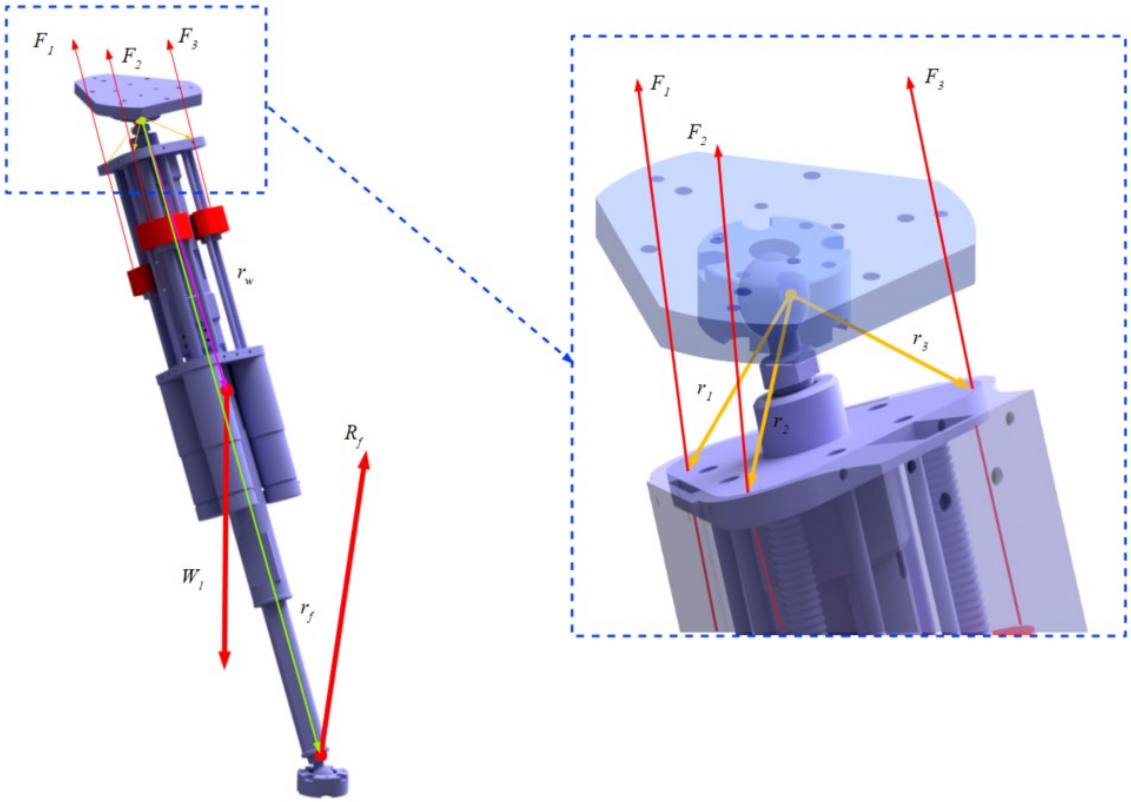


Figure 6-11. Representation of the moments actuating on the limbs.

The equation describing the system is:

$$\sum_{i=1}^{3} F_i(\boldsymbol{r_i} x \boldsymbol{D_i}) + \boldsymbol{W_l}(\boldsymbol{r_w} x \boldsymbol{g}) + (\boldsymbol{r_f} x \boldsymbol{R_f}) = 0 \qquad (32)$$

Where:

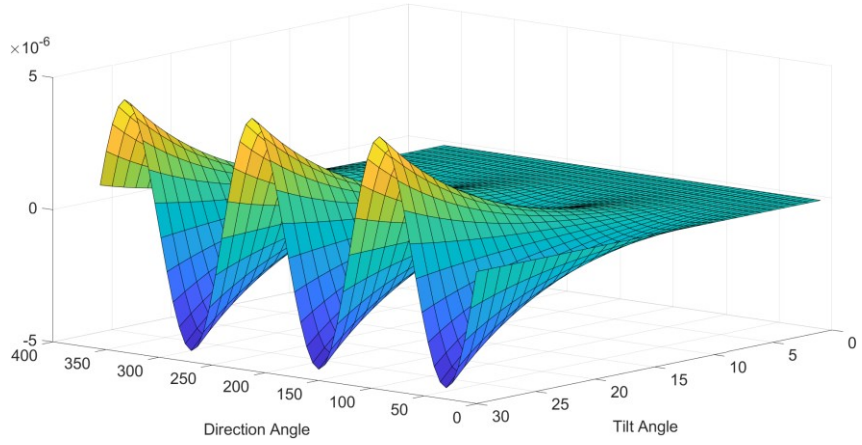
- F_i is the force exerted by *ith* tendon.
- $\boldsymbol{r_i}$ the vector from the centre of the spherical joint to the lower tendon guide.
- $\boldsymbol{D_i}$ the direction vector for the *ith* tendon (as a unit vector).
- $\boldsymbol{W_l}$ is the mass of the limb.
- $\boldsymbol{r_w}$ represents the radius of action of the limb's mass.
- $\boldsymbol{g}$ is the acceleration produced by the gravity.

- $\boldsymbol{r_f}$ is the radius of action of the reaction force of the foot.
- $\boldsymbol{R_f}$ **is** the reaction force on the foot.

Which can be expressed in a matrix form as

$$[T]\{F_i\} + \{T_{Wlimb}\} + \{T_{Feet}\} = 0 \qquad (33)$$

Where T represents the transformation matrix for the moments exerted by the tendons, T_{Wlimb} represents the torque exerted by the weight of the limb and T_{Feet} Represents the torque exerted by the reactions on the feet. However, when the determinant of T is analysed, it can be observed that the system is singular. This can be seen when the determinant of T is analysed on the operational ranges of the S-joint, as is shown in Figure *6-12*



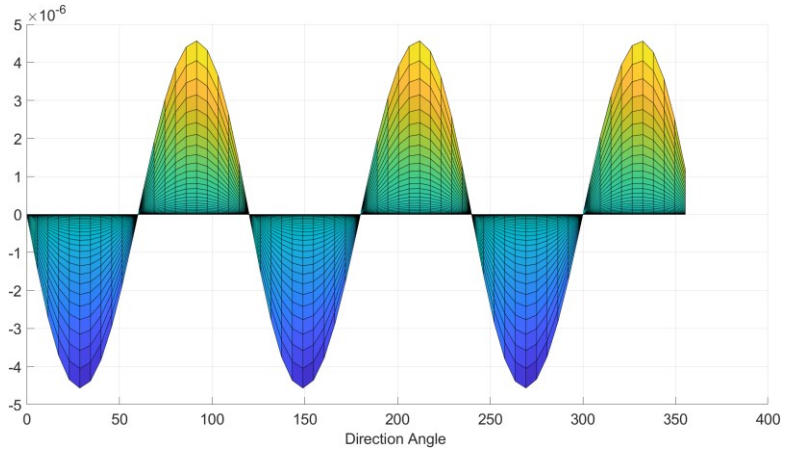


Figure 6-12. Determinant of matrix T.

Figure 6-12 shows that the determinant of T is close to zero, especially for certain orientation angles (e.g.0, 60, 120, 180, 240). From Figure 6-11 is possible to see that the tendons can not fully control the rotation around the Z-axis, and infinitesimal displacements will occur in these locations. However, based on the small error presented in Chapter 4 with the actuation of the spherical joints, the following assumptions are considered:

- The upper joints are considered to work as universal joints, as the tendons constraint the rotation around the z-axis when these are tensed.
- The tendons can actuate only under tensile forces.

Furthermore, considering the upper joint restricted to actuate as a universal joint Equation (32) is expressed as:

$$\begin{bmatrix} T_{x1} & T_{x2} & T_{x3} \\ T_{y1} & T_{y2} & T_{y3} \end{bmatrix} \begin{Bmatrix} F_{T1} \\ F_{T2} \\ F_{T3} \end{Bmatrix} + \begin{Bmatrix} T_{Wlimbx} \\ T_{Wlimby} \end{Bmatrix} + \begin{Bmatrix} T_{Feetx} \\ T_{Feety} \end{Bmatrix} = 0 \tag{34}$$

Solving (34) represents the results for a link element for the tendons (tensile and compressive forces). However, the solution is imposed on working only under

tensile forces. For this reason, for any F_{Ti}<0, $T_{xi} = T_{yi}$=0. This presents that Equation (34) must be solved in an iterative form when any of the force F_{Ti}<0, as mathematically, the tendons would be working under compressive forces. More importantly, the determinant of T represents that the system will alternate between 3 tendons working in the best case scenario and in the worst-case scenario, a single tendon will carry the full load exerted on the limb. For this reason, it becomes predominant to analyse each configuration and select the conditions that diminish the loads on the tendons, as higher loads on the tendon could lead to failure in the walking process.

6.3 **Walking Performance Analysis**

As the RPKM proposed can modify its upper joint configuration, different layouts can be arranged to increase the performance of the RPKM over different walking conditions (i.e. low friction surfaces, slopes, obstacle avoidance). However, as presented in previous sections, four configurations are considered in this thesis: Sym-Hex, Insect, G-S and Asy-Hex. More importantly, the advantages of an RPKM are presented when these configurations are compared in different terrain conditions. The next subsections present the capabilities of each configuration considering different inclinations on the terrain (i.e. no inclination, inclined at 4 and 10 degrees).

6.3.1. Levelled Ground

For levelled ground conditions, the two configurations considered are the Insect configuration and the Sym-Hex layouts. Table 1 considers the maximum step size over flat terrain for the Insect and Sym-Hex configurations over the same general layout, with one difference. A lateral offset of 90 mm is considered between the upper joints and the feet for the Sym-Hex configuration. Furthermore, the height of

the platform is modified between the operational limits of the limbs. This increase in height is targeted to prevent and avoid possible collisions with steps and obstacles that the RPKM may find in its path. More importantly, having enough eight to prevent the collision with obstacles inhibits the need to modify the trajectory, resulting in fewer manoeuvres required from the RPKM and less energy consumption. Table 4 also summarises the conditions limiting the maximum step size.

Table 4. Table of comparison between Insect and Sym-Hex configuration for maximum step size over flat terrain.

Height	**Insect Max Step (mm) and limiting condition**		**Sym-Hex Max Step (mm) and limiting condition**	
504.4	80	Collision	300	Stability
514.4	80	Collision	280	Stability
524.4	80	Collision	280	Stability
534.4	90	Collision	280	Stability
544.4	90	Collision	280	Stability
554.4	94	Collision	280	Stability
564.4	96	Collision	280	Stability
574.4	96	Collision	220	Out of limits
584.4	98	Collision	120	Out of limits
594.4	100	Collision	20	Out of limits
604.4	100	Out of limits	0	Out of limits
614.4	100	Out of limits	0	Out of limits
624.4	100	Out of limits	0	Out of limits

Further this table is also represented in Figure 6-13 where the maximum step size is compared against the height at which the RPKM is effectuating the walking.

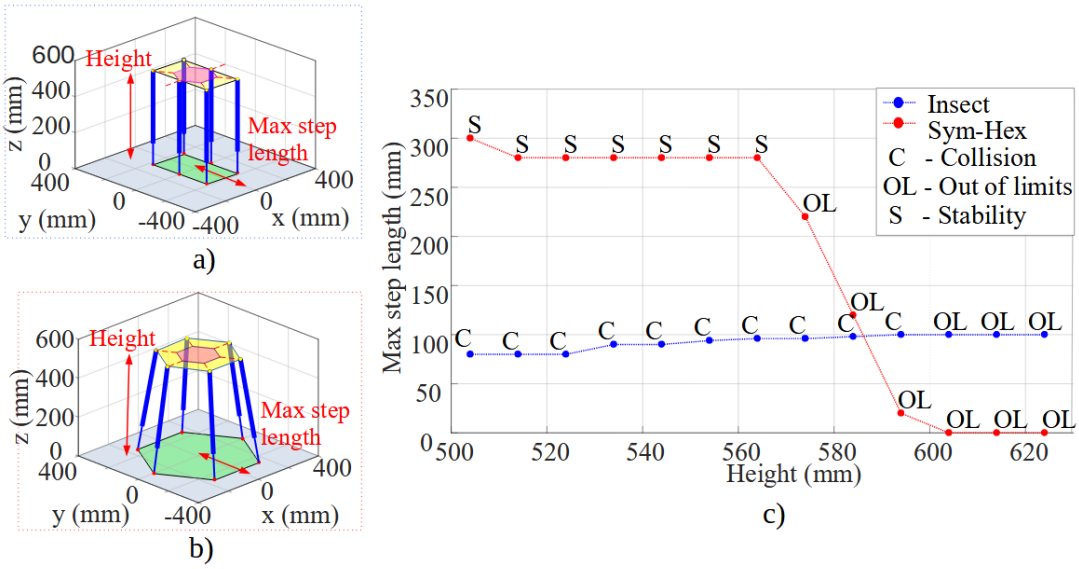


Figure 6-13. Maximum step length comparison a) Maximum step length vs height, showing limitations to extend steps size) insect configuration; c) Sym-Hex configuration.

From Figure 6-13 is possible to observe a consistent step size from the Insect configuration as the height is modified. More importantly the maximum step size is only limited by possible lateral impacts between the components of the RPKM, meaning that the limbs can make better use of their workspace in the vertical directions meaning allowing maximum and minimum strokes as its operation is towards the centre of their workspace. While in the Sym-Hex configuration the limitation is given as the limbs are closer to the limits of the workspace of each limb. Furthermore, the Insect configuration present a more stable step size over different operation heights, which means that a single configuration can be utilised even if the terrain present small variations, resulting in an advantage if Rule-based gait generations are used. This is as a single steps size can be utilised with similar

actuations for imperfections or variations on the terrain (such as small uneven ground or small obstacles in the path of the limbs).

Nevertheless, a more stable pattern (higher stability margins) are observed for the Sym-Hex configuration and this becomes the main objective when the RPKM is traversing over inclined slopes, for this reason the Sym-Hex configuration is selected when climbing over inclined slopes. However, different possible configurations are considered such as non-symmetric hexagonal configurations and the well known Gough-Stewart configuration. This considerations take into account the walking direction, attitude angles (yaw, pitch and roll) of the RPKM, and the configuration of the upper joints on the moving platform which directly affects the maximum usage of the workspace of each limb.

Force analysis for tendons: Insect and Sym-Hex configuration

The forces exerted on the tendons are evaluated in this section as a criterion to reduce conditions that can affect the displacement of the RPKM. Furthermore, this criterion can be utilised to prevent situations that could induce damage to the components. In this case, the maximum load forces on the tendons are traced between tripod and wave gait for the Insect and Sym-Hex configurations as high forces will induce larger deformations on the tendons and deviate the limbs from their ideal position. The comparison between gaits is presented in Figure 6-14b and Figure 6-14d and is expressed as:

$$T_{i\%} = \left(\frac{T_{Ti} - T_{Wi}}{T_{Wi}}\right) x\ 100 \qquad (35)$$

Where T_{Ti} and T_{Wi} represent the maximum tensile force on the *ith* tendon with the tripod and the wave gait, respectively. More importantly, the Insect and Sym-Hex

configurations are evaluated considering the tripod and wave gaits (summarised in *Figure 6-14*b and *Figure 6-14*d). Furthermore, *Figure 6-14* shows the maximum tensile forces(for each tendon) and the difference between gaits (wave and tripod).

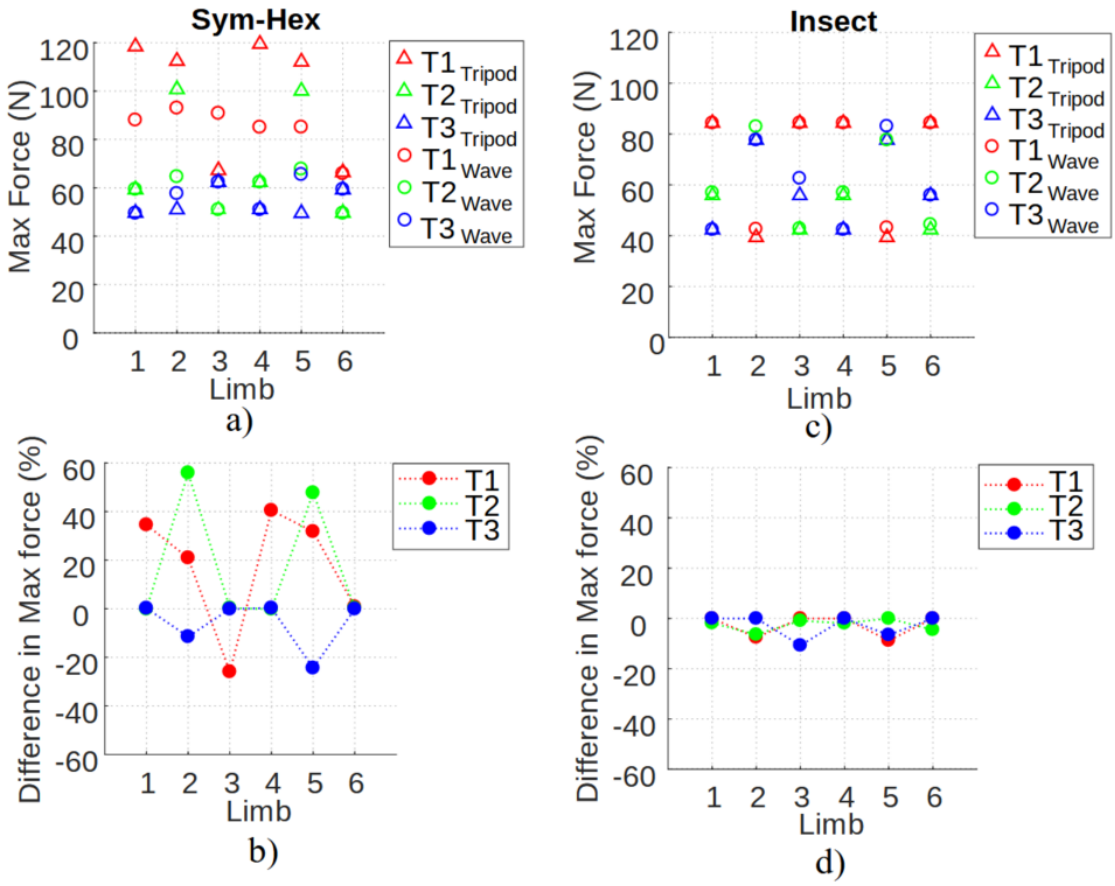


Figure 6-14. Force analysis for the tendons. Sym-Hex configurations: a) Tripod gait max force; b) Wave gait max force; c) Difference between gaits. Insect configuration: d) Tripod gait max force; e) Wave gait max force; f) Difference between gaits.

Figure 6-14b shows that the most significant variation in forces occurs with the Sym-Hex configuration (tripod and wave gaits). The Sym-Hex configuration with tripod gait represents an increment of up to 60% of the forces exerted on the tendons for the wave gait (Limb 2- T2). More importantly, the maximum force found in the tendons for the Sym-Hex gait is reduced from 119.5 N to 80 N, with the wave gait (Limb 4-

T1) representing a difference of 40%. For these reasons, the wave gait is selected for the Hexagonal(symmetric and non-symmetric) and G-S configurations. However, for the Insect configuration, the maximum forces exerted on the tendons are similar in both cases (tripod and wave gait). The case of the Insect configuration represents that the wave and tripod gaits can be used without significantly modifying the load conditions on the critical components of the RPKM. However, the time required to perform each displacement of the moving platform is reduced. For this reason, the tripod gait is selected for the insect configuration

6.3.2. Inclined ground

Traversing over inclined ground affects the stability of an RPKM, and configurations with increased stability must be considered. This section presents a study of the effects of traversing over inclined surfaces with different configurations. First, the Sym-Hex gait and the Insect are compared considering different inclinations from the ground; a third configuration is proposed to traverse over the inclined ground. Later the effect of traversing inclined ground with different pitch angles is presented.

The analysis begins proposing the first three configurations, considering an increment from zero to ten degrees in the inclined ground. Nevertheless, the Asy-Hex configuration is not considered for this analysis, as its performance is only considered for higher angles and when the rest of the configurations are not capable to operate. For this analysis, the three configurations consider the RPKM platform parallel to the inclined ground (Figure 6-13a). This is the normal vector of the plane n is parallel to the $+Z_H$. The results of this analysis are presented in Figure 6-13b.

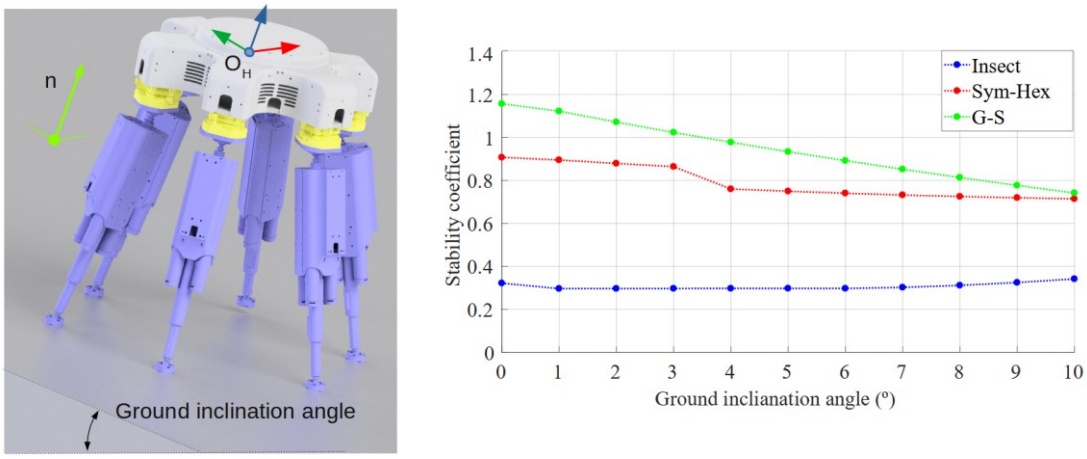


Figure 6-15. RPKM over an inclined surface. a) Illustration of the RPKM, the platform is considered parallel to the inclined surface; b) Stability margins between 0 and 10 ° of inclination for the inclined surface.

Figure 6-15 shows that the stability margins of the insect configuration remain stable and close to constant. However, when the stability margins of the insect configuration are compared against the Gough-Stewart and Sym-Hex configurations is possible to observe that the last two presents higher stability margins (of an order of three times of the Insect). More importantly, the reduced stability margins of the insect configuration could lead to unstable conditions while traversing inclined surfaces and thus damaging the RPKM. For these reasons, the next sections focus on the analysis of the Gough-Stewart and Hexagonal configurations for inclined surfaces.

The first part of this analysis is focused on the effect of the pitch angles and the ground inclination angle over the stability margins, as changing the relative angles between the normal vector ***n*** leaving the ground and the ***Z*** axes of the RPKM affects the relative location of the centre of mass against the support polygon and the

distances to its support (Figure 6-16). For this study, the ground is considered to change its inclination between zero to ten degrees. Similarly, the pitch angle of the RPKM is changed between zero and then degrees. The effect of these changes is focused on the effect of the angles between the platform and the slope, so the best configuration can be chosen to traverse over different terrains.

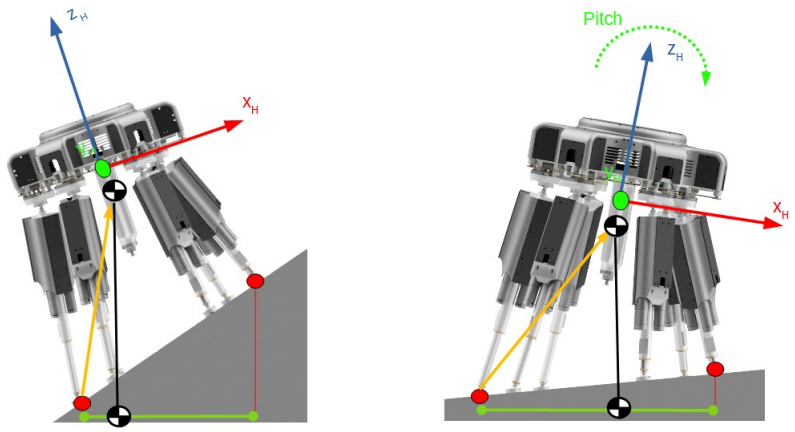


Figure 6-16. Illustration of the RPKM showing the effect of the attitude angles of the platform with respect to the ground.

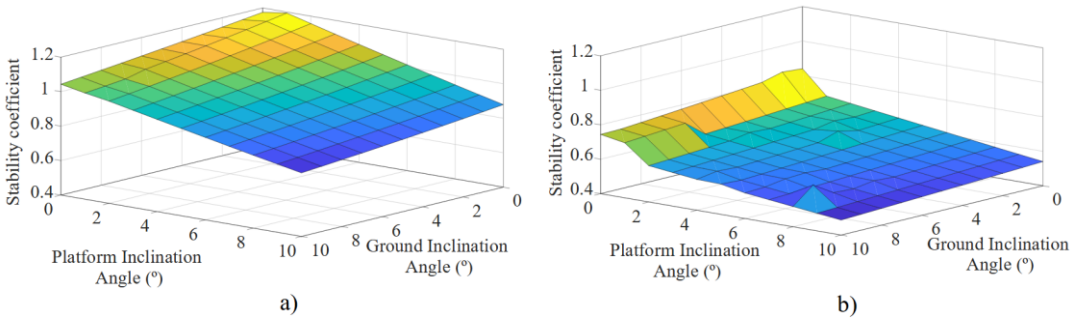


Figure 6-17. Case study for the optimal attitude of the RPKM. Variation of the stability coefficients considering different platform inclinations and ground inclinations. a) Gough-Stewart configuration stability coefficients; b) Sym-Hex configuration stability coefficients.

Figure 6-17 presents the results of computing the stability margins for the Gough-Stewart and the Sym-Hex configurations. From Figure 6-17a and Figure 6-17b is possible to observe that for both configurations, increasing the ground inclination while maintaining the platform parallel to the inclined ground (the angles of the RPKM and the ground increase evenly) has a negative effect on the stability margins. This means that the stability coefficients are reduced, and thus, the system can be considered less stable. Furthermore, positive angles could be considered; however, this also negatively affects the stability margins and creates a negative effect on the workspace of each limb, as the usable workspace of each limb is reduced. Where the maximum usable workspace of each limb is obtained when the platform of the RPKM and the inclined surface are parallel. Considering the previous statements, the maximum stability coefficients are obtained at zero degrees of the pitch for the platform, meaning that the Z_H and the Z axes are parallel. However, these assumptions consider the locations of the upper joints to be symmetrical for the Gough-Stewart and Sym-Hex configurations, meaning that all the joints on the upper platform remain at the same radial distance from Oh. As previously stated, these configurations restrain the maximum allowable workspace from being obtained when the Z_H and n are parallel. These conditions are imposed as the following restrictions are present over high inclination conditions:

1. Frontal limbs operate at the top of the workspace of each limb, restricting the minimum limb length (Figure 6-18 red rectangle).
2. Rear limbs operate at the bottom of the workspace of each limb, restricting the maximum limb length (Figure 6-18 yellow rectangle).

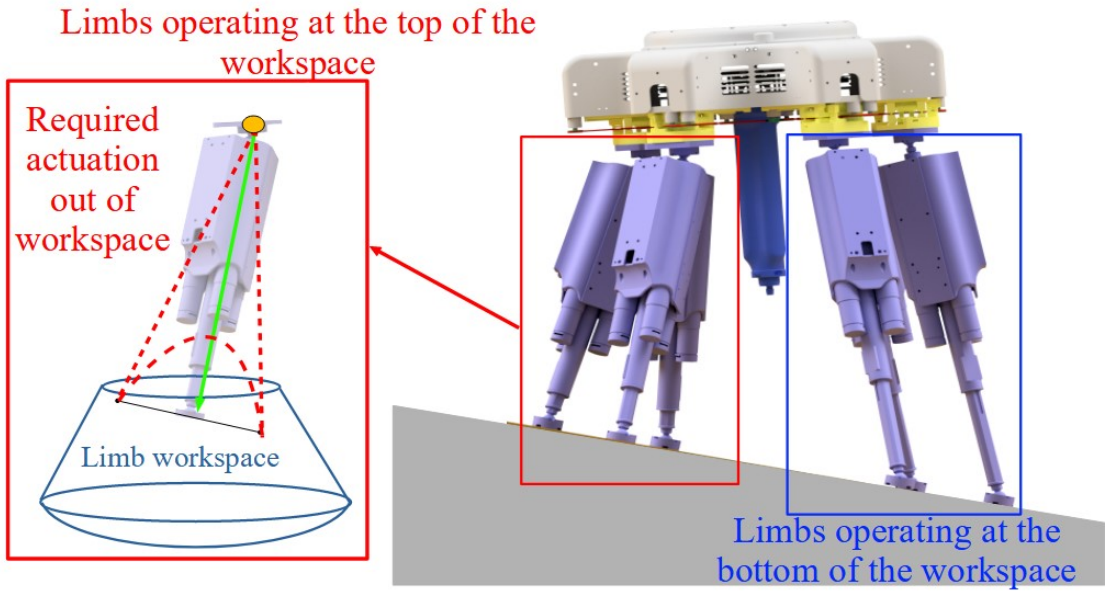


Figure 6-18. Illustration of the RPKM operating at a high inclined surface. The frontal limbs work at the top of the workspace, while the rear limbs operate at the bottom of the workspace, limiting the displacement of the RPKM.

Furthermore, these conditions would limit fixed PKM to operate at lower angles of inclination for the terrain under Sym-Hex and symmetrical Gough-Stewart configurations. However, as the upper joints are repositionable the joints on the moving platform can be reconfigured to increase the maximum slope that the RPKM can traverse.

6.4 **Results**

In this section the theoretical results are validated. First, the Insect and Sym-Hex are tested considering two gait types: tripod and wave gait. Then these two configurations are compared utilising a motion tracking system. Later the G-S and the Sym-Hex configurations are compared by means of the achieved displacements on an inclined terrain at four degrees. Finally, this section presents non-symmetrical configurations of the G-S and Hexagonal configurations traversing an inclined terrain at 10 degrees. More importantly, this section remarks the adaptability

characteristics of RPKM and the kinematic model presented in previous sections to traverse different terrains without the need of extensive condition tables.

6.4.1. Gait selection for the different configurations

The first comparison started testing the tripod and wave gaits for the Insect and Sym-Hex configurations. It is observed that the tripod gait failed in the Hexagonal configuration in each test. This was produced as the load on the tendons increases as three limbs are lifted from the ground; this increase in the forces actuating in the tendons has been proved in Chapter 3, where a difference of 60% is computed between the tripod and wave gait for the Sym.-Hex configuration. The effect of these increased forces results in deformations which lead the position of each limb to become inaccurate, and thus the gait failed. However, the Insect configuration can achieve tripod gaits as the forces on the tendons are reduced compared to the Sym-Hex, which is proved with the analysis presented in Chapter 6. More importantly, when the forces acting on the tendons are computed in Chapter 6 is possible to observe a more stable pattern present with the Insect configuration. This also means that the load conditions on the tendons are more stable, and a longer operational life can be expected from the tendons that actuate each joint, further preventing a possible failure during its walking operations.

Once the appropriated gaits where selected for each configuration the next stage consisted of the capabilities to traverse over different terrains. To evaluate the motion capabilities of the RPKM a system based on motion tracking was implemented and the relative displacements were recorded. The motion tracking system is a Vicon system with four Vantage cameras placed around the RPKM, with an accuracy between 7 μm to 25 μm [116]. Seven markers have been declared and tracked on each configuration, one marker is placed on the top of the platform and

one on each foot (Figure 6-19a), then the relative displacements are recorded (Figure 6-19b). To validate the capabilities of the proposed RPKM three scenarios are proposed: flat ground, inclined ground at 4 degrees and inclined ground at 10 degrees.

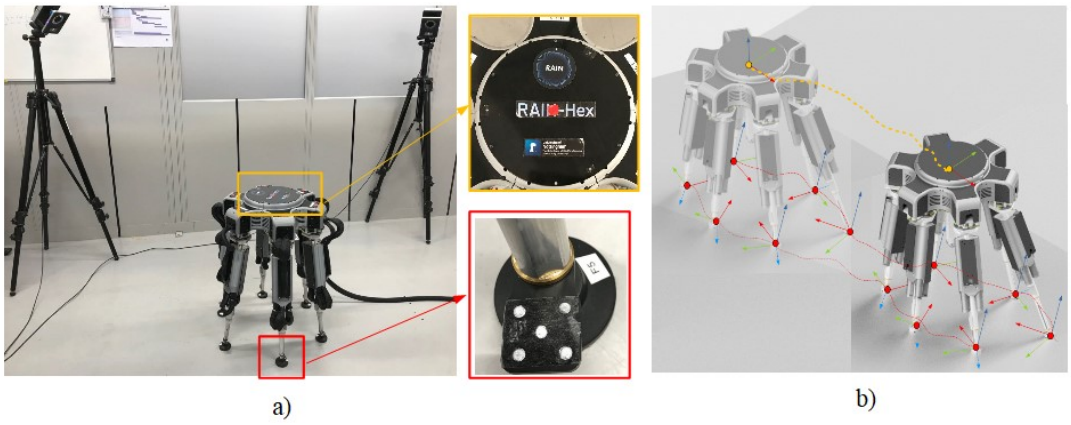


Figure 6-19. Motion tracking implementation. a) Image of the locations where the markers have been located; b) Illustration of the recorded motion, the markers are traced at each state of the terrain traverse.

Figure 6-20a represents 5 steps effectuated with the G-S configuration, similarly between each step (movement of the platform) each limb has to be repositioned in respect to the wave or tripod gaits. This movements are effectuated between each step of the system and is illustrated in Figure 6-20b. Similarly the tracking motion systems allows to record each of the movements of the RPKM. However, for brevity the platform displacements are the main source of interest as the error from each limb will be reflected on the platform displacement.

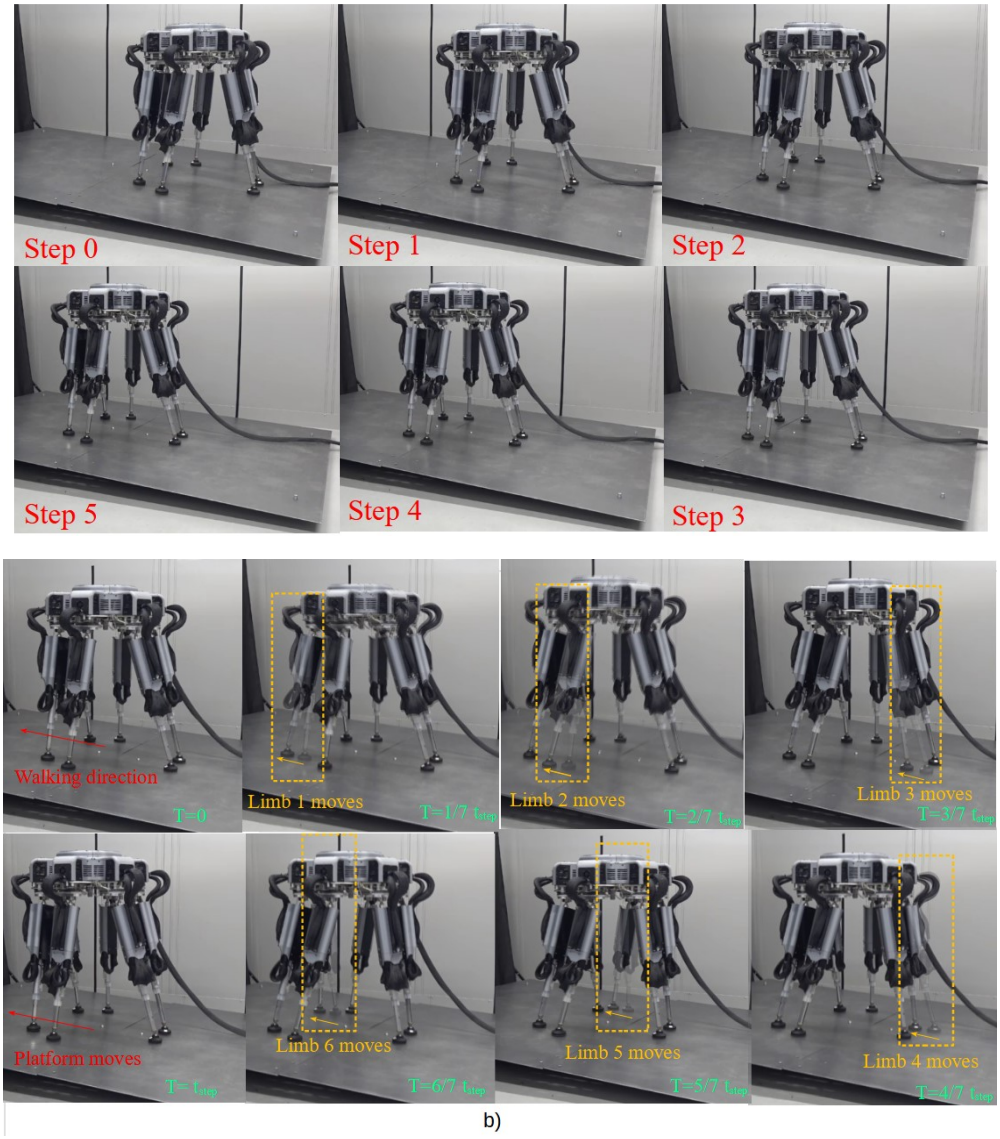
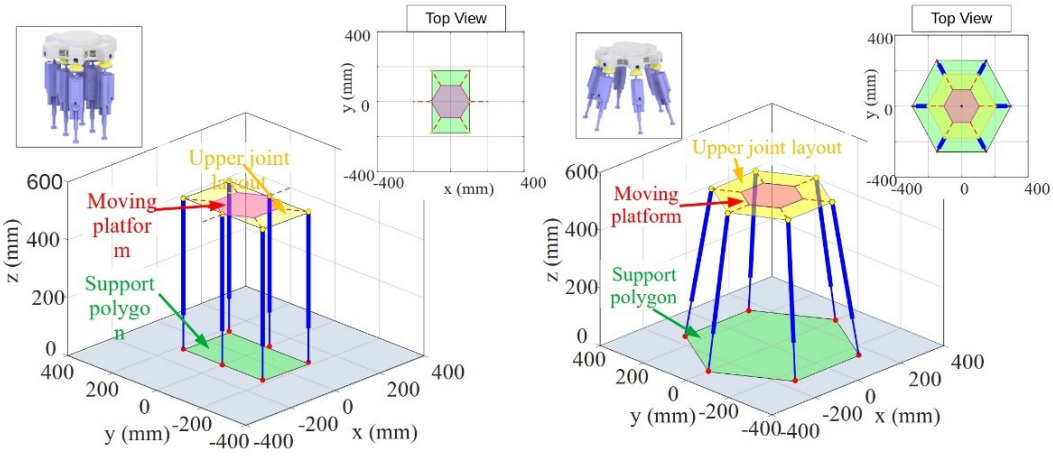
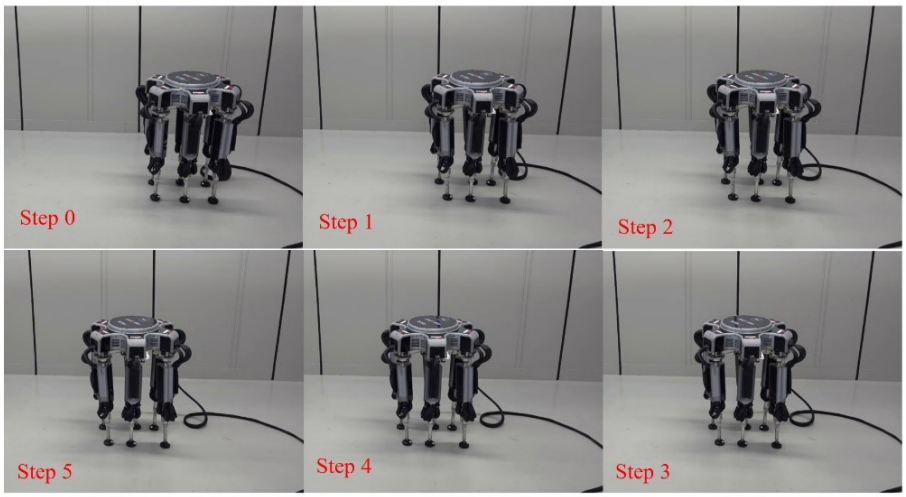


Figure 6-20. Snapshots of the recorded motion. A) G-S configuration during the first 5 steps of the walking; b) Snapshots of the gait between full steps.

6.4.2. Flat ground

The Insect and Sym-Hex configurations are proposed to test the motion capabilities on flat ground; the characteristics of interest are the time required to traverse the same distance and the quality of the real displacements against the ideal displacements. For this analysis the total distance traversed, and the orientation of the displacement are utilised to compere the walking ability under the different configurations (i.e. Insect and Sym-Hex). Figure 6-21 presents the configurations.





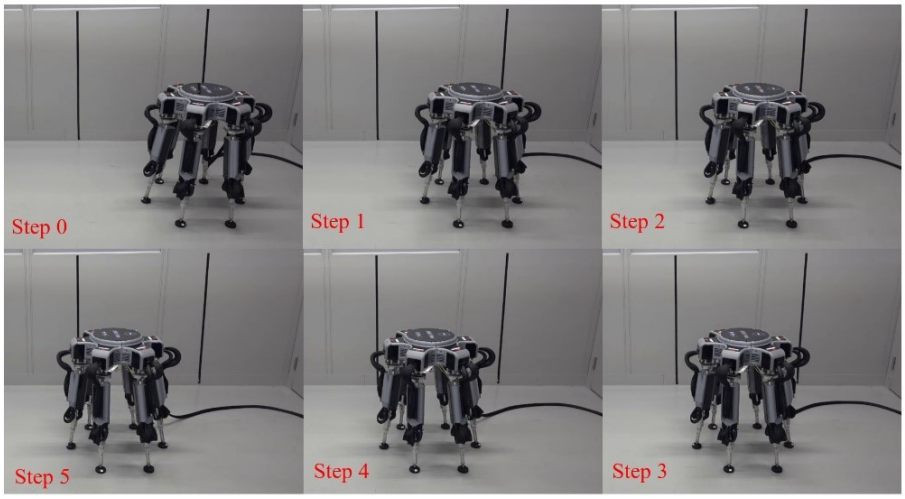


Figure 6-21. a) Illustration of the: a) Insect configuration; b) Sym-Hex configuration. c) First five steps of the Insect configuration; d) First five steps of the Sym-Hex l configuration.

Both configurations, Insect and Sym-Hex, have considered a total displacement of 880 mm in 10 steps; each full step considers a displacement of 88 mm. These displacements are recorded using a motion tracking system and the relative displacements are presented in Figure 6-22 for the Sym-Hex and the Insect configurations respectively.

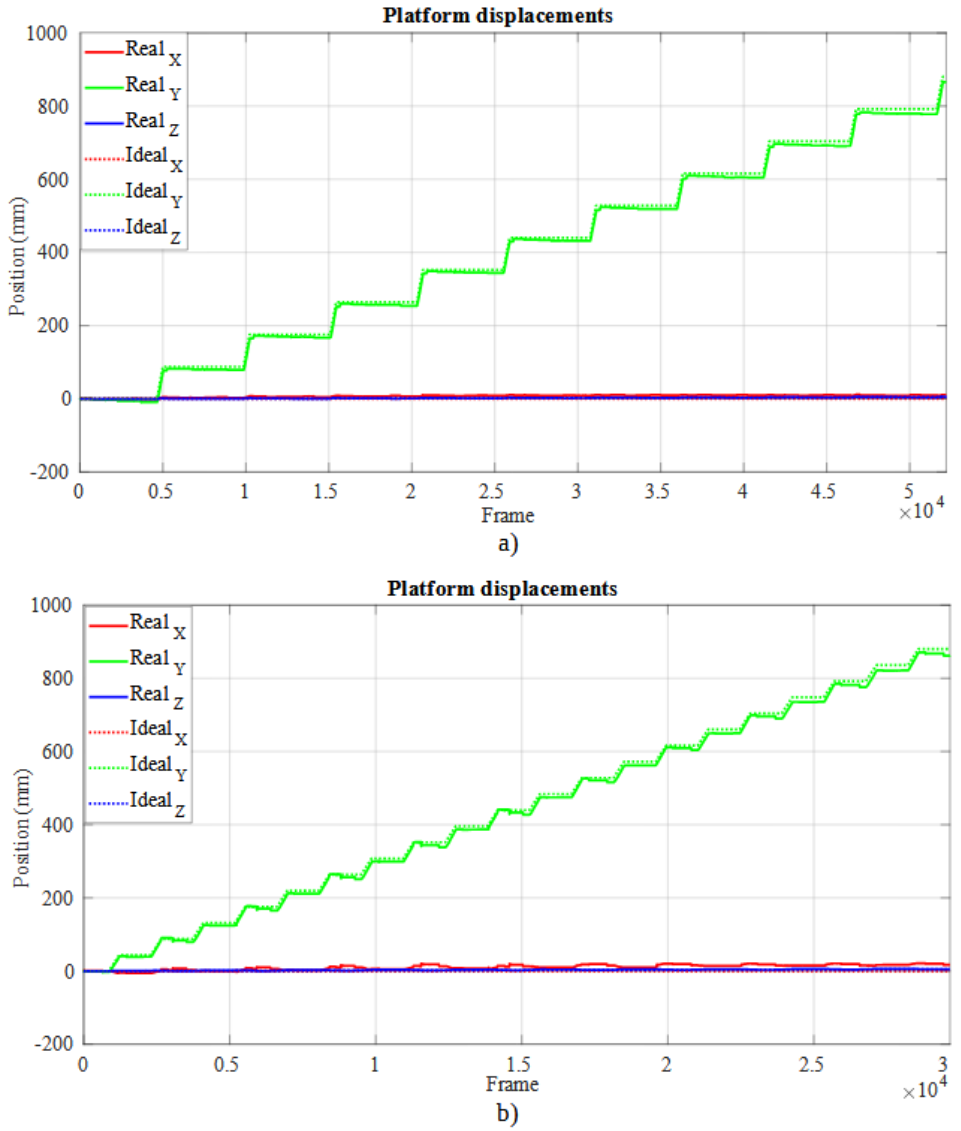


Figure 6-22. Recorded motion of the moving platform for the: a) Sym-Hex configuration; b) Insect configuration.

However, these plots are complicated to illustrate the displacement and the direction of the walking. To better illustrate the effect over the displacement capabilities Figure 6-24 is proposed as a rapid mean to compere the quality between the ideal displacements as well as between configurations. Figure 6-24a represents the polar representation of the recorded walking of the RPKM, where the grey semi-circles represent a full step (the norm of the desired displacement) and the inclined grey lines represent the direction around the platform (spaced every 1 degree.

Furthermore, in Figure 6-24 the error of the displacements and angles are evaluated at the end of each step. Figure 6-24b and Figure 6-24c present the displacement error and direction errors for both configurations. Figures 6-24, 6-26 and 6-27 present the two configurations which presented the best performance during the testing, this has been included in this way to make more clear the fittest configuration in each condition of the terrain.

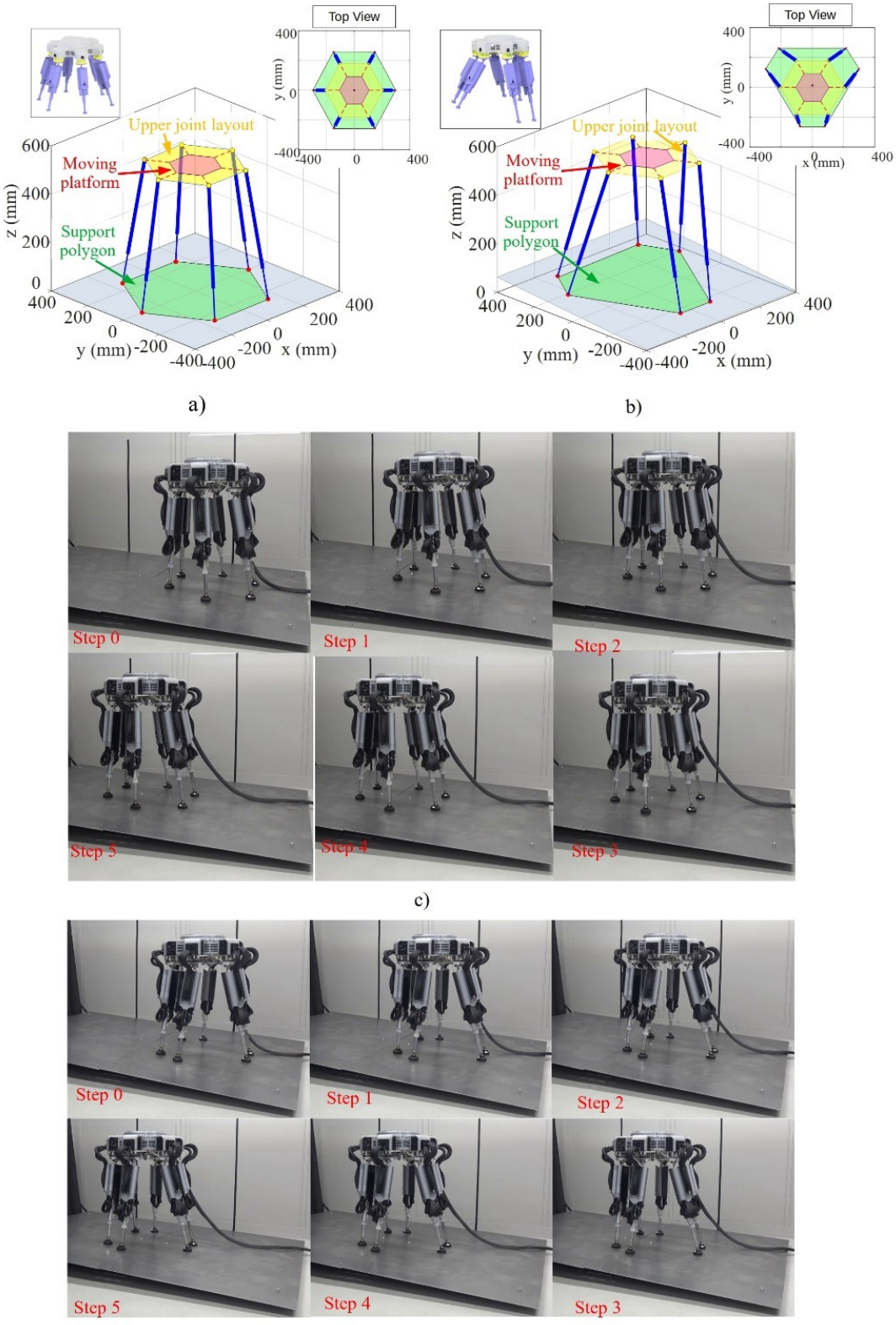


Figure 6-23. a) Illustration of the: a) Sym-Hex configuration; b) G-S configuration. c) First five steps of the Sym-Hex configuration; d) First five steps of the G-Sl configuration.

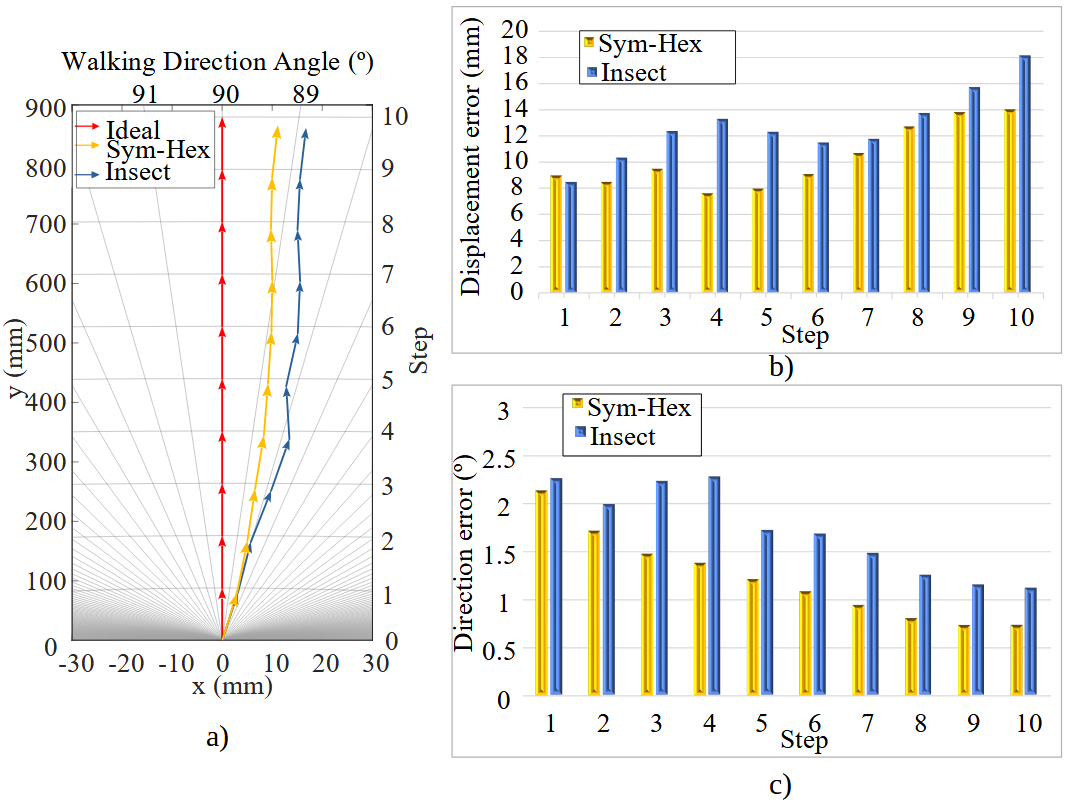


Figure 6-24. Comparison between the Sym-Hex and Insect configurations. a) Displacements of the Sym-Hex and Insect configuration against the ideal displacement. b) Displacement error. c) Direction error.

The results presented in Figure 6-21e and f, represent the error on each step and how these errors accumulate as the RPKM keeps displacing. In both configurations the maximum angle error is present at the beginning of the walking; for both configurations these errors are reduced at each step. Nevertheless, the Insect configuration represents the configuration with higher error at each step both in the direction of displacement and the total displacement effectuated. Nevertheless, no significant difference is found between both configuration as the maximum difference in the displacement errors between both configurations is smaller 5.72 mm and 1.14 degrees. Furthermore, the Insect configuration is found to complete a full step every 1.6 minutes while the Sym-Hex completed a step every 2.94 minutes.

This represents that the Insect configuration displaces the RPKM 1.8 times faster compared to the Sym-Hex configuration.

6.4.3. Inclined ground at 4 degrees

The Hexagonal and G-S configurations are selected for its increased stability coefficients compared with those of the Insect configuration, and are illustrated in Figure 6-23. Similarly to the test on flat ground, the required displacement comprehends a total displacement of 880 mm in 10 steps. Nevertheless, these displacements are performed on an inclined terrain at 4 degrees.

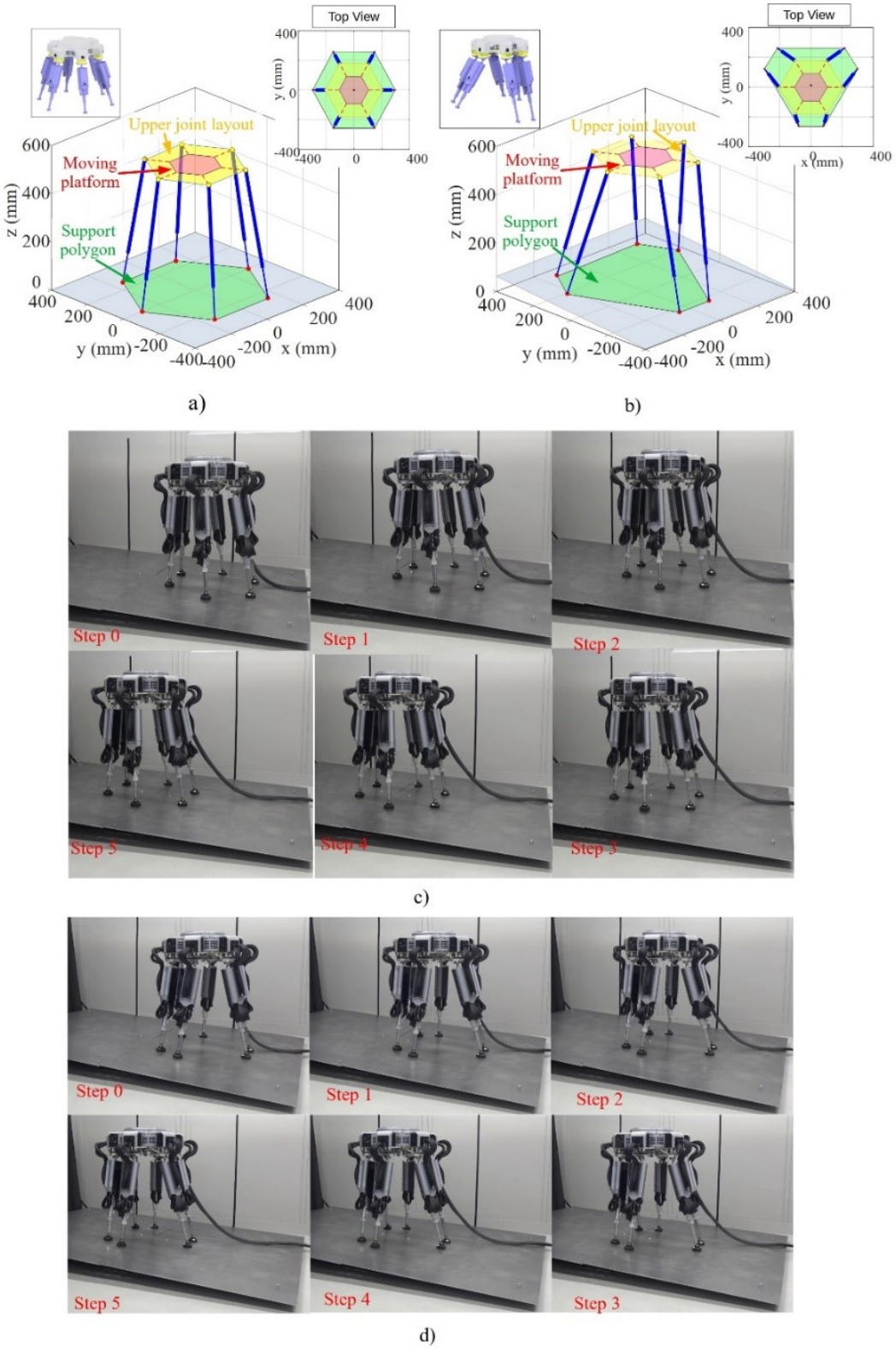


Figure 6-25. a) Illustration of the: a) Sym-Hex configuration; b) G-S configuration. c) First five steps of the Sym-Hex configuration; d) First five steps of the G-S configuration.

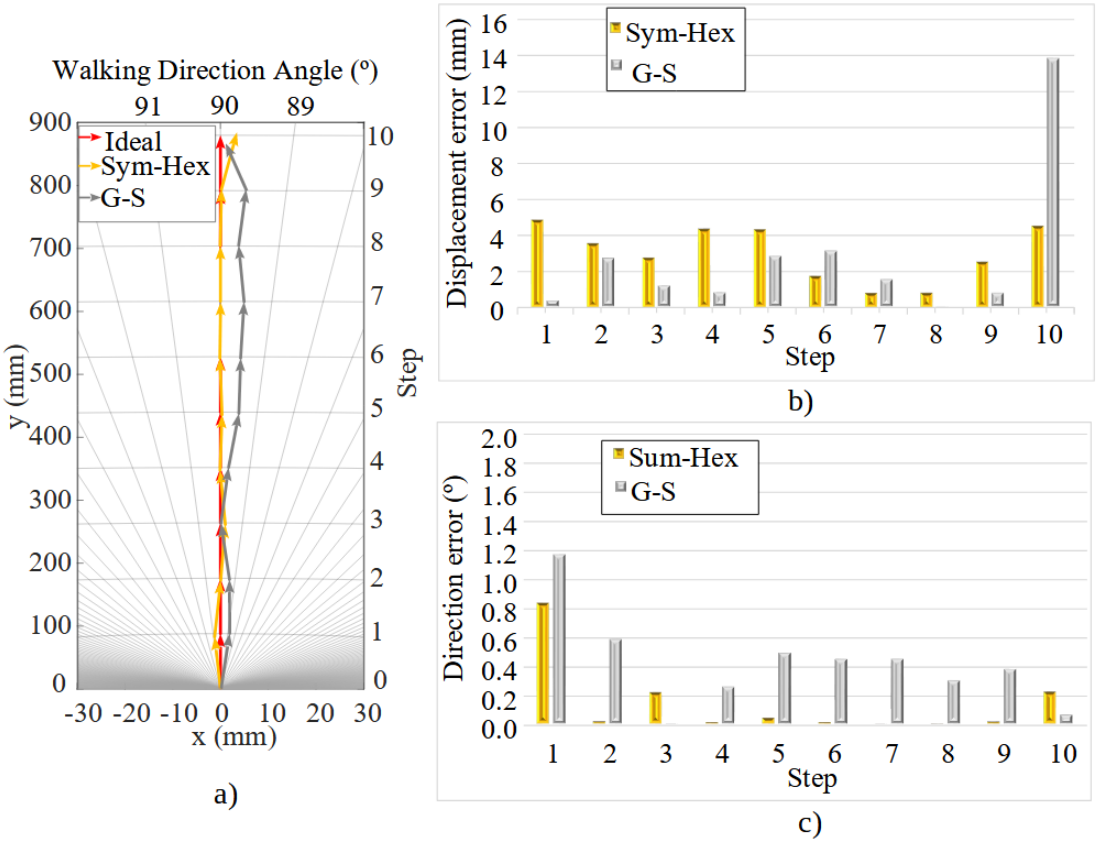


Figure 6-26. Comparison between the Sym-Hex and G-S configurations. a) Displacements of the Sym-Hex and G-S configuration against the ideal displacement. b) Displacement error. c) Direction error.

The results at 4 degrees show that the maximum error occurs at the first step for the Sym-Hex configuration in the traverse distance and the deviation angle. Similarly, the G-S presents the maximum deviation angle during the first step of the walking. However, the maximum the maximum displacement error occurs during the last step of the walking, while the deviation angles are significantly higher than those of the Sym-Hex configuration, indicating a more erratic patter in the walking angles.

6.4.4. Inclined ground at 10 degrees

The Sym-Hex and G-S configurations are selected for their increased stability coefficients when compared with those of the Insect configuration. However, when

the ground inclination is increased, the usable workspace of each limb is reduced, as mentioned in Section III-D2. Two non-symmetrical configurations are proposed as a modification to the G-S and Sym-Hex to achieve stable displacements. In these configurations, the upper S-joints of frontal limbs are brought closer to the centre of the platform, while the ones in the rear limbs are brought to the end of the slides. The required displacement comprehends a total t of 660 mm in 10 steps and is performed on an inclined ground at 10º. However, when the G-S configuration is tested, considerable slippage is observed, and thus this configuration is discarded for further test. More importantly, the Asy-Hex configuration proved to be capable of displacing on inclined ground at 10º, and the results are presented Figure 6-27a-c.

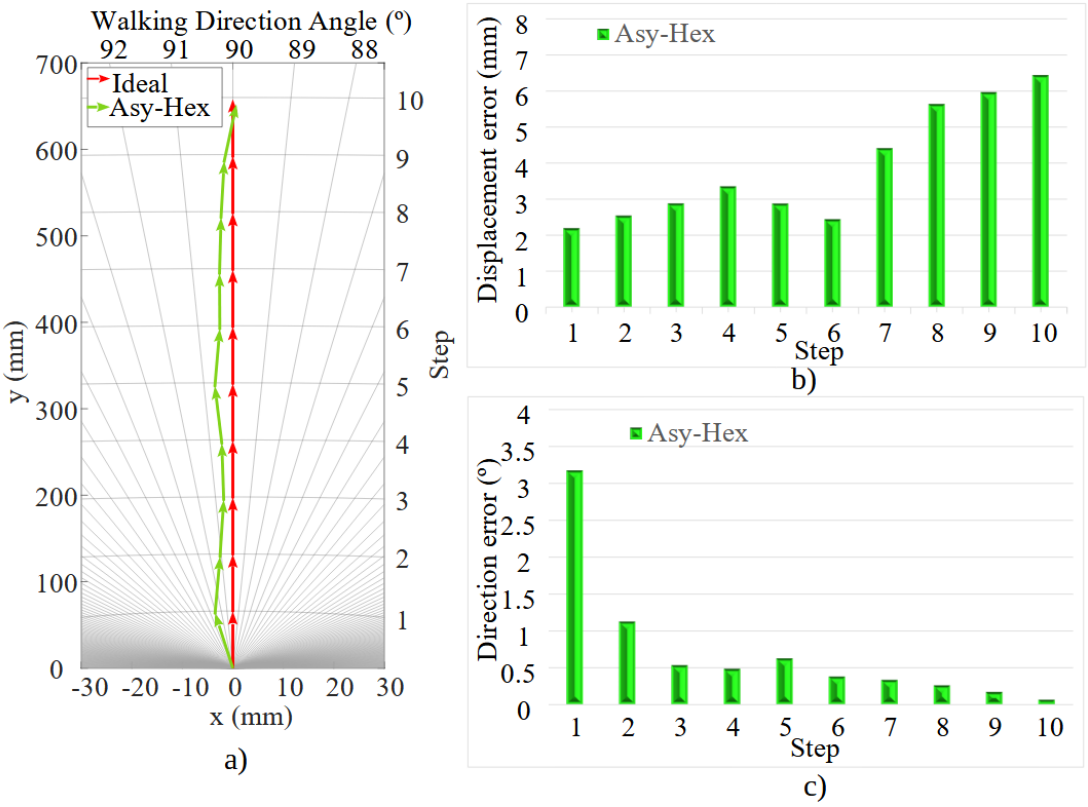


Figure 6-27. Comparison Asy-Hex configuration. a) Displacements of the Asy-Hex configuration against the ideal displacement. b) Displacement error. c) Direction error.

The results for the Asy-Hex configuration show a maximum displacement error at the last step with a total error of 6.42 mm. Similarly to previous configurations, the

maximum deviation angle occurs at the first step, and is reduced in subsequent steps. More importantly, no significant error is acquired and it is concluded that the proposed RPKM can modify its configuration to achieve save traverse on conditions that would limit conventional parallel kinematic walking machines.

6.5 **Discussion of Results**

Figure 6-21 presented the comparison between the Insect and Sym-Hex configurations; from Figure 6-21c and Figure 6-21d is possible to conclude a higher direction error with the Insect configuration. Even though the total displacement presents no significant deviation with the Insect and Sym-Hex configurations (smaller than 6 mm). Furthermore, from Table 6-5 is possible to observe the reduced stability margin of the Insect configuration compared to the Sym-Hex, which indicates that the effect of reduced stability coefficient had an impact in the total displacement of the RPKM. However, in these cases, the maximum lateral deviation remained smaller than 2º with the advantage of a higher displacement speed (1.8 times faster than the Sym-Hex, as shown in Table 6-5). This also is related to the time consumed to place each group of limbs, this is the tripod gait against the wave gait. More importantly, the direction error over long distances can solved as the Insect configuration presents the capability displace laterally. This represents that the configuration allows to change the direction of displacement by 90 degrees without major modifications to the gaits, as the limbs operate at all times close to the neutral position of the upper spherical joints. Furthermore, this also represents that the Insect configuration can avoid obstacles in the path of the RPKM.

Table 6-5. Performance Comparison of the Insect, Sym-Hex, G-S and Asy-hex configurations.

	Insect	**Sym-Hex**		**GS**	**Asy-Hex.**
Ground inclination (º)	0	0	4	4	10
Max displacement error (mm)	18.2	10.1	4.9	13.9	6.4
Max direction error (º)	9.6	2.4	0.8	1.2	3.2
Average displacement error (mm)	12.8	10.2	3	2.7	3.8
Min stability coefficient	0.3	0.9	0.9	1.11	0.8
Speed (step/min)	0.6	0.34	0.34	0.34	0.34

Furthermore, the relationship between the stability coefficient, the configuration and the errors on the true displacement are reinforced when the G-S and the Hexagonal configurations are compared at the inclined ground; the Hexagonal configuration presented a better performance in terms of direction error over the full trajectory presented in Figure 6-26c and d. More importantly, this represents that the Hexagonal configuration is the most suited for traversing over inclined grounds, showing that more symmetrical configurations present a better performance with respect to the real displacements achieved. This is statement is reinforced when non-symmetrical G-S and Hexagonal configurations where compared; at higher angles slippage was presented with the G-S configuration, rendering the last configuration as non-suitable for safe traverse. Regarding Hexagonal configurations, the symmetrical configuration shows a better performance at low inclination angles, while steeper slopes require non-symmetrical configurations for safety (operate within limits of components).

In conclusion, three configurations of the RPKM are proposed to traverse different terrain conditions optimally:

- *Insect configuration:* Proposed to traverse over flat grounds when the main concern is the speed of displacement and avoiding possible obstacles.

- *Symmetric Hexagonal:* Proposed to traverse over inclined grounds when the limbs operate within allowable limits.
- *Non-Symmetric Hexagonal:* Proposed to traverse over highly inclined ground when the limbs are required to operate at their maximum actuation limits.

6.6 Conclusions

This chapter proved the concept and the design of an RPKM for different terrain conditions able to:

a) Modify its configuration to adopt symmetric and non-symmetric layouts by repositioning the joints on the moving platform. Thanks to a novel clutch mechanism based on Shape Memory Alloys, the proposed RPKM can modify its kinematic chain and achieve several configurations. This metamorphic characteristic allowed the adaptability of the RPKM to different terrain conditions, where conventional PKM would be limited. Furthermore, the proposed repositioning system is lightweight and compact when the system is compared with conventional actuation packages.
b) Prove the versatility of a reconfigurable parallel kinematic walking machine to traverse over inclined and levelled terrain. By adopting different configurations (i.e. Sym-Hex, Insect, Gough-Stewart and Asy-Hex) different capabilities where adopted, such as the higher speed of displacement, increased stability for lower displacement errors and climbing over higher inclination angles for machines intended for in-situ repair and maintenance.
c) Open the opportunity for the development of future portable machine tools by utilising the reconfigurable characteristics of RPKMs, as the concept, design, kinematic models, and different configurations have been presented. Therefore, designers and researchers can use this paper as a reference for the design and analysis of RPKM.

Chapter 7 **Conclusions and further research**

In this chapter, the overall outcomes and achievements of the thesis are summarised and discussed, emphasising the contributions to overcome the current limitations of PKMs.

The identified objectives for the PhD have been defined as:

- Develop the kinematic models that describe the metamorphic characteristics of a novel reconfigurable parallel manipulator for its safe operation.
- Develop the models that describe the optimum configuration of the RPKM for machining operations and the avoidance of singularities. As one drawback of PKMs is the presence of singularities in the workspace that can lead to loss of control and damage to the PKMs, this thesis aims to overcome this issue by taking advantage of the reconfiguration capabilities of the proposed design.

Propose the models that lead to optimised walking of the RPKM considering different conditions such as the effects of the terrain on the RPKM to produce stable and optimal gaits.

7.1 **Discussion on challenges in PKMs vs project objectives**

In this section, the challenges of this research project are discussed in terms of the proposed models and the design implemented. The final scope is to transfer the PhD achievements into a broader academic and industrial context.

According to the literature review in Chapter 2, there are several limitations of PKMs forbidding their wider popularity in industrial applications. These limitations

are related to the need for well-prepared environments for operation, small workspaces, complicated workspace characterisation and singularities. The aim of this thesis is to overcome these obstacles by developing a Reconfigurable Parallel Kinematic Manipulator (RPKM) capable of effectuating machining and walking operations with increased adaptability (able to comply to uneven surfaces, modify its workspace, stiffness and avoid singular configurations). Furthermore, the system has been designed to modify its performance to walk in different terrain conditions (i.e. inclined ground) while maintaining a safe operational performance. Hence the novelty claimed by this project. To overcome the limitations of conventional PKM the following challenges have been addressed:

- The workspace of conventional PKMs is dependant on the architecture selected during the design phase and remains constant during the operational life of the PKMs. However, in a RPKM the workspace changes as the RPKM adopts a new configuration. To ensure a safe operation of the RPKMs the workspace must be evaluated and characterised (collision avoidance, operation of subcomponents in the appropriated range and singularity avoidance) prior to any operation, which often is linked to high resource consumption (time of analysis). *Therefore, the thesis developed a kinematic model capable to evaluate the safe workspace of the proposed RPKM and its many possible configurations considering the limits of subcomponents (spherical joints, linear actuators, slides), collision avoidance and singularity avoidance.*
- Complex environments require new concepts of adaptive robotic systems with higher versatility to adjust to unstructured environments. However, conventional PKMs required dedicated installations to operate efficiently.

RPKMs represent an opportunity to develop highly adaptive systems capable to operate in different conditions. *For this reason, this thesis proposed four concepts of RPKMs able to modify the location of the upper and lower joints*. It has been shown that the feet of the RPKM allow the system to adapt to un-even surfaces (inclined, steps, curved) and modified the workspace allowing the RPKM to operate in non-dedicated spaces for manufacturing and repair. Furthermore, by allowing the reconfigurability of the upper joints the workspace can be enhanced to avoid singular configurations and optimise the stiffness of the RPKM proposed. Similarly, by reconfiguring the upper and lower joints, symmetric and non-symetric configurations where used to enhance the walking characteristics of the RPKM proposed and allowed it to safely traverse in conditions that would limit the use of conventional PKMs.

- PKMs are well known for their high stiffness and precision characteristics. However, certain orientations and positions in the workspace of PKMs are singular. These conditions are known to make the stiffness of PKMs vanish and therefore lead to a loss of control which can result in damage to the system. Furthermore, the identification of these conditions is exhaustive and often resource-consuming, frequently resulting in a reduced workspace by limiting the singular regions. *The proposed RPKM in this thesis aims to modify the kinematic chain of the RPKM by repositioning the upper joints to avoid unstable conditions to comply with the specified task.*
- Current research of walking robots has extensively relied on nature-inspired mechanism in the search for more efficient, higher load capability and increased gait adaptability. In such circumstances, limb distribution and their configuration play a crucial role in the performance of walking robots.

However, most walking robots present fixed structures, and their performance may be compromised when the environment changes from the ideal conditions. For this reason, *this thesis proposed an RPKM capable of modifying its walking speed, stability coefficients and climbing capabilities (regarding inclined terrain) to enable its safe operation in different environments by allowing the reconfiguration of the upper joints*.

The objectives and challenges and the details of their fulfilment are as follows:

7.1.1. To Study suitable architectures to allow a reconfigurable parallel kinematic machine

Four concepts were proposed in Chapter 3; each concept proposed a design to enhance the adaptability of conventional PKMs to unstructured environments. However, a concept utilising linear slides was selected to provide suitable means to modify the RPKM performance while maintaining a relatively low level of complexity. Furthermore, this concept aid in maintaining a compact and lightweight system, so the performance of the proposed RPKM would not be hindered (mobility and machining capabilities).

7.1.2. To propose the kinematic models that describe the safe actuation of an RPKM

In order to take advantage of the selected concept in Chapter 3, a kinematic study was required. Chapter 4 presented a novel methodology for obtaining the inverse kinematics of the proposed system. Furthermore, the kinematic model proposed presented considered all the possible concepts presented in Chapter 3, aiming to further optimise the design in later stages and considering the safe working limits of its components and potential collisions. In this regard, this methodology proposed an efficient algorithm to identify the distance between the components of the RPKM without the need for any optimisation process, which can be resource consuming.

Similarly, the methodology proved to be suitable for irregular workspaces, whilst conventional methodologies proposed simplified geometries,

which often result in the loss of part of the workspace.

7.1.3. To optimise the architecture of an RPKM to enhance its workspace

Regarding the concept selected for the RPKM, it was proposed a fixed orientation of the slides. However, to increase the adaptability to different scenarios, the system should present the maximum workspace, optimising the direction of the linear slides and the upper platform geometry. A novel methodology based on genetic algorithms was utilised to reduce the time of analysis. This methodology showed that the maximum workspace volume could be achieved when the linear slides are aligned with the radius of the platform (symmetrically distributed on the platform).

Similarly, one of the disadvantages of conventional PKMs is the presence of singularities in the workspace. Standard methodologies are focused on identifying singular regions and then forbidding the PKM to operate in these zones. However, this represents a reduction of the usable workspace. In this regard, this thesis presented a novel methodology capable of identifying and proposing new configurations free of singularities for a given task. This methodology is based on the analysis of the Jacobian of the RPKM. By analysing the Jacobian ‘s determinant in respect to different orientations for several points of interest. Based on the analysis of these values, the Fourier Analysis is implemented to trace singular conditions and to reposition the upper joints in the system to produce singular free configurations. This methodology proved to be efficient as a mean to avoid and propose new singular-free configurations. Furthermore, this methodology has been validated by

comparing the stiffness of the system by means of the analytical results against a model implemented in ANSYS APDL.

7.1.4. To propose a novel design of an RPKM

This thesis demonstrated that a novel design capable of modifying the position of the upper joints would enhance the performance during machining operations. However, to avoid heavy and bulky repositioning systems, a novel design based on shape memory alloys was developed. This system not only proved to be lightweight and compact, but it also provided the actuation to reposition six joints to effectively modify the kinematic chain of the RPKM. In this regard, the characterisation of the SMA wire and the design of the clutch mechanism has been performed in chapter 5. Furthermore, Chapter 5 presented the integration of several subsystems to enable the design of the RPKM and the prototype developed for further test.

7.1.5. To develop the kinematics for enabling the RPKM to walk in different terrain conditions

With respect to the walking characteristics, Chapter 6 presented the kinematics for enabling the proposed RPKM to walk on different terrain conditions (i.e. flat terrain, inclined terrain). These models considered the safe actuation of the system from possible collisions, the forces exerted on the sub-components and the stability during the walking. Regarding the stability of the RPKM, Chapter 6 considered a new approach to include the vertical position of the CoM and its influence on the stability of the RPKM. The methodology proposed the required force to tip over the RPKM and compared it against its weight. The closer the coefficient to zero, the less stable the system, while if the coefficient presented a negative value represented an unstable configuration. Similarly, the methodology to evaluate the forces acting on the RPKM during the different stages of the walking was proposed based on commercial FEA software. This methodology reduced the burden of analysis

involved with extensive models by reducing the number of components and the characteristics of each element to its most basic structural representation. This not only allowed to evaluate the forces exerted on each component during the walking but provided helpful information towards the most feasible gaits for the Sym-Hex and Insect configurations. More importantly, this methodology showed a reduction of 60 % between the wave and tripod gait in the Sym-Hex configuration. Whilst the Insect configuration presented similar load cases in both gaits.

Chapter 7 recorded the details of the experimental testing of the proposed RPKM in different terrain conditions. These conditions included the walking of the system in level ground and inclined ground at 4 and 10 degrees. The system showed to be capable of operating in conditions that would have limited conventional PKMs. Furthermore, the advantages of a reconfigurable system were established in these different terrain conditions as the system allowed to operate different gaits in other terrain conditions. For instance, the Insect configuration presented the fastest displacement speed as this configuration allowed the use of tripod gaits. However, the Insect configuration presented the lowest stability coefficients, and as such, it presented the maximum error in terms of its displacement. The more symmetrical and higher stable configurations proved to present the smallest error in terms of displacement and their capabilities to climb on medium inclined surfaces. However, when the inclination of the terrain was increased, the major limitations for the displacement was related to the individual workspace of each limb. In this regard, asymmetric configurations (Asy-Hex) allowed better use of each limb and allowed the RPKM to climb on surfaces inclined at 10 degrees.

7.2 Overall Achievement

The proposed RPKM based on a novel concept to enable emerging robotics to adapt to different environment conditions. More importantly, this research project has been able to combine the theoretical aspects of a novel system with a practical application in the current needs of industry, especially in the ones that forbid the intervention of human operators.

7.3 Further Research

Since the proposed RPKM is novel in terms of the concepts proposed, more testing and further research could benefit its wider application in real environments. Developing a methodology to integrate the hardware designed with current technologies communication technologies would increase its possible applications.

7.3.1. Feet

During the experimental test developed for Chapter 7, it became apparent that gaits that deviated from ideal resulted in the system effectively walk. However, this could be prevented if sensors to detect the deviation from the ideal force exerted on each limb could be compensated. This means that in failing gaits, some feet would support most of the weight of the RPKM whilst others would be kept without contact with the ground. This was compensated by making the analysis of the forces acting on the RPKM. However, the inclusion of sensors on the feet could compensate for errors generated by the deformation of critical components of the RPKM.

7.3.2. Walking

The existing prototype proved the advantages of a reconfigurable system in different terrains. However, the methodologies proposed are based on a static analysis as the displacements speeds of the designs are limited by the hardware itself (heating and cooling times of the SMA, deformation of the tendons actuating the limbs, etc.). In this regard, optimising the actuation of the limbs could increase the achieved

displacements speed. Furthermore, the developed methodologies should include the dynamic effects and take advantage of the redundancy of the limbs.

7.3.3. Machining

The proposed RPKM has yet to be studied extensively in terms of its capabilities in real environments and its performance with different tools and manufacturing technologies, such as in the case of including additive manufacturing tools.

7.3.4. Power Consumption

A reduction in power consumption has a crucial impact on reducing the size of the actuators that operate the robot and the total weight of the walking robot for systems operating on batteries. Furthermore, enabling systems to operate on batteries could increase the autonomy and capabilities of PKMs to be deployed in hazardous and hard to reach zones. Then it is crucial to the creation of models capable of accounting for energy-efficient gaits. With the energy optimisation, different parameters can be considered, such as force distribution on the supporting limbs[117], gait speeds [118], ground reaction forces, forces and torques required at the joints [119] and the conditions that lead to feet slippage. Other optimisation strategies target to maximisation of stability margins and maximisation of walking displacements. In this regard, Gonzalez et al. [9] studied the leg distribution in a hexapod and concluded on the advantages of arranging the middle limbs, by a reduction of 15% of the forces on the legs was experienced, reducing the energy required to operate the hexapod. Mahapatra et al. [120] calculated the force distribution of a hexapod using the quadratic programming method to minimise the energy consumption, concluding that increasing the body stroke and leg offset had a negative impact on power consumption. Then Mustapha performed an energy efficiency analysis of a hexapod with metachronal gaits to propose the modified

parameter wave gait [121] for an increased efficiency hexapod. Although all these efforts provide a significant improvement in the analysis and understanding of hexapods and to the effects of leg distribution and configuration for gait energy consumption, these also consider several simplifications. These simplifications are mainly neglecting the mass effects of the limbs, as the majority of the walking robotic systems consider the centre of mass to depend only on the main body [95]. Others consider a single direction of displacement or simplified kinematic models without pondering the interaction with the ground as the displacement have been considered to take effect on flat ground, which results in a significant impact on the stability margins, energy efficiency and collision avoidance. However, a connected model would be beneficial to improve the walking performances (i.e. centre of mass, stability) when the legs are repositioned, this is proposed as future work as to the authors best knowledge including these estudies could benefit the future development of RPKMs.

7.4 **Conclusion**

This thesis presented a family of concepts of RPKMs. From the initial concepts, concept 2 is selected to create a detailed design and later manufacturing. To achieve the mechanical design of the system, several subsystems where integrated. One significant system relates to the SAS, which allowed the repositioning of the upper joints. Furthermore, a new methodology to detect and later propose new configurations is presented in chapter 4. The main advantage of this methodology relies in it capability to propose new configurations of the RPKM, by repositioning the upper joints, supported by the design of the SAS. Later on in chapter 6, this thesis presents the advantages of considering a reconfigurable system, enabling the displacement of the proposed RPKM over different terrain and showing the

advantages of each configuration. The experiments developed in this thesis proved the versatility of an RPKM to traverse over inclined and levelled terrain. By adopting different configurations (i.e. Sym-Hex, Insect, Gough-Stewart and Asy-Hex) different capabilities where adopted, such as the higher speed of displacement, increased stability for lower displacement errors and climbing over higher inclination angles for machines intended for in-situ repair and maintenance. Overall this thesis presented and proved the concept, design and testing of a RPKM capable to adapt to different operational conditions.

References

1. *Executive Summary WR 2017 Industrial Robots.* International Federation of Robotics 2018: p. 15-24.
2. Xu, P., et al., *Novel hybrid robot and its processes for precision polishing of freeform surfaces.* Precision Engineering, 2020. **64**: p. 53-62.
3. Escorcia-Hernández, J.M., et al., *A new solution for machining with RA-PKMs: Modelling, control and experiments.* Mechanism and Machine Theory, 2020. **150**: p. 103864.
4. Chen, T.-C., et al., *Design analysis of machine tool structure with artificial granite material.* Advances in Mechanical Engineering, 2016. **8**(7): p. 168781401665653.
5. Stewart, D., *A Platform with Six Degrees of Freedom.* Institution of Mechanical Engineers, 1965. **180**(1): p. 371-386.
6. Merlet, J.-P., *Parallel Robots*. Second ed. ed. Vol. 128. 2006: Springer.
7. Ji, W. and L. Wang, *Industrial robotic machining: a review.* The International Journal of Advanced Manufacturing Technology, 2019. **103**(1-4): p. 1239-1255.
8. Axinte, D.A., et al., *Free-leg Hexapod: A novel approach of using parallel kinematic platforms for developing miniature machine tools for special purpose operations.* CIRP Annals, 2011. **60**(1): p. 395-398.
9. Gonzalez de Santos, P., J. Estremera, and E. Garcia, *Optimizing Leg Distribution Around the Body in Walking Robots.* Proceedings of the 2005 IEEE International Conference on Robotics and Automation, 2005: p. 3207-3212.
10. Y. Li, B.L., J. Ruan X Rong, *Research of Mammal Bionic Quadruped Robots A Review.* IEEE 5th International Conference on Robotics, Automation and Mechatronics 2011: p. 166-171.
11. Sun, J. and J. Zhao, *An Adaptive Walking Robot With Reconfigurable Mechanisms Using Shape Morphing Joints.* IEEE Robotics and Automation Letters, 2019. **4**(2): p. 724-731.
12. Roy, R., et al., *Continuous maintenance and the future – Foundations and technological challenges.* CIRP Annals, 2016. **65**(2): p. 667-688.
13. Fraser, K., H.-H. Hvolby, and T.-L. Tseng, *Maintenance management models: a study of the published literature to identify empirical evidence.* International Journal of Quality & Reliability Management, 2015. **32**(6): p. 635-664.
14. Mobley, R.K., *An introduction to predictive maintenance*. Vol. Second edition. 2002: Butterwrth Heinemann. 1-61.
15. Dhillon, B.S., *Engineering Maintenance a modern approach*. 2002: CRC Press.
16. Neugebauer, R., et al., *Structure principles of energy efficient machine tools.* CIRP Journal of Manufacturing Science and Technology, 2011. **4**(2): p. 136-147.
17. Chang, M.M.L., S.K. Ong, and A.Y.C. Nee, *AR-guided Product Disassembly for Maintenance and Remanufacturing.* Procedia CIRP, 2017. **61**: p. 299-304.
18. Y.G. Li, H.T.L., X.M. Zhao, T. Huang, Derek G. Chetwynd, *Design of a 3-DOF PKM module for large structural component machining* Mechanism and Machine Theory, 2010. **45**: p. 941-954.

19. Checchi, A., et al., *Offline tool trajectory compensation for cutting forces induced errors in a portable machine tool.* Procedia CIRP, 2019. **82**: p. 527-531.
20. Lee, D., et al., *Development of a mobile robotic system for working in the double-hulled structure of a ship.* Robotics and Computer-Integrated Manufacturing, 2010. **26**(1): p. 13-23.
21. Dong, X., et al., *Development of a slender continuum robotic system for on-wing inspection/repair of gas turbine engines.* Robotics and Computer-Integrated Manufacturing, 2017. **44**: p. 218-229.
22. Hazel, B., et al., *A portable, multiprocess, track-based robot for in situ work on hydropower equipment.* Journal of Field Robotics, 2012. **29**(1): p. 69-101.
23. Legoff, O., et al., *Mobile Machines for the Machining of Large Dimension Parts.* MM Science Journal, 2019. **2019**(04): p. 3142-3147.
24. de la Torre, H. and E. Rodriguez-Leal, *Instantaneous Kinematics Analysis via Screw-Theory of a Novel 3-CRC Parallel Mechanism.* International Journal of Advanced Robotic Systems, 2016. **13**(3): p. 128.
25. Gallardo-Alvarado, J., *Kinematic Analysis Of Parallel Manipulators by Algebraic Screw Theory*. 2016: Springer.
26. A. Youseff, H.A.E.-H., Mohamoud H. Ahmed, *Manufacturing Technology: Materials, Processes and Equipment*. 2012: CRC Press.
27. Fassi, I. and G.J. Wiens, *Multiaxis Machining: PKMs and Traditional Machining Centers.* Journal of Manufacturing Processes, 2000. **2**(1): p. 1-14.
28. Palpacelli, M., et al., *Design of a Lockable Spherical Joint for a Reconfigurable 3-URU Parallel Platform.* Robotics, 2018. **7**(3): p. 42.
29. Dash, A.K., et al., *Task-oriented configuration design for reconfigurable parallel manipulator systems.* Int. J. Computer Integrated Manufacturing, 2005. **18**: p. 615-634.
30. Shaw, D. and Y.-S. Chen, *Cutting path generation of the Stewart-Platform-Based Milling Machine using an end-mill.* International Journal of Production Research, 2001. **39**(7): p. 1367-1383.
31. Chong, Z., et al., *Design of the parallel mechanism for a hybrid mobile robot in wind turbine blades polishing.* Robotics and Computer-Integrated Manufacturing, 2020. **61**: p. 101857.
32. Reid, E., *Development of a Mobile Drilling and Fastening System Based on a PKM Robotic Platform.* 2015. **1**.
33. Olarra, A., et al., *Machining with the WalkingHex: A walking parallel kinematic machine tool for in situ operations.* CIRP Annals, 2017. **66**(1): p. 361-364.
34. Keil, C. *Ultra motion Stewart-Gough platform* 2020; Available from: https://www.colinkeil.com/robotics.
35. Jiang, Y., T. Li, and L. Wang, *Novel Method for Designing High Precision Parallel Kinematic Machines Based on the Smart Structure.* IEEE/ASME Transactions on Mechatronics, 2017. **22**(4): p. 1889-1902.
36. Industry, D. *V100* 2020; Available from: https://pdf.directindustry.com/pdf/index-werke/v100/5689-301437.html.
37. Quinchuan Li, J.M.H.W.Y., *Geometric Method For Type Synthesis of Parallel Manipulators*. 2020: Springer.
38. Industry, D. *5 Axis machining center Scharmann Ecospeed*. 2020; Available from: https://www.directindustry.com/prod/starrag/product-122219-1369143.html.

39. Popovik, M.b., *Biomechatronics*. 2019: Elsevier Science.
40. Angel, L. and J. Viola, *Fractional order PID for tracking control of a parallel robotic manipulator type delta.* ISA Trans, 2018. **79**: p. 172-188.
41. Pierrot, F., et al., *Optimal Design of a 4-DOF Parallel Manipulator: From Academia to Industry.* IEEE Transactions on Robotics, 2009. **25**(2): p. 213-224.
42. Weiss. *Delta robot DR 4*. 2020; Available from: https://www.weiss-gmbh.de/Delta-Robot-DR.4188.0.html?&L=1.
43. Omron, *X-Delta 3+1*. 2020.
44. Garcia, L. and A. Campos, *Maximal Singularity-Free Orientation Subregions Associated with Initial Parallel Manipulator Configuration.* Robotics, 2018. **7**(3): p. 57.
45. Yu, J., et al., *Mobility and singularity analysis of a class of two degree of freedom rotational parallel mechanisms using a visual approach.* Journal of Mechanisms and Robotics, 2011. **4**: p. 1027-1036.
46. Liu, G., et al., *Singularity analysis and detection of 6-UCU parallel manipulator.* Robotics and Computer-Integrated Manufacturing, 2014. **30**(2): p. 172-179.
47. Slavutin, M., et al., *A complete Geometric Singular Characterisation Of The Stewart Platform.* Journal of Mechanisms and Robotics, 2018. **10**(4).
48. Marc Raibert, K.B., Gabriel Nelson, Rob Playter, *BigDog, the ROugh-Terrain Quadruped Robot.* Boston Dynamics, 2008.
49. Bledt, G., et al., *MIT Cheetah 3 Design and Control of a Robust Dynamic Quadruped Robot.pdf.* International Conference on Intelligent Robots and Systems 2018: p. 2245-2252.
50. McGhee, R.B., *Some Finite State Aspects of Legged Locomotion.* Mathematical Biosciences, 1966. **2**: p. 67-84.
51. Frank, A.A., *Automatic Control System For Legged Locomotion Machines*. 1968, University of Southern California.
52. Mosher, R.S., *Exploring the Potential of a Quadruped.* SAE Transactions, 1969. **78**: p. 836-843.
53. Shingeo Hirose, K.K., *Study on Quadruped Walking Robot in Tokyo Institute of Technology -Past, Present and Future.* International Conference on Intelligent Robotics and Automation, 2000: p. 414-419.
54. D.M. Gorinevsky, A.Y.S., *Force Control in Locomotion of Legged Vehicles over Rgid and Soft Surfaces.* The International Journal of Robotics Research, 1990: p. 4-23.
55. Scheneider A., S.U., Ihme T. , Devjanin E. Savitsky K., *Force Control in Locomotion of Legged Vehicle and for Service Operations.* World Automation Congress, 1996.
56. Robert B. McGhee, G.i.I., *Adaptative Locomotion of a Multilegged Robot over Rough Terrain.* IEEE Transactions on Systems, Man, and Cybernetics 1979. **9**.
57. Kenzo Nonami, R.K.B., Addie Irawan, Mohd Razali Daud, *Hydraulically Actuated Hexapod Robots*. 2014: Springer.
58. Raibert, M.H., *Legged Robots That Balance*. 1986: The MIT Press.
59. Marc H. Reibert, I.E.S., *Machines that walk*, in *Scientific American* 1983. p. 32-41.
60. Hirose, S., et al., *Quadruped walking robots at Tokyo Institute of Technology.* IEEE Robotics & Automation Magazine, 2009. **16**(2): p. 104-114.

61. Kenneth J. Waldron, R.B.M., *The Adaptative Suspension Vehicle.* IEEE Control Systems Magazine, 1986: p. 7-12.
62. Junichi Akizono, M.I., Takashi Nemoto, Osamu Asakura, *Field Test of Aquatic Walking Robot for Underwater Inspection*. Port and Harbour Research Institutu, Ministry of Transport: Yokosuka, Japan.
63. Raibert, M.H., *Trotting, pacing and bouncing by quadruped robot.* Journal of Biomechanics, 1990. **23**: p. 79-98.
64. Hironori Adachi, N.K., Eiji Nakano, *Mechanism and Control of a Quadruped Walking Robot.* IEEE Systems Magazine 1988. **8**(5): p. 14-19.
65. Coilin M. Angle, R.A.B., *Small Planetary Rovers.* IEEE International Workshop on Intelligent Robots and Systems 1990: p. 383-388.
66. K.K. Hartikainen A.J. Halme, H.L.K.O.K., *MECANTI: A Six Legged Walking Machine for Research Purposes in Outdoor Enviroment.* International Conference on Intelligent Robotics and Automation, 1992: p. 157-163.
67. K. Berns, S.C., W. Ilg., *Adaptative, Neural Control Architecture for the Walking Machine Lauron.* International Conference on Intelligent Robots and Systems, 1994: p. 1172-1177.
68. S. Cordes, K.B., L. Lappanen, *Sensor Components of the Six-Legged Walking Machine Lauron II.* international Conference on Advanced Robotics, 1997: p. 71-76.
69. Shigeo Hirose, A.N., Ryosei Toyama, *Machine That Can Walk and Climb on Floors, Walls and Ceilings.* IEEE, 1991: p. 753-758.
70. Shigeo Hirose, K.A., *Coupled and Decoupled Actuation of Robotic Mechanisms.* International Conference on Robotics & Automation, 2000: p. 33-39.
71. Phillippe De Beaucoun, P.G., P. Morganh, *Field Test of the Mobile Robot SHERPA*. 1994.
72. Keisuke Arikawa, S.H., *Development of Quadruped Walking Robot TITAN-VIII.* International Conference on Intelligent Robots and Systems, 1996: p. 208-214.
73. G.M Nelson, R.D.Q., R.J. Bachmann. W.C. Flanningan, *Design and Simulation of a Cockroach-like Hexapod Robot.* International Conference on Intelligent Robotics and Automation, 1997.
74. Roger D. Quinn, G.M.N., Richard J. Bachamann, Daniel A. Kingsley, John Offie, Roy E. Ritzmann, *Insect Designs for Improved Robot Mobiity.* International Conference on Climbing and Walking Robots, Berns and Dillmann, 2001: p. 69-76.
75. Juan Carlos Grieco, M.P., Manuel Armada, Pablo Gonzalez Santos, *A six-Legged Climbing Robot for High Payloads.* International Conference on Control Applications, 1998: p. 446-450.
76. Lisbeth Mena, H.M., Roemi Fernandez, Javier Sarria, Manuel Armada, *Reconfiguration of a Climbing Robot in an All-terrain Hexapod Robot.* Robot 2015: Second Iberian Robotics Conference. Advances in Intelligent Systems and Computing, 2015. **418**.
77. Bernd Gabmann, K.-U.S., Karsten Berns, *Locomotion of Lauron III in rough terrain.* Internation Conference on Advanced Intelligent Mechatronics Procedings, 2001: p. 959-964.
78. Eric Celaya, J.A., *Implementation of a hierarchical walk controller for the LAURON III hexapod robot.* 2003.

79. P. Gonzalez de Santos, M.A.A., M.A. Jimenez, *Shipbuiding with ROWER.* Roboti & Automation Magazine, 2000. **7**(4): p. 35-43.
80. Kennedy, B., et al., *LEMUR: Legged excursion mechanical utlity rover.* Autonomous Robots, 2001. **11**(3): p. 201-205.
81. Keisuke Kato, S.H., *Development of the Quadruped Walking Robot TITAN-IX.* 26th Annual Conference of the IEEE Industrial Electronics Society. IECON 2000. IEEE International Conference on Industrial Electronics, Control and Instrumentation, 2000: p. 40-45.
82. Murphy, M.P., et al., *The LittleDog robot.* The International Journal of Robotics Research, 2010. **30**(2): p. 145-149.
83. Hae-Won Park, S.K., *The MIT Cheetah, an Electrically-Powered Quadrupedal Robot for High-speed Running.* Journal of the Robotics Society of Japan 2014. **32**(4): p. 323-328.
84. de Waard, M., M. Inja, and A. Visser, *Analysis of flat terrain for the atlas robot.* 2013: p. 1-6.
85. Saltaren, R., R. Aracil, and E. Yime, *Teleoperathed Parallel Climbing Robots in Nuclear Installations.pdf.* Industrial Robot, 2006. **33**(5): p. 381-386.
86. Yang, H., et al., *Locomotion approach of REMORA: A reonfigurable mobile robot for manufacturing Applications.* International Conference on Intelligent Robots and Systems, 2011: p. 5067-5072.
87. Axinte, D., et al., *MiRoR—Miniaturized Robotic Systems for Holistic In-Situ Repair and Maintenance Works in Restrained and Hazardous Environments.* IEEE/ASME Transactions on Mechatronics, 2018. **23**(2): p. 978-981.
88. Chen, X.D., K. Watanabe, and K. Izumi, *Kinematic solution of a quadruped walking robot - posture analysis of TITAN-VIII.* IFAC Proceedings Volumes, 1999. **32**(2): p. 827-832.
89. Da Xi, F.G., *Criteria of type complexity for legged robots.* Mechanism and Machine Theory, 2019. **144**.
90. Barreto, J.P., et al., *FED-the free body diagram method. Kinematic and dynamic modeling of a six leg robot.* 1998: p. 423-428.
91. Min, B., Z. Bien, and S. Hwangt†, *Basic characteristics and stability properties of quadruped crab gaits.* Robotica, 1993. **11**(3): p. 233-243.
92. Shigeo Hirose, H.T., Kan Yoneda, *Normalized energy stability margin and its contour of walking vehicles on rough terrain.* Internation Conference on Robotics and Automation, 2001. **1**: p. 181-186.
93. P. Gonzalez de Santos, M.A.A., M.A. Jimenez, *Path tracking with quadruped walking machines using discontinuous gaits.* Computer and Electrical Engineering, 1995. **21**(6): p. 383-396.
94. Wang, Z., et al., *Mobility analysis of the typical gait of a radial symmetrical six-legged robot.* Mechatronics, 2011. **21**(7): p. 1133-1146.
95. Roy, S.S. and D.K. Pratihar, *Effects of turning gait parameters on energy consumption and stability of a six-legged walking robot.* Robotics and Autonomous Systems, 2012. **60**(1): p. 72-82.
96. Vázquez, J.A. and M. Velasco-Villa, *Experimental Estimation of Slipping in the Supporting Point of a Biped Robot.* Journal of Applied Research and Technology, 2013. **11**(3): p. 348-359.
97. Amine, S., et al., *Singularity analysis of 3T2R parallel mechanisms using Grassmann–Cayley algebra and Grassmann geometry.* Mechanism and Machine Theory, 2012. **52**: p. 326-340.

98. Li, B., et al., *Singularity property and singularity-free path planning of the Gough–Stewart parallel mechanism.* International Journal of Advanced Robotic Systems, 2017. **14**(6): p. 1-16.
99. Rushworth, A., et al., *A concept for actuating and controlling a leg of a novel walking parallel kinematic machine tool.* Mechatronics, 2016. **40**: p. 63-77.
100. R. Stamper, L.T.a.G.W., *Optimization of a three DoF translational platform for well conditioned workspace.pdf.* Proceedings of the 1997 IEEE International Conference on Robotics and Automation, 1997: p. 3250-3255.
101. Tsai, L.-W., *Robot Analysis, The Mechanics of Serial and Parallel Manipulators.* 1999: p. 239-240.
102. R.C.a.J.L., *Fourier Analysis.* John Wiley & Sons, 2017.
103. Singh, B., *Computational Tools and Techniques for Biomedical Signal Processing.* 2016: p. 277.
104. Golberg, D.E., *Genetic Alforithms in Search, Optimization and Machine Learning.* Addison-Wesley, Boston, Mass, , 1989.
105. Ma, N., X. Dong, and D. Axinte, *Modeling and Experimental Validation of a Compliant Underactuated Parallel Kinematic Manipulator.* IEEE/ASME Transactions on Mechatronics, 2020. **25**(3): p. 1409-1421.
106. Ma Nan , X.D., Josue Camacho Arreguin., *A Novel Shape Memory Alloy (SMA) Wire-Based Clutch Design and Performance Test.* In Annual Conference Towards Autonomous Robotic Systems, 2020(Springer,Cham): p. 369-376.
107. Motzki, P., et al., *Design and Validation of a Reconfigurable Robotic End-Effector Based on Shape Memory Alloys.* IEEE/ASME Transactions on Mechatronics, 2019. **24**(1): p. 293-303.
108. Hartl, D., et al., *Thermomechanical Characterization and Modeling of Ni60Ti40 SMA for Actuated Chevrons.* 2006: p. 281-290.
109. Jang, N., et al., *Compact and Lightweight End-Effectors to Drive Hand-Operated Surgical Instruments for Robot-Assisted Microsurgery.* IEEE/ASME Transactions on Mechatronics, 2020. **25**(4): p. 1933-1943.
110. Mohd Jani, J., et al., *A review of shape memory alloy research, applications and opportunities.* Materials & Design (1980-2015), 2014. **56**: p. 1078-1113.
111. Ma, N., et al., *Design and stiffness analysis of a class of 2-DoF tendon driven parallel kinematics mechanism.* Mechanism and Machine Theory, 2018. **129**: p. 202-217.
112. Wittlinger, M., R. Wehner, and H. Wolf, *The desert ant odometer: a stride integrator that accounts for stride length and walking speed.* J Exp Biol, 2007. **210**(Pt 2): p. 198-207.
113. Grabowska, M., et al., *Quadrupedal gaits in hexapod animals - inter-leg coordination in free-walking adult stick insects.* J Exp Biol, 2012. **215**(Pt 24): p. 4255-66.
114. Camacho, J., et al., *A Novel Class of RPKM Concepts and Fourier-base Singularity Analysis* Mechanism and Machine Theory, 2020. **153**.
115. Yuan, C., R. Gexue, and D. ShiLiang, *Vibration control of gough-stewart platform on flexible suspension.* IEEE Transactions on Robotics and Automation, 2003. **19**(3): p. 489-493.
116. Merriaux, P., et al., *A Study of Vicon System Positioning Performance.* Sensors (Basel), 2017. **17**(7).

117. Y. Liu, L.D., H. Gao, G. Liu, Z. Deng and H. Yu, *Efficient Force distribution on walking on uneven terrain.* International Conference on Robotics and Biomimetics, 2016: p. 432-437.
118. Manuel Solva, R.B., Jose Tenreiro Machado, *GA Optimization of an Hexapod Robot Parameters for Periodic Gaits.* International Symphosium on Computational Intellignence For Engineering, 2009. **1**.
119. Jin, B., C. Chen, and W. Li, *Power Consumption Optimization for a Hexapod Walking Robot.* Journal of Intelligent & Robotic Systems, 2012. **71**(2): p. 195-209.
120. Mahapatra, A., S.S. Roy, and D.K. Pratihar, *Study on feet forces' distributions, energy consumption and dynamic stability measure of hexapod robot during crab walking.* Applied Mathematical Modelling, 2019. **65**: p. 717-744.
121. Suphi Erden, M. and K. Leblebicioğlu, *Analysis of wave gaits for energy efficiency.* Autonomous Robots, 2007. **23**(3): p. 213-230.